Università degli Studi del Piemonte Orientale “Amedeo Avogadro”

Dipartimento di Medicina Traslazionale

Università degli Studi di Torino

Dipartimento di Scienze Agrarie, Forestali e Alimentari

Corso di Dottorato di Ricerca in Food, Health and Longevity

Ciclo XXXVII

“Effect of Tannins on the Stability of Sterols in Food Emulsions”

Settore Scientifico Disciplinare: AGR/15 – Scienze e Tecnologie Alimentari

Dottoranda Ambra Bonciolini

Coordinatrice Prof.ssa Antonia Follenzi

Tutor Prof. Vladimiro Cardenia

Co-tutor Prof.ssa Virginia Teresa Glicerina

UNIVERSITÀ DEL PIEMONTE ORIENTALE

CORSO DI DOTTORATO DI RICERCA
FOOD, HEALTH AND LONGEVITY STUDIES

DECLARATION AND AUTHORISATION TO ANTIPLAGIARIM DETECTION

The undersigned Ambra Bonciolini student of the Food, Health and Longevity Studies Ph.D course (XXXVII Cycle)

DECLARES

- to be aware that the University has adopted a web-based service to detect plagiarism through a software system called “Turnit.in”,

- his/her Ph.D thesis was submitted to Turnit.in scan and reasonably it resulted an original document, which correctly cites the literature;

ACKNOWLEDGES

- his/her Ph.D thesis can be verified by his/her Ph.D tutor and/or Ph.D Coordinator in order to confirm its originality.

Date: 15/04/2025

Signature

... e va bene così,

senza parole.

Table of Contents

Chapter 1

Literature Review

1.1 Lipid Oxidation

Lipids play a crucial role in food systems and biological processes. They act as a vital source of energy, as precursors for essential biomolecules, and are integral components of cell membranes and signaling pathways. In the context of food, lipids contribute to nutritional, structural and key sensory attributes – such as aroma, flavour, mouthfeel, and texture – and serve as carriers of fat-soluble vitamins and essential fatty acids (Frankel, 2005). Food lipids encompass a variety of compounds, including fatty acids (saturated, monounsaturated, and polyunsaturated), mono-, di-, and triacylglycerols, phospholipids, and minor unsaponifiable components such as sterols, carotenoids, and tocopherols (McClements & Decker, 2018). Again, lipids can be broadly categorized as saponifiable and unsaponifiable matter. Whole saponifiable lipids (e.g. triglycerides, phospholipids) are susceptible to both hydrolytic and oxidative degradation, unsaponifiable lipids (e.g. sterols, fat-soluble vitamins) are primarily prone to oxidation (Frankel, 2005; McClements & Decker, 2018). Hydrolytic rancidity results from enzymatic activity, particularly lipases, which cleave fatty acids from the glycerol backbone of triacylglycerols, generating free fatty acids associated with undesirable off-flavour. In contrast, oxidation involved complex reaction between unsaturated lipids and oxygen, leading to the formation of volatile compounds such as aldehydes and ketones, which contribute to rancid odours, nutrients loss, and the production of potentially toxic substances (Shahidi & Hossain, 2022; Shahidi & Zhong, 2010).

Among the two degradation pathways, lipid oxidation is more challenging and widespread. It not only impairs the sensory and nutritional quality of food but also raises significant concerns in nutrition, medicine, and biochemistry due to its role in the development of various health disorders

(Frankel, 2005). Factors such as light, heat, metal ions, and enzymes can initiate oxidation via autoxidation, photooxidation, or thermal mechanisms – most of which proceed through free radical intermediates. Autoxidation, the most prevalent form, is a self-propagating reaction involving the formation of lipid hydroperoxides, which subsequently decompose into a range of secondary oxidation products including alcohols, hydrocarbons, organic acids, and epoxides – many with extremely low odour thresholds (Waraho et al., 2011). Despite decades of intensive study and considerable advances in our understanding of lipid oxidation, it continues to represent a major hurdle in food science and related disciplines. Control of lipid oxidation is thus critical for preventing food quality, extending shelf-life, and ensuring the health safety of lipid-containing products. Among the lipid components, sterols play a pivotal role due to their susceptibility to oxidation; thus, the significant impact of their degradation products on both nutritional quality and safety, warranting detailed investigation.

1.2 Sterols

Sterols are a class of amphipathic lipids derived from isoprenoid biosynthesis, characterized by a tetracyclic cyclopenta[α]phenanthrene ring system with a hydroxyl group at C3 and a flexible side chain at C17 (Nes, 2011). Despite containing a hydroxyl group, sterols are classified as lipids due to their lipophilic nature and biological roles. Structurally, they are part of the broader steroid group and occur naturally in most eukaryotic organism and even in some bacteria (Ferreira-Guerra et al., 2025). Sterols play essential roles in maintaining membrane fluidity, rigidity, and permeability. In animals, cholesterol is the primary sterol, while in plants, phytosterols like sitosterol and campesterol are predominant. They serve as precursors for a variety of biologically active molecules, including steroid hormones, bile acids, vitamin D (in animals), and brassinosteroids (in plants). Sterols are classified as unsaponifiable lipids depending on their susceptibility to alkaline hydrolysis, with cholesterol and phytosterols being the most common dietary sterols. They also contribute to structural and

developmental functions in fungi and plants, including roles in cellulose biosynthesis and stress adaptation. In addition to their biological significance, sterols represent minor yet important constituents of the unsaponifiable fraction in edible fats and oils. A crucial property of sterols is their amphipathic nature, meaning they possess both a hydrophilic region—conferred by the hydroxyl group at C3—and a hydrophobic region formed by the fused carbon ring system and aliphatic side chain. This dual character is fundamental to their biological role, particularly in the organization, formation, and maintenance of cellular membranes (Cercaci et al., 2007; Gifer et al., 2022).

1.2.1 Cholesterol

Cholesterol is a vital lipid molecule that plays a central role in maintaining the structural and functional integrity of eukaryotic cell membranes. It constitutes approximately 50% of membrane lipids on a molar basis and is essential for regulating membrane fluidity, permeability, and rigidity. Beyond its structural role, cholesterol serves as a biosynthetic precursor for several critical compounds, including steroid hormones, bile acids, and vitamin D (Iuliano, 2011). The majority of cholesterol in the human body (around 60–70%) is endogenously synthesized, primarily in the liver, with additional contributions from the intestines, adrenal glands, and skin (Li et al., 2019). Although the brain contains the highest concentration of cholesterol in the body, its metabolism operates independently from that of other tissues. Neurons, astrocytes, and oligodendrocytes are primarily responsible for synthesizing cholesterol, that is kept remarkably stable thanks to the cholesterol homeostasis. When this delicate balance is disturbed, it can contribute to the development of neurodegenerative diseases such as Alzheimer's, Parkinson's, and Huntington's disease (Gao et al., 2023). Alongside endogenous synthesis, a significant portion of cholesterol (about 20–25%) is derived from dietary intake, particularly from animal-based foods such as eggs, lard, cream, fatty meats, and full-fat dairy products (Li et al., 2019). In the digestive system, dietary cholesterol (mostly in its free (non-esterified) form) is incorporated into bile salt micelles and delivered to the brush

border of intestinal enterocytes for absorption. Once absorbed, the body tightly regulates cholesterol levels through homeostatic mechanisms involving feedback inhibition of endogenous synthesis and modulation of intestinal uptake. This compensatory response explains why most individuals maintain stable cholesterol levels despite variations in dietary intake. Historically, dietary guidelines in the United States strongly recommended restricting cholesterol intake to no more than 300 mg per day, based on the assumption that high dietary cholesterol would directly elevate serum low-density lipoprotein cholesterol (LDL-C), thereby increasing cardiovascular risk. These recommendations were endorsed by authoritative bodies such as the American Heart Association (AHA) and the American College of Cardiology (ACC). However, growing scientific evidence has shown that the relationship between dietary cholesterol and blood cholesterol levels is more complex and varies significantly between individuals. As highlighted by DiMarco & Fernandez, (2019), while a small subgroup of people—known as hyper-responders—may exhibit greater sensitivity to dietary cholesterol, the vast majority experience negligible effects due to the aforementioned regulatory mechanisms. Despite cholesterol's indispensable physiological roles, dysregulation of its metabolism can lead to severe health outcomes. Elevated cholesterol levels, particularly in LDL form, are associated with an increased risk of atherosclerosis, coronary heart disease, gallstones, type 2 diabetes, non-alcoholic fatty liver disease (NAFLD), certain cancers, and neurodegenerative disorders (Dai et al., 2021; Mortensen & Nordestgaard, 2020; Silbernagel et al., 2013). As a result, the development of safe and effective strategies to control cholesterol levels remains a major focus of current biomedical and nutritional research.

1.2.2. Phytosterols

Phytosterols, also known as plant sterols, are plant-derived compounds that are structurally similar to cholesterol found in animals with 28 or 29-carbon atoms and a double bond in the C5-C6 position. They are composed of a steroid nucleus with a hydroxyl group attached to the 3-carbon of the A-sing

and an alkyl side chain at the 17-carbon position. With respect to cholesterol, phytosterols contain an extra methyl group, or double bond with a side chain of 9-10 carbon atoms in length, instead of a C8 cholesterol side chain (Figure 1.1).

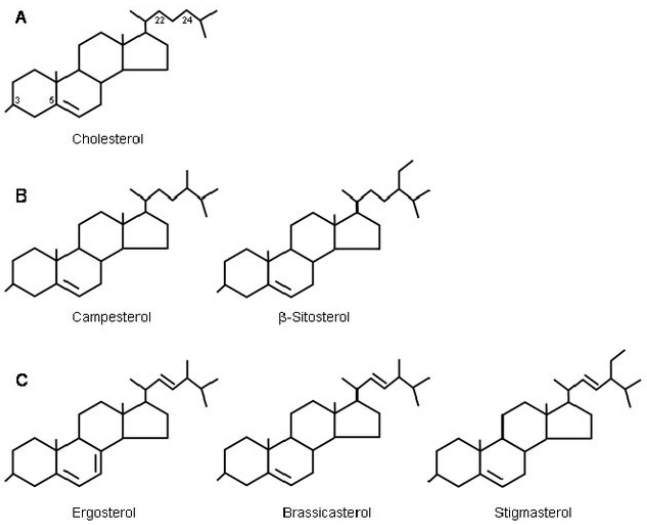

Figure 1.1. Chemical structures of cholesterol and the main phytosterols. From (Calpe-Berdel et al., 2010)

Phytosterols are mostly found in the endoplasmic reticulum and mitochondrial outer membranes and play essential roles in maintaining cell membrane structure and fluidity in plants. They also serve as precursors for various plant hormones, contributing to growth and development process (Kilvington et al., 2020). Phytosterols can promote a variety of bioactive features in the human body, as anticancer effects and attenuating central nervous system (CNS) disorder, but the one of the most well-known benefits of phytosterols is their ability to reduce cholesterol absorption in the intestines (Shen et al., 2024). This property has led to their use in cholesterol-lowering and reducing the level of low-density lipoprotein (LDL) in bloodstream strategies, potentially contributing to improved cardiovascular health. This reduction may be mediated by some mechanisms (Figure 2). After passing through the gastrointestinal tract, phytosterols, by specific enzymes able to break down all ester bonds, are released in their free form. Due to their greater hydrophobicity, phytosterols have a higher affinity for the bile salt micelles than cholesterol, competing for space. As a result, they displace cholesterol, reducing its incorporation into micelles and thereby limiting its absorption while promoting its

excretion. This displacement in mixed micelles within the intestinal lumen is the primary mechanism by which phytosterols contribute to lowering cholesterol level. In addition, authors proposed other mechanisms including 1) the modification in the expression of genes that encode the proteins (Niemann-Pick C1-like 1; NPC1L1) that move cholesterol into enterocytes in one direction, promoting the efflux of cholesterol to the intestinal lumen; 2) trans-intestinal cholesterol efflux (TICE) theory that refers to the excretion of endogenous cholesterol from the intestinal epithelium into the intestinal lumen via ABCG5/8; and 3) decreases the activity of microsomal triglyceride transport protein (MTP, which helps package these cholesterol esters into newly formed chylomicrons, which transport fats into circulation) and acyltransferase-2 (ACAT-2) that converts free cholesterol into esterified stored form. The free form is then pump out of enterocytes (through ABCG5/8) and back to intestine for excretion. However, only the micellar theory has gained experimental support by literature (Cabral et al., 2017; Dumolt & Rideout, 2018; Xiang Li et al., 2022).

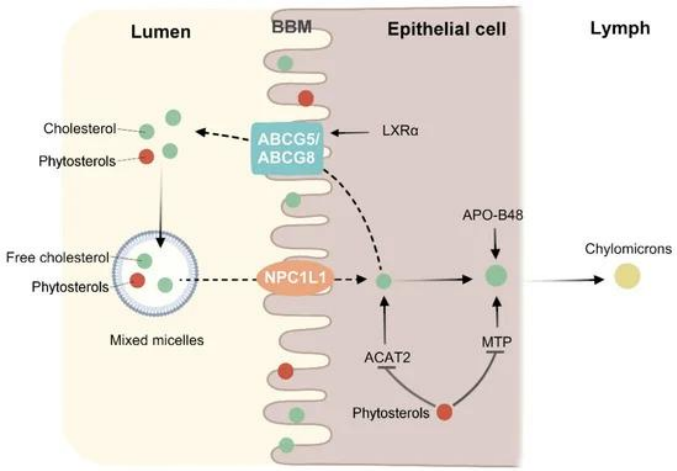

Figure 1.2. Cholesterol lowering mechanism of phytosterols. From Li et al. 2022

1.2.2.1 Phytosterols in food system

Phytosterols are naturally found in various plant-based foods, with vegetable oils being the richest sources. Among them, corn oil contains approximately 909 mg/100 mL, followed by sunflower (411 mg/100 mL), soybean (320 mg/100 mL), and olive oil (300 mg/100 mL) (Cabral et al., 2017). More than 250 phytosterols have been identified, but the most found in the diet are β-sitosterol, campesterol, and stigmasterol. In addition to these, saturated forms of phytosterols, known as plant stanols (such as β-sitostanol and campestanol), are also present in lower concentrations. Over the past two decades, more than 200 clinical trials have confirmed the efficacy, effectiveness, and safety of phytosterols in treating hypercholesterolemia (AbuMweis et al., 2014). A daily intake of 2-4 g of phytosterols is required to achieve an LDL-cholesterol reduction of approximately 10% (Cabral et al., 2017). However, a typical western diet provides only about 300 mg of phytosterols and 30 mg of plant stanols per day, while vegetarian diets contain slightly higher amounts, ranging from 300 to 500 mg/day—still insufficient to produce a significant cholesterol-lowering effect (Cabral & Klein, 2017; Poli et al., 2021). To bridge this gap, functional foods enriched with phytosterols have been developed, commonly including as esterified to improve their solubility and dispersibility within food matrices, such as margarines, dairy products, and beverages. However, due to their high hydrophobicity, phytosterols are challenging to incorporate into many food and beverage systems. Their poor water solubility at room temperature makes it difficult to achieve a uniform dispersion in aqueous-based matrices. To address this issue, emulsion-based systems are commonly used to enhance their water dispersibility, chemical stability, bioavailability, and integration into food matrices. Despite these strategies, incorporating phytosterols into emulsified systems presents several technological challenges, particularly in terms of stability at the oil-in-water interface, which can compromise both their functionality and safety (Zhang et al., 2022). Due to their amphiphilic nature, phytosterols contain both hydrophilic and hydrophobic regions, allowing them to migrate and accumulate at the interface region in emulsion droplet, makes them highly susceptible to oxidative

reactions (Cercaci et al., 2007). In fact, the emulsion interface droplet represents the site where lipids, oxygen, and pro-oxidant agent interact, creating an environment favourable to oxidation, leading to a faster lipid degradation compared to bulk oils. Among the key pro-oxidant agents, transition metals such as iron (Fe) and copper (Cu) are significant catalysts of oxidation, significantly accelerating oxidative degradation and further compromising the stability of the system (Figure 1.3).

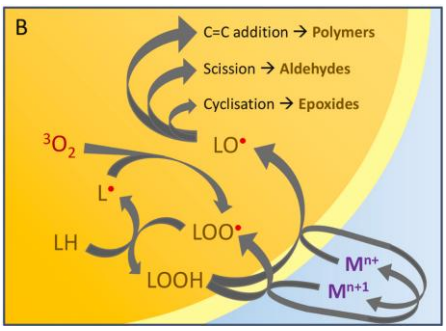

Figure 1.3. Main chemical pathways of lipid oxidation at the interface in O/W emulsion. From Hennebelle et al. (2024)

Specifically, these metals not only contribute to the initiation of oxidation but also act as catalysts in the breakdown of lipid hydroperoxides, leading to the formation of highly reactive peroxyl (LOO•) and alkoxyl (LO•) radicals, pathways that will discuss in the next paragraph. This process occurs through redox cycling, where ferric ions (Fe^{3+}, Mn^{+1}) or ferrous ions (Fe^{2+}, Mn) react with hydroperoxides, accelerating oxidative degradation.

Given these oxidation-related challenges, there is an increasing need to reassess current approaches to oxidative stabilization. In this context, significant attention has been directed toward the development of functional foods enriched with phytosterols, as they contain substantially higher sterol levels than conventional foods. However, this enrichment also leads to a notable rise in sterol oxidation products (oxysterols) formation, with concentrations increasing up to three to five times compared to non-enriched alternatives. (Conchillo et al., 2005). Given the above-mentioned harmful effects in human cell lines, their formation should be minimized. Thus, emerging trends focus on

natural antioxidants sources derived from plant extracts, agri-food by-products and plant-based emulsifiers as potential oxidation inhibitors.

1.3 Sterol Oxidation Products (SOPs)

Sterols, including cholesterol and phytosterols, are highly susceptible to oxidation, leading to the formation of Cholesterol Oxidation Products (COPs) and Phytosterol Oxidation Products (POPs), respectively. Some of these compounds have been shown to exert harmful effects, including atherosclerosis, cytotoxicity, and mutagenesis (Fuhrmann et al., 2018; Valenzuela et al., 2004; Vigne & Pot, 2024). The presence of polar Sterol Oxidation Products (SOPs) has been widely documented across a broad range of foods (Deng et al., 2023; Derewiaka & Obiedziński, 2012; Risso et al., 2022; Scholz, Guth, et al., 2015). The susceptibility of sterols to oxidation is strongly influenced by their chemical structure, particularly the presence of C=C double bonds, which are highly reactive to free radical attacks. Oxidation introduces functional groups such as hydroxyl, carbonyl, epoxy, hydroperoxide, or carboxyl moieties into the fused ring system or side chain of sterols, significantly altering their chemical and biological properties (García-Llatas & Rodríguez-Estrada, 2011; Vigne & Pot, 2024). Cholesterol oxidation can occur through both enzymatic and non-enzymatic pathways. In contrast, phytosterols are less prone to enzymatic oxidation due to structural differences—specifically, the presence of an additional ethyl or methyl group at C24 and/or a double bond at C22—which reduces their interaction with cellular enzymes. As a result, the formation of COPs and POPs in foods is mainly due to auto-oxidation and heat-induced auto-oxidation (also known as thermo-oxidation), in which free radicals attack sensitive sites within the A and B rings of the steroid backbone, initiating a chain mechanism (Zerbinati & Iuliano, 2017) involving the following step as reported in Figure 1.4.

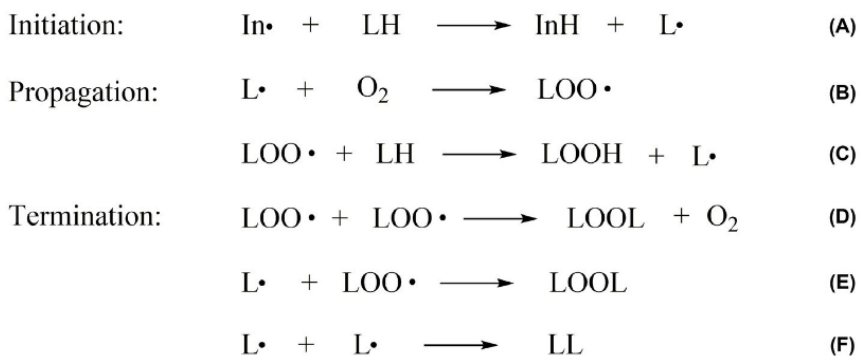

Figure 1.4. The mechanism of lipid auto-oxidation in food. (A) initiation period; (B-C) propagation period of lipid oxidation; (D-F) termination period. In •: free radicals; LH: unsaturated molecules; LOO•: lipid peroxyl radical; L•: lipid free radicals; O_2: Oxygen, LOOH: lipid hydroperoxides; LOOL, LL: lipid polymer. From (Geng et al., 2023).

In cholesterol molecules, oxidation follows two primary pathways (Figure 1.5): C7 oxidation and epoxidation. The initial formation of free radicals predominantly occurs at the C7 and C25 positions, leading to the production of 7α/β-hydroperoxycholesterol (7-OOH) and 25-hydroperoxycholesterol (25-OOH). Among these, the 7-OOH epimers remain stable at room temperature, whereas 25-OOH is typically found in solid, dry cholesterol and, to a lesser extent, in dispersion solutions. When subjected to heat, the 7-OOH epimers undergo reduction, resulting in their respective hydroxyl derivatives: 7α/β-hydroxycholesterol. Epoxide formation, on the other hand, occurs through a bimolecular reaction mechanism. Specifically, the interaction between hydroperoxyl radicals and cholesterol gives rise to 5,6α/β-epoxycholesterol (Lercker & Rodriguez-Estrada, 2002). The formation of oxygenated compounds from sterols and their oxidation products varies depending on the duration and intensity of exposure. Specifically, the dehydration of 7-hydroperoxycholesterol (7-OOH) and the dehydrogenation of 7-hydroxycholesterol (7-OH) results in the production of 7-ketocholesterol (Iuliano, 2011). On the other hand, the acid-catalyzed hydration of epoxides begins with the protonation of the oxygen in the epoxide ring, making it more susceptible to nucleophilic attack. In this case, water acts as the nucleophile, approaching the more substituted carbon from the side opposite to the protonated oxygen. In the case of the α-epoxide, steric hindrance caused by the

angular methyl group at C19 restricts access to the rear side of C5. As a result, nucleophilic attack occurs preferentially at C6 rather than C5, leading to the formation of triol form.

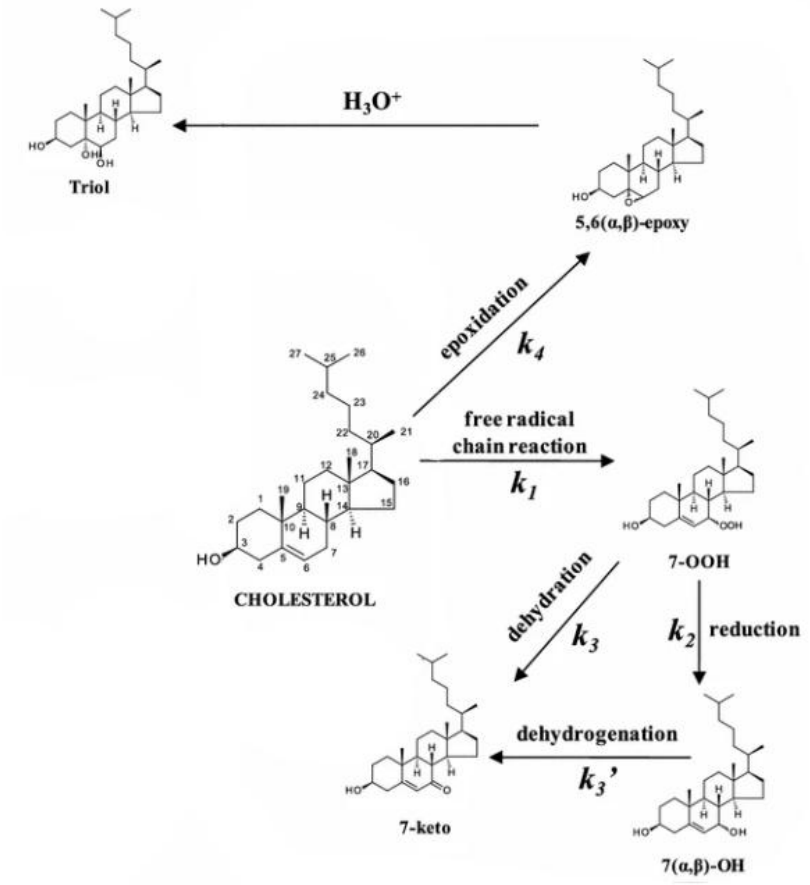

Figure 1.5. The formation pathways of some COPs during thermos-oxidation. Modified from Chien et al., (1998)

1.3.1. Biological effect

Due to the introduction of polar functional groups, oxysterols exhibit greater water solubility than their non-oxidized isomers, allowing them to diffuse more readily between lipid membranes. This increased mobility enables interactions with cellular proteins and receptors, influencing gene expression, enzymatic activity, and cell signaling pathways. Consequently, oxysterols have been implicated in inflammatory responses, apoptosis, and cellular differentiation. While the biological effects of COPs are well documented (Chalubinski et al., 2013; Deiana et al., 2017; Mascia et al., 2010; Rossin et al., 2017), the impact of dietary POPs remains debated. Some studies reported

negative effects similar to those of COPs, including proatherogenic and inflammatory properties, while others suggest potential benefits associated with the consumption of oxidized phytosterols (Gachumi et al., 2021; O'Callaghan et al., 2014). Researches on the presence of POPs in food has primarily focused on vegetable oils, where they occur naturally, and on the effects of heat processing on oxidation rates (Bonciolini et al., 2024). However, data on POP levels in phytosterol-enriched foods remain limited due to variations in fortification methods (free vs. esterified phytosterols) and processing conditions (heat treatment, storage duration, and exposure to oxygen). Estimates of daily POP intake vary depending on food type and processing. In non-heated products (e.g., spreads, milk), intake ranges from 1.2 to 2.9 mg/day. Upon heat exposure, the POPs levels could increase to 3.5–4.2 mg/day for milk and up to 29.6 mg/day for cooking and baking spreads (Scholz, Guth, et al., 2015). In 2020, the EFSA evaluated the safety of extending the use of phytosterol esters as a novel food (Regulation EU 2015/2283 (Turck et al., 2020)). In this assessment, a maximum authorized intake of 3 g of phytosterol per person per day was considered, with oxidation rates of 0.5% and 2.28%. Under those conditions, the estimated daily intake of POPs for a 70 Kg adult would be 0.21 and 0.98 mg/Kg of body weight per day, respectively, highlighting the importance of their monitoring.

1.3.2 Analytical method

The analysis of oxidized phytosterols (POPs) presents significant challenges due to the lack of a commonly validated analytical method. This absence makes it impossible to directly compare studies in the literature, leading to substantial variability in reported data and undermining their reliability. In addition, the scarce availability of POPs commercial standards to be used as reference material, except for 7-ketositosterol, make arduous a robust and reproducible determination. In light of this shortage, many studies have based their quantifications on calibration curves build using commercial cholesterol oxidation products assuming a similar analytical behavior. However, as doubts have emerged regarding the validity of this assumption, more recent research has focused on the

purification or synthesis of POPs to enable more accurate quantification (Calaminici et al., 2024; Scholz, Wocheslander, et al., 2015). The situation is further deepen by the lack of standardized instrumental approaches, since researchers employed gas chromatography (GC) (Grandgirard et al., 2004; Menéndez-carreño & Steenbergen, 2023), liquid chromatography (LC) (Calaminici et al., 2024; Foley et al., 2010; Poudel et al., 2022; Scholz, Wocheslander, et al., 2015), and different mass spectrometry approach in an inconsistent and often arbitrary manner. This methodological inconsistency not only compromises data comparability but also poses a serious risk to consumer health, as inaccurate assessments of oxidized phytosterols could lead to misjudgments regarding their dietary exposure and potential biological effects.

1.4 Antioxidants

One of the most effective and widely adopted strategies to control and delay lipid oxidation in food systems is the use of antioxidants. Antioxidants are defined as compounds that, even at low concentrations relative to an oxidizable substrate, significantly delay or prevent its oxidation, extending shelf-life and preserve the sensory and nutritional quality of lipid-rich products (Shahidi & Zhong, 2010). Depending on their origin, antioxidants are generally categorized into synthetic and natural. Synthetic antioxidants, such as butylated hydroxytoluene (BHT), butylated hydroxyanisole (BHA), tert-butylhydroquinone (TBHQ), ethylenediaminetetraacetic acid (EDTA), and gallates, are industrially synthesized with optimized structures to maximize stability and activity. On the other hand, natural antioxidants are typically secondary metabolites found in plants, fungi, and microorganisms, and include phenolic compounds, carotenoids, tocopherols, ascorbic acid.

Antioxidants act via several mechanisms, but the most relevant in the context of lipid oxidation include free radical scavenging, metal chelation, and singlet oxygen quenching (Choe & Min, 2009):

i) Free radical scavengers inhibit the propagation phase of oxidation by donating a hydrogen atom to lipid radicals, forming more stable radical species. Phenolic

antioxidants are particularly effective due to their low bond dissociation energy and the resonance stabilization of the resulting phenoxyl radicals. This makes them fast enough to outcompete lipid substrates in reacting with radicals.

ii) Metal chelators inhibit oxidation by binding prooxidant transition metals (e.g., Fe^{2+}, Cu^{2+}), which would otherwise catalyze the decomposition of lipid hydroperoxides. However, improper use of metal chelators can also induce prooxidant activity if they solubilize redox-active metals or alter their oxidation states (Frankel, 2005).

iii) Singlet oxygen quenchers operate either chemically, by reacting directly with singlet oxygen to form non-radical products, or physically, by transferring energy from singlet oxygen to the antioxidant, converting it into harmless triplet oxygen.

Among the various strategies employed to control lipid oxidation, the use of antioxidants remains the most effective, practical, and economically viable approach. Their application is widespread in the food industry, where they are employed to preserve the quality, nutritional value, and sensory attributes of lipid-rich products

Antioxidants can be broadly categorized based on their mechanism of action into two main types: preventive antioxidants and chain-breaking antioxidants. Preventive antioxidants act by inhibiting the formation of reactive oxygen species (ROS) or by directly scavenging initiators of oxidation, such as superoxide anions ($O_2^{\bullet -}$) and singlet oxygen ($^1O_2$). By doing so, they block the initiation phase of lipid oxidation. On the other hand, chain-breaking antioxidants act during the propagation phase of oxidation. These molecules neutralize peroxyl and alkoxyl radicals, thereby interrupting the radical chain reaction that leads to the formation of harmful oxidation products. In addition to direct radical scavenging, chain-breaking antioxidants can exert their effects indirectly by chelating prooxidant transition metals (e.g., Fe^{2+}, Cu^{2+}), or by deactivating singlet oxygen, further preventing lipid peroxidation cascades. Together, these two classes of antioxidants offer complementary protective

mechanisms and are often used in combination to enhance oxidative stability in complex food systems.

1.5 Tannins

The term “tannin” indicates a plant material which allows the transformation of hide into leather. Throughout the history a lot of definition and application was attribute to tannins: from the 1800 in which tannins were comparable to gallic acid, mixture of green colouring compound and other molecules to 1891 in which tannins were defined as the whole class of astringent substances. Nowadays, the common definition of tannin is the one given in 1962, i.e., tannins are water-soluble phenolic compounds with molecular weights between 500 and 3000 Dalton and up to 20 hydroxyl groups (Arbenz & Avérous, 2015). They are widely distributed in plants, food, and beverages, naturally occurring in leaves, seeds, bark, fruits, and vegetables. In vascular plants, tannins represent the fourth most abundant group of compounds after cellulose, hemicellulose, and lignin, accounting for up to 20% of the plant’s dry weight, though this amount can vary in response to environmental conditions (Adamczyk et al., 2017; Pizzi, 2019). Although they are secondary metabolites and do not play a direct role in plant growth and development, tannins are crucial in plant-environment interactions. Their primary function is defense against herbivores and pathogens, relying on their ability to irreversibly bind protein compounds, forming complexes that inhibit enzymatic activity (Pizzi, 2019). This phenomenon also occurs in the human body, where tannins bind to the —NH groups of peptides and proteins, preventing their hydrolysis and digestion in the stomach, making them known as antinutritional compounds (Smeriglio et al., 2017). Tannins are broadly classified into two main groups: hydrolysable tannins and condensed tannins. Hydrolysable tannins are further divided into gallotannins, which release sugar and gallic acid upon hydrolysis, and ellagitannins, which yield sugar, gallic acid, and ellagic acid. These compounds are susceptible to hydrolysis by weak acids and decompose at high temperatures, potentially forming toxic compounds such as

pyrogallol. Condensed tannins, also known as proanthocyanidins or catechin tannins, are more structurally complex and not yet fully characterized. They are the most abundant plant-derived polyphenols, consisting of oligomers of flavan-3-ol (catechin monomers) and/or flavan-3,4-diol, typically linked by C-C (4-8 or 6-8) and occasionally by C-O-C bonds, resulting in significant structural diversity. Unlike hydrolysable tannins, condensed tannins are not readily hydrolyzed; instead, they degrade in acidic alcoholic conditions, forming red pigments known as phlobaphenes.

1.5.1 Classification

Many tannins can undergo hydrolysis when treated with hot water or tannases, breaking down into monomeric products. This characteristic place them under the category of hydrolysable tannins. In contrast, those that do not hydrolase and are composed of oligomeric and polymeric proanthocyanidins fall into the group of "condensed tannins". However, this binary classification does not fully capture the structural diversity of tannins.

1.5.1.1 Hydrolysable tannins

Hydrolysable tannins are present in lower quantities compared to the total tannin content in biological matters. Their availability is relatively limited, with a global production accounting for less than 10% of the total commercial tannin market. Due to their scarcity and relatively high cost, they are considered less attractive than condensed tannins. These tannins share a common structural feature: a central carbohydrate core, typically D-glucose, whose hydroxyl groups are partially or fully esterified with gallic acid, ellagic acid, or digallic acid (Arbenz & Avérous, 2015; Pizzi, 2019). Based on their chemical structure, hydrolysable tannins can be further classified according to the reaction products obtained through hydrolysis (Table 1.1):

i. Gallotannins, consisting of a polyphenolic and a polyol residue. They are defined as tannins in which galloyl units or their meta-depsidic derivatives are attached to various polyol,

catechin, or triterpenoid units. Although a wide range of polyol residues can be found, the majority of gallotannins isolated from plants contain a polyol core derived from a saccharide, most commonly *d*-glucose. The hydroxyl (-OH) groups of the polyol residue may be partially or fully substituted by galloyl units. In the cases of partial substitution, the remaining hydroxyl groups may either remain unmodified or be replaced by other functional groups.

ii. Ellagitannins, constituted from gallotannins by at least two galloyl units which are C–C linked to each other, leading to the axially chiral monomer hexahydroxydiphenoyl (HHDP) unit, and they do not contain a glycosidically linked catechin unit (Lamy et al., 2016). This HHDP unit is then ester-linked to some sugar, typically glucose. The carbon positions involved in this reaction are generally C3-C6, C2-C4, or C1-C6 (Chávez González et al., 2017; Smeriglio et al., 2017).

1.5.1.2 Condensed tannins

Condensed tannins are the most abundant class of naturally occurring tannins, accounting for nearly 90% of global tannin production. In nature, they are often found complexed with proteins, a characteristic influenced by their chemical structure and affinity for these macromolecules. To be classified as condensed tannins, these compounds must consist of oligomeric structures composed of three to eight repeating units, derived from flavan-3-ols (such as catechin) or flavan-3,4-diols (leucoanthocyanidins). Each flavonoid unit contains two distinct phenolic rings (A and B), which differ in reactivity and structural configuration (Figure 1.6). The structure of monoflavonoid in figure 1.4.3 shows that it is possible to have two configurations for each ring: with or without OH in position 5 and 5'. These various configurations generate four possibilities and corresponding basic building blocks from condensed tannins.

Table 1.1. Structure of tannins. From Arbenz & Avérous, (2015)

Type of tannins		**Examples of structures**
Hydrolysable tannins	Gallotannins	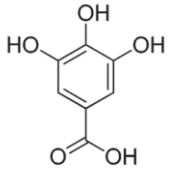 gallic acid 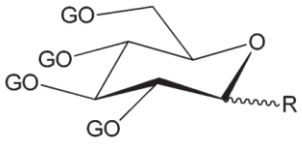 R = α,β-OH (1) TGG R = β-OG (2) β–PGG 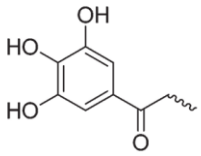 G = Galloyl unit
	Ellagitannins	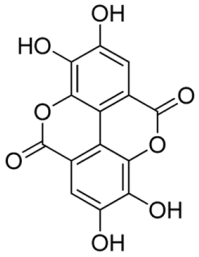 ellagic acid 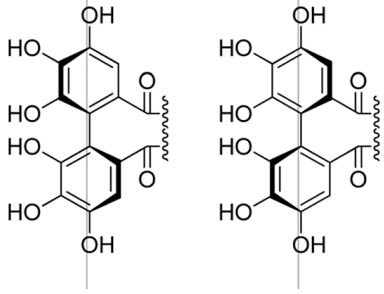 biaryl axis biaryl axis (3) HHDP
Condensed tannins		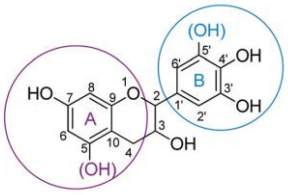 Structure of monoflavanoid

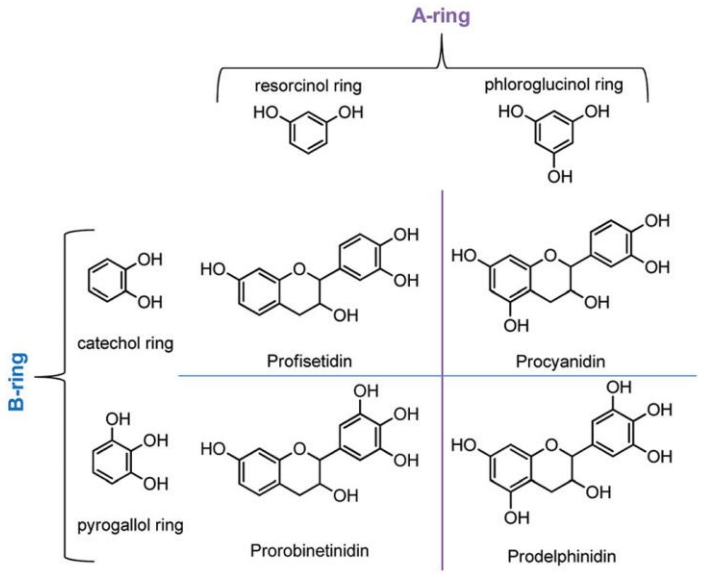

Figure 1.6. Structure of the four monoflavonoid building blocks. Modified from Arbenz & Avérous, (2015)

While monomeric catechins and leucoanthocyanidins do not exhibit tanning properties on their own, they can be transformed into oligomeric and polymeric structures with tanning capabilities through enzymatic or acidic reactions. The way flavonoid units are linked together depends on the nature of the rings. In all oligomeric and polymeric proanthocyanidins, the linkage occurs between the C4 position of one unit and either the C6 or C8 position of the next. The C4-C6 bond is more commonly found in tannins primarily composed of profisetidins and prorobinetidins, whereas the C4-C8 bond is predominant in procyanidins and prodelphinidins. The degree of polymerization (DP) varies significantly, ranging from as few as two to more than fifty flavonoid units. Oligomers and polymers containing two to ten catechin units are often referred to as flavolans. In addition to their size, condensed tannins also exhibit a considerable diversity in the way catechin units are linked together, resulting in different structural patterns (Arbenz & Avérous, 2015; Sieniawska & Baj, 2017).

1.5.2 Sources

Throughout history, numerous plant species have been identified and utilized as significant sources of tannins, both for large-scale industrial applications and traditional uses. Among the primary

industrial sources several tree species were considered. Notably, *Schinopsis balansae* Engl. and *Schinopsis lorentzii* (Griseb.) Engl. (quebracho) are valued for their exceptionally hard wood, which can contain up to 20% tannins by weight. *Castanea sativa* Mill. (chestnut) has long been used in Europe not only for its edible fruits but also for its durable wood and high tannin content. *Acacia mearnsii* De Wild. (black wattle or mimosa) is another major industrial source, with bark tannin levels ranging from 30% to 45%. *Caesalpinia spinosa* (Molina) Kuntze (tara), a South American shrub, produces tannin-rich pods with a concentrations range between 35-55%. Additionally, galls formed on oaks (*Quercus infectoria* Oliv.) and *Rhus chinensis* Mill. in response to insect activity are among the most concentrated sources, containing 50% to 75% tannins. In the following table (Table 1.2) are reported the major sources of tannins.

Table 1.2. Main source of tannins and respectively molecules extract

Source	Category	Main tannic compounds	*Reference*
Black mimosa bark (*Acacia mearnsii* De Wild)	Condensed 1-2% hydrolysable tannin	Prorobinetinidin	*(Missio et al., 2017)*
Quebracho wood (*Schinopsis balansae* Engl. or *lorentzii* (Griseb.) Engl.)	Condensed tannin	Profisetinidin	*(Moccia et al., 2020)*
Oak bark (*Quercus* spp.)	Hydrolysable and Condensed	Ellagitannin, Gallotannin, Catechin	*(Ştefănescu et al., 2022)*
Chestnut wood (*Castanea sativa* Mill.)	Hydrolysable	Tannic acid, vescalagin, castalagin	*(Khatib et al., 2023)*
Gallnut	Hydrolysable	Gallotannin	*(Tian et al., 2009)*
Tara (*Caesalpinia spinosa* (Molina) Kuntze)	Hydrolysable	Gallic Acid	*(Aguilar-Galvez et al., 2014)*

On a more traditional level, tannins are also found in various fruits (e.g., apples, blueberries, persimmons, gooseberries), leaves (e.g., bay, blackberry, raspberry, nettle), seeds and nuts (e.g., acorns, beechnuts, hazelnuts, walnuts), and spices (e.g., cinnamon, clove).

1.5.2.1 Quebracho

The term *quebracho* generally refers to species within the *Schinopsis* genus (*Schinopsis lorentzii* (Griseb.) Engl, and *Schinopsis balansae* Engl..), members of the Anacardiaceae family, which are distinguished by their dense, reddish hardwood. This classification differentiates them from *Aspidosperma quebracho*-blanco Schltdl (white quebracho), which belongs to the Apocynaceae family. In industrial contexts, *quebracho* typically denotes the *Schinopsis* species (Venter et al., 2012), which are native to the Chaco forest, covering regions of northern Argentina and eastern Paraguay. Quebracho wood is highly appreciated not only for its mechanical strength, long utilized in construction, but also for its high tannin content. Tannin concentrations range from 15–21% in *S. lorentzii* (Griseb.) Enlg. and 20–21% in *S. balansae* Engl. and may reach up to 30% in the heartwood. The tannins extracted from quebracho wood belong to the condensed tannin category, primarily composed of profisetinidins. These tannins are predominantly built from resorcinol, catechol, and pyrogallol units. Other compounds identified in quebracho heartwood include catechin, and gallic acid, all contributing to its chemical complexity and functional properties.

1.5.2.2 Chestnut

Sweet chestnut (*Castanea sativa* M., Fagaceae) is the dominant species of chestnut tree in central Europe. While its primary use is for timber production, it also holds significant economic value in the food and feed industries. One of the key components that enhances the chestnut's value is the presence of various phytocomplexes, particularly tannins, which offer a broad spectrum of potential applications. The tannins content in the spray-dried extract is approximately 75% with about 89% of this comprised of hydrolysable tannins, including both gallotannins and ellagitannins. The dominant

ellagitannins in chestnut are castalagin (53%), vescalagin (35%), castalin (3%), and vescalin (8%). Other bioactive compounds found in chestnut include acutissim A, kurigalin, and chestanin (Caprarulo et al., 2021).

1.5.3 Properties of tannins

Tannins are effective antioxidants due to their benzene ring skeleton and phenolic hydroxyl groups, which can readily stabilize free radical intermediates by harboring singlet electrons. Their direct antioxidant action consists of maintaining balance through rapid redox reactions between pro-oxidant molecules and tannins themselves. Tannins primarily act through hydrogen atom transfer, neutralizing free radicals and preventing oxidative damage. However, the exact mechanism of tannins' antioxidant activity remains unclear. The ability to scavenge free radicals depends on the number and degree of polymerization of hydroxyl groups (Tong et al., 2022) with specific phenolic hydroxyl groups playing a crucial role in their antioxidant efficacy (Wang et al., 2022). However, their effectiveness can vary significantly based on several factors, such as the extraction method and the presence of other compounds. Notably, antioxidant activity does not always correlate with total phenolic content (Nguyen et al., 2023) but rather depends on the molecular composition and type of tannins. Research demonstrated that hydrolysable tannins, such as those found in pomegranates, are particularly effective in this role. In fact, since many chronic diseases, including cardiovascular conditions and diabetes involve oxidative stress, the use of appropriate antioxidants could be crucial to counteract the inflammation processes (Omar et al., 2022; Smeriglio et al., 2017). For instance, a previous study (Bonciolini et al., 2023) showed that hydrolysable tannins (esters of gallic acid) increased radical scavenging activity in fresh egg pasta and reduced the formation of cholesterol oxidation products.

Beyond their direct antioxidant capacity, a significant portion of tannins' antioxidant activity is due to their indirect action. These bioactive molecules can also act as preventive antioxidants by acting

as co-antioxidant agents or inhibitors of oxidation catalysts, thereby helping to maintain the appropriate antioxidant/pro-oxidant balance. In this context, tannins exert their antioxidant effects through their ability to form complexes with other molecules, such as metals or proteins (Molino et al., 2023). The high content of hydroxyl and carboxyl functional groups, allow tannins to bind metal ions effectively. Thus, ability to form stable complexes with metal ions, such as iron (Fe^{2+}), copper (Cu^{2+}), and zinc (Zn^{2+}), plays a crucial role in various biological and technological applications. The chelating properties of tannins contribute to their antioxidant activity by reducing the availability of transition metals that catalyze oxidative reactions, thereby preventing the formation of reactive oxygen species (ROS). This mechanism is particularly important in mitigating oxidative stress, which is implicated in both aging and several chronic diseases (including neurodegenerative and cardiovascular disorders) and food quality preservative by inhibiting lipid oxidation. However, while metal chelation is beneficial in many contexts, excessive chelation of essential minerals in the human diet could interfere with nutrient absorption, contributing to the antinutritional properties of tannins. That dual role highlights the complexity of tannins and the importance of their controlled application in nutrition and health sciences.

1.5.4 Interaction activity

Tannins are distinguished by their remarkable ability to interact with a wide range of molecules, a characteristic so fundamental that it plays a key role in their very definition. Historically, their application in leather tanning became widespread long before the molecular mechanisms behind this process were understood. Over time, tannins have been recognized for their capacity to bind and precipitate proteins, alkaloids, and metals, a property that has led to their use across various industries, including food technology, leather processing, and pharmaceuticals.

In the fields of nutrition and food science, studies on tannins have largely focused on their interactions with proteins and metals, particularly due to their antinutritional effects. However, like other

polyphenols, tannins engage with a broader spectrum of molecules, revealing potential applications in nutraceuticals and food stabilization. One of the most well-known associations with tannins is their contribution to astringency in foods such as red wine. The latter arises from their strong affinity for salivary proteins, especially proline-rich proteins, forming complexes that can be either soluble or precipitate depending on the structural characteristics of both the tannin and the protein (Sarni-Manchado et al., 2008; Watrelot et al., 2017). The polyphenolic structure of tannins is central to their molecular interactions. The high abundance of hydroxyl (-OH) groups on their aromatic rings enables them to form strong hydrogen bonds with other molecules, particularly polar compounds such as proteins and the polar heads of phospholipids. These tannin-biomolecule complexes can remain soluble or become insoluble depending on factors such as concentration, molecular size, and environmental pH. Their interactions are primarily stabilized by non-covalent forces, including hydrogen bonding and hydrophobic interactions (Adamczyk et al., 2017).

However, the vast structural diversity of tannins in nature presents a challenge in predicting specific interaction mechanisms. For instance, Stern et al. (1996) reported that in oxidative conditions, phlorotannins can undergo oxidation themselves, leading to covalent binding with proteins—a phenomenon not observed in other tannin classes such as procyanidins, profisetinidins, and gallotannins. Moreover, tannins are widely recognized for their inhibitory effects on enzymes, an attribute that has contributed to their classification as antinutritional factors. For instance, condensed tannins have been shown to inhibit pancreatic lipase, a key enzyme in triglyceride hydrolysis and absorption, which, despite its inhibitory nature, results in a reduction of plasma triglyceride levels (Xiangxin Li et al., 2019).

1.5.4.1 Lipid interaction

Tannins are amphiphilic molecules, composed of hydrophobic aromatic rings surrounded by hydroxyl groups, a structural arrangement that enables effective interaction with lipids. That dual nature—both

hydrophilic and hydrophobic—is fundamental to their ability to associate with polar and non-polar regions of lipid molecules (Dufourc, 2024). Among condensed tannins, catechins represent a particularly noteworthy subgroup due to their strong complexing activity. These flavonoid compounds contain hydroxyl groups on both A and B rings, while certain derivatives—such as epigallocatechin gallate (EGCG) and epicatechin gallate (ECG)—also feature a galloyl moiety. That structural component provides specific binding sites that allow for selective interactions with lipid components, facilitating the formation of stable complexes (Sirk et al., 2008). However, it might be highlighted that *in vitro* and *in vivo* studies have demonstrated that catechins obtained from green tea (especially EGCG) can interfere with key processes involved in lipid digestion and absorption. Specifically, they have been shown to disrupt emulsification, enzymatic digestion, and micellar solubilization of lipids—critical steps for the intestinal uptake of triglycerides, cholesterol, and other dietary lipids (Koo & Noh, 2007).

References

AbuMweis, S. S., Marinangeli, C. P. F., Frohlich, J., & Jones, P. J. H. (2014). Implementing Phytosterols Into Medical Practice as a Cholesterol-Lowering Strategy: Overview of Efficacy, Effectiveness, and Safety. Canadian Journal of Cardiology, 30(10), 1225–1232.https://doi.org/10.1016/j.cjca.2014.04.022

Adamczyk, B., Simon, J., Kitunen, V., Adamczyk, S., & Smolander, A. (2017). Tannins and Their Complex Interaction with Different Organic Nitrogen Compounds and Enzymes: Old Paradigms versus Recent Advances. ChemistryOpen, 6(5), 610–614. https://doi.org/10.1002/open.201700113

Aguilar-Galvez, A., Noratto, G., Chambi, F., Debaste, F., & Campos, D. (2014). Potential of tara (Caesalpinia spinosa) gallotannins and hydrolysates as natural antibacterial compounds. Food Chemistry, 156, 301–304. https://doi.org/10.1016/j.foodchem.2014.01.110

Arbenz, A., & Avérous, L. (2015). Chemical modification of tannins to elaborate aromatic biobased macromolecular architectures. Green Chemistry, 17(5), 2626–2646. https://doi.org/10.1039/c5gc00282f

Bonciolini, A., Cantele, C., Piochi, M., Di Lecce, G., Risso, D., & Cardenia, V. (2024). New insights on phytocannabinoids role in antioxidant activity of hemp inflorescences extract in high-oleic sunflower oil. LWT, 194(January), 115807. https://doi.org/10.1016/j.lwt.2024.115807

Bonciolini, A., Cantele, C., Salgarella, N. I., Zeppa, G., Bertolino, M., & Cardenia, V. (2023). Effect of Tannins on Cholesterol Content and Its Oxidation in Egg Pasta as Related to Different Pasta Shapes. Food and Bioprocess Technology, 16(7), 1541–1554. https://doi.org/10.1007/s11947-023-03016-1

Cabral, C. E., & Klein, M. R. S. T. (2017). Phytosterols in the Treatment of Hypercholesterolemia and Prevention of Cardiovascular Diseases. Arquivos Brasileiros de Cardiologia. https://doi.org/10.5935/abc.20170158

Cabral, C. E., Regina, M., & Torres, S. (2017). Review Article Phytosterols in the Treatment of Hypercholesterolemia and Prevention of Cardiovascular Diseases. 475–482. https://doi.org/10.5935/abc.20170158

Calaminici, R., Salgarella, N. I., Cardenia, V., & Forte, E. (2024). Optimization and validation of an HPLC-HRMS method through semipreparative HPLC system for determining phytosterol oxidation products during refining processing and storage of vegetable oils. Journal of the American Oil Chemists' Society, 101(8), 735–751. https://doi.org/10.1002/aocs.12826

Calpe-Berdel, L., Méndez-Gonzàlez, J., Llaverias, G., Escolà-Gil, J. C., & Blanco-Vaca, F. (2010). Plant sterols, cholesterol metabolism and related disorders. In L. Avigliano & L. Rossi (Eds.), Biochemical Aspects of Human Nutrition (pp. 223–242). Transworld Research Network.

Caprarulo, V., Giromini, C., & Rossi, L. (2021). Review: Chestnut and quebracho tannins in pig nutrition: the effects on performance and intestinal health. Animal, 15(1), 100064. https://doi.org/10.1016/j.animal.2020.100064

Cercaci, L., Rodriguez-Estrada, M. T., Lercker, G., & Decker, E. A. (2007). Phytosterol oxidation in oil-in-water emulsions and bulk oil. Food Chemistry, 102(1), 161–167. https://doi.org/10.1016/j.foodchem.2006.05.010

Chalubinski, M., Zemanek, K., Skowron, W., Wojdan, K., Gorzelak, P., & Broncel, M. (2013). The effect of 7-ketocholesterol and 25-hydroxycholesterol on the integrity of the human aortic endothelial and intestinal epithelial barriers. Inflammation Research, 62(12), 1015–1023. https://doi.org/10.1007/s00011-013-0660-x

Chávez González, M. L., Buenrostro-Figueroa, J., Rodríguez Durán, L. V., Zárate, P. A., Rodríguez, R., Rodríguez-Jasso, R. M., Ruiz, H. A., & Aguilar, C. N. (2017). Tannases. In Current Developments in Biotechnology and Bioengineering (pp. 471–489). Elsevier. https://doi.org/10.1016/B978-0-444-63662-1.00020-8

Chien, J. T., Wang, H. C., & Chen, B. H. (1998). Kinetic Model of the Cholesterol Oxidation during Heating. Journal of Agricultural and Food Chemistry, 46(7), 2572–2577. https://doi.org/10.1021/jf970788d

Choe, E., & Min, D. B. (2009). Mechanisms of Antioxidants in the Oxidation of Foods. Comprehensive Reviews in Food Science and Food Safety, 8(4), 345–358. https://doi.org/10.1111/j.1541-4337.2009.00085.x

Conchillo, A., Cercaci, L., Ansorena, D., Rodriguez-Estrada, M. T., Lercker, G., & Astiasarán, I. (2005). Levels of Phytosterol Oxides in Enriched and Nonenriched Spreads: Application of a Thin-Layer Chromatography−Gas Chromatography Methodology. Journal of Agricultural and Food Chemistry, 53(20), 7844–7850. https://doi.org/10.1021/jf050539m

Dai, L., Zou, L., Meng, L., Qiang, G., Yan, M., & Zhang, Z. (2021). Cholesterol Metabolism in Neurodegenerative Diseases: Molecular Mechanisms and Therapeutic Targets. Molecular Neurobiology, 58(5), 2183–2201. https://doi.org/10.1007/s12035-020-02232-6

Deiana, M., Calfapietra, S., Incani, A., Atzeri, A., Rossin, D., Loi, R., Sottero, B., Iaia, N., Poli, G., & Biasi, F. (2017). Derangement of intestinal epithelial cell monolayer by dietary cholesterol oxidation products. Free Radical Biology and Medicine, 113, 539–550. https://doi.org/10.1016/j.freeradbiomed.2017.10.390

Deng, C., Li, M., Liu, Y., Yan, C., He, Z., Chen, Z.-Y., & Zhu, H. (2023). Cholesterol Oxidation Products: Potential Adverse Effect and Prevention of Their Production in Foods. Journal of Agricultural and Food Chemistry, 71(48), 18645–18659. https://doi.org/10.1021/acs.jafc.3c05158

Derewiaka, D., & Obiedziński, M. (2012). Phytosterol oxides content in selected thermally processed products. European Food Research and Technology, 234(4), 703–712. https://doi.org/10.1007/s00217-012-1681-3

DiMarco, D. M., & Fernandez, M. L. (2019). Differences in response to egg-derived dietary cholesterol result in distinct lipoprotein profiles while plasma concentrations of carotenoids and choline are not affected in a young healthy population. Journal of Agriculture and Food Research, 1, 100014. https://doi.org/10.1016/j.jafr.2019.100014

Dufourc, E. J. (2024). Wine tannins and their aggregation/release with lipids and proteins: Review and perspectives for neurodegenerative diseases. Biophysical Chemistry, 307(December 2023), 107178. https://doi.org/10.1016/j.bpc.2024.107178

Dumolt, J. H., & Rideout, T. C. (2018). The Lipid-lowering Effects and Associated Mechanisms of Dietary Phytosterol Supplementation. Current Pharmaceutical Design, 23(34). https://doi.org/10.2174/1381612823666170725142337

Ferreira-Guerra, M., Coleto-Alcudia, V., Mora-García, S., & Caño-Delgado, A. I. (2025). The Evolutionary Journey of Sterol Synthesis Pathways in Eukaryotes. Plant And Cell Physiology. https://doi.org/10.1093/pcp/pcaf016

Foley, D., O'Callaghan, Y., O'Brien, N., McCarthy, F., & Maguire, A. (2010). Synthesis and Characterization of Stigmasterol Oxidation Products. 23, 1165–1173. https://doi.org/10.1021/jf9024745

Frankel, E. (2005). Lipid Oxidation (Second Edi).

Fuhrmann, A., Weingärtner, O., Meyer, S., Cremers, B., Seiler-mußler, S., Schött, H., Kerksiek, A., Friedrichs, S., Ulbricht, U., Zawada, A. M., Laufs, U., Scheller, B., Fliser, D., Christian, P., Böhm, M., Heine, G. H., Lütjohann, D., Chemie, K., & Bonn, U. (2018). Plasma levels of the oxyphytosterol 7α-hydroxycampesterol are associated with cardiovascular events. Atherosclerosis, 279(April), 17–22. https://doi.org/10.1016/j.atherosclerosis.2018.10.010

Gachumi, G., Poudel, A., Wasan, K. M., & El-Aneed, A. (2021). Analytical Strategies to Analyze the Oxidation Products of Phytosterols, and Formulation-Based Approaches to Reduce Their Generation. Pharmaceutics, 13(2), 268. https://doi.org/10.3390/pharmaceutics13020268

Gao, Y., Ye, S., Tang, Y., Tong, W., & Sun, S. (2023). Brain cholesterol homeostasis and its association with neurodegenerative diseases. Neurochemistry International, 171, 105635. https://doi.org/10.1016/j.neuint.2023.105635

García-Llatas, G., & Rodríguez-Estrada, M. T. (2011). Current and new insights on phytosterol oxides in plant sterol-enriched food. Chemistry and Physics of Lipids, 164(6), 607–624. https://doi.org/10.1016/j.chemphyslip.2011.06.005

Geng, L., Liu, K., & Zhang, H. (2023). Lipid oxidation in foods and its implications on proteins. Frontiers in Nutrition, 10. https://doi.org/10.3389/fnut.2023.1192199

Gifer, P. K., Popova, M. M., & Batishchev, O. V. (2022). Effect of Sterols on the stability of bilayer lipid membranes. Biophysical Journal, 121(3), 365a-366a. https://doi.org/10.1016/j.bpj.2021.11.914

Grandgirard, A., Martine, L., Joffre, C., Juaneda, P., & Berdeaux, O. (2004). Gas chromatographic separation and mass spectrometric identification of mixtures of oxyphytosterol and oxycholesterol derivatives Application to a phytosterol-enriched food. 1040, 239–250. https://doi.org/10.1016/j.chroma.2004.04.008

Iuliano, L. (2011). Pathways of cholesterol oxidation via non-enzymatic mechanisms. Chemistry and Physics of Lipids, 164(6), 457–468. https://doi.org/10.1016/j.chemphyslip.2011.06.006

Khatib, M., Campo, M., Bellumori, M., Cecchi, L., Vignolini, P., Innocenti, M., & Mulinacci, N. (2023). Tannins from Different Parts of the Chestnut Trunk (Castanea Sativa Mill.): a Green and Effective Extraction Method and Their Profiling by High-Performance Liquid Chromatography-Diode Array Detector-Mass Spectrometry. ACS Food Science & Technology, 3(11), 1903–1912. https://doi.org/10.1021/acsfoodscitech.3c00272

Kilvington, A., Maldonado-Pereira, L., Torres-Palacios, C., & Medina-Meza, I. (2020). Phytosterols and their oxidative products in infant formula. Journal of Food Process Engineering, 43(5), 1–46. https://doi.org/10.1111/jfpe.13151

Koo, S., & Noh, S. (2007). Green tea as inhibitor of the intestinal absorption of lipids: potential mechanism for its lipid-lowering effect. The Journal of Nutritional Biochemistry, 18(3), 179–183. https://doi.org/10.1016/j.jnutbio.2006.12.005

Lamy, E., Pinheiro, C., Rodrigues, L., Capela e Silva, F., Lopes, O. S., Tavares, S., & Gaspar, R. (2016). Determinants of tannin-rich food and beverage consumption: Oral perception vs. psychosocial aspects. Tannins: Biochemistry, Food Sources and Nutritional Properties, 29–58.

Lercker, G., & Rodriguez-Estrada, M. T. (2002). Cholesterol Oxidation Mechanisms. In F. Guardiola, P. C. Dutta, R. Codony, & G. Savage (Eds.), Cholesterol and Phytosterol Oxidation Products: Analysis, Occurence, and Biological Effects (pp. 1–25).

Li, L.-H., Dutkiewicz, E. P., Huang, Y.-C., Zhou, H.-B., & Hsu, C.-C. (2019). Analytical methods for cholesterol quantification. Journal of Food and Drug Analysis, 27(2), 375–386. https://doi.org/10.1016/j.jfda.2018.09.001

Li, Xiang, Xin, Y., Mo, Y., Marozik, P., He, T., & Guo, H. (2022). The Bioavailability and Biological Activities of Phytosterols as Modulators of Cholesterol Metabolism. Molecules, 27(2), 1–15. https://doi.org/10.3390/molecules27020523

Li, Xiangxin, Jiang, H., Pu, Y., Cao, J., & Jiang, W. (2019). Inhibitory Effect of Condensed Tannins from Banana Pulp on Cholesterol Esterase and Mechanisms of Interaction. Journal of Agricultural and Food Chemistry, 67(51), 14066–14073. https://doi.org/10.1021/acs.jafc.9b05212

Mascia, C., Maina, M., Chiarpotto, E., Leonarduzzi, G., Poli, G., & Biasi, F. (2010). Proinflammatory effect of cholesterol and its oxidation products on CaCo-2 human enterocyte-like cells: effective protection by epigallocatechin-3-gallate. Free Radical Biology and Medicine, 49(12), 2049–2057. https://doi.org/10.1016/j.freeradbiomed.2010.09.033

McClements, D. J., & Decker, E. (2018). Interfacial Antioxidants: A Review of Natural and Synthetic Emulsifiers and Coemulsifiers That Can Inhibit Lipid Oxidation. Journal of Agricultural and Food Chemistry, 66(1), 20–25. https://doi.org/10.1021/acs.jafc.7b05066

Menéndez-carreño, M., & Steenbergen, H. (2023). Development and validation of a comprehensive two-dimensional gas chromatography – mass spectrometry method for the analysis of phytosterol oxidation products in human plasma. 2012, 2023–2032. https://doi.org/10.1007/s00216-011-5432-2

Missio, A. L., Tischer, B., dos Santos, P. S. B., Codevilla, C., de Menezes, C. R., Barin, J. S., Haselein, C. R., Labidi, J., Gatto, D. A., Petutschnigg, A., & Tondi, G. (2017). Analytical characterization of purified mimosa (Acacia mearnsii) industrial tannin extract: Single and sequential fractionation. Separation and Purification Technology, 186, 218–225. https://doi.org/10.1016/j.seppur.2017.06.010

Moccia, F., Piscitelli, A., Giovando, S., Giardina, P., Panzella, L., D'Ischia, M., & Napolitano, A. (2020). Hydrolyzable vs. Condensed Wood Tannins for Bio-based Antioxidant Coatings: Superior Properties of Quebracho Tannins. Antioxidants, 9(9), 804. https://doi.org/10.3390/antiox9090804

Molino, S., Pilar Francino, M., & Ángel Rufián Henares, J. (2023). Why is it important to understand the nature and chemistry of tannins to exploit their potential as nutraceuticals? Food Research International, 173(July). https://doi.org/10.1016/j.foodres.2023.113329

Mortensen, M. B., & Nordestgaard, B. G. (2020). Elevated LDL cholesterol and increased risk of myocardial infarction and atherosclerotic cardiovascular disease in individuals aged 70–100 years: a contemporary primary prevention cohort. The Lancet, 396(10263). https://doi.org/10.1016/S0140-6736(20)32233-9

Nes, W. D. (2011). Biosynthesis of Cholesterol and Other Sterols. Chemical Reviews, 111(10), 6423–6451. https://doi.org/10.1021/cr200021m

Nguyen, C., Nirmal, N., Sultanbawa, Y., & Ziora, Z. (2023). Antioxidant and Antibacterial Activity of Four Tannins Isolated from Different Sources and Their Effect on the Shelf-Life Extension of Vacuum-Packed Minced Meat. Foods, 12(2), 354. https://doi.org/10.3390/foods12020354

O'Callaghan, Y., McCarthy, F. O., & O'Brien, N. M. (2014). Recent advances in Phytosterol Oxidation Products. Biochemical and Biophysical Research Communications, 446(3), 786–791. https://doi.org/10.1016/j.bbrc.2014.01.148

Omar, N., Ismail, C. A. N., & Long, I. (2022). Tannins in the Treatment of Diabetic Neuropathic Pain: Research Progress and Future Challenges. Frontiers in Pharmacology, 12. https://doi.org/10.3389/fphar.2021.805854

Pizzi, A. (2019). Tannins: Prospectives and actual industrial applications. Biomolecules, 9(8). https://doi.org/10.3390/biom9080344

Poli, A., Marangoni, F., Corsini, A., Manzato, E., Marrocco, W., Martini, D., Medea, G., & Visioli, F. (2021). Phytosterols, Cholesterol Control, and Cardiovascular Disease. Nutrients, 13(8), 2810. https://doi.org/10.3390/nu13082810

Poudel, A., Gachumi, G., Purves, R., Badea, I., & El-Aneed, A. (2022). Determination of phytosterol oxidation products in pharmaceutical liposomal formulations and plant vegetable oil extracts using novel fast liquid chromatography - Tandem mass spectrometric methods. Analytica Chimica Acta, 1194, 339404. https://doi.org/10.1016/j.aca.2021.339404

Risso, D., Leoni, V., Canzoneri, F., Arveda, M., Zivoli, R., Peraino, A., Poli, G., & Menta, R. (2022). Presence of cholesterol oxides in milk chocolates and their correlation with milk powder freshness. PLOS ONE, 17(3), e0264288. https://doi.org/10.1371/journal.pone.0264288

Rossin, D., Calfapietra, S., Sottero, B., Poli, G., & Biasi, F. (2017). HNE and cholesterol oxidation products in colorectal inflammation and carcinogenesis. Free Radical Biology and Medicine, 111, 186–195. https://doi.org/10.1016/j.freeradbiomed.2017.01.017

Sarni-Manchado, P., Canals-Bosch, J.-M., Mazerolles, G., & Cheynier, V. (2008). Influence of the Glycosylation of Human Salivary Proline-Rich Proteins on Their Interactions with Condensed Tannins. Journal of Agricultural and Food Chemistry, 56(20), 9563–9569. https://doi.org/10.1021/jf801249e

Scholz, B., Guth, S., Engel, K.-H., & Steinberg, P. (2015). Phytosterol oxidation products in enriched foods: Occurrence, exposure, and biological effects. Molecular Nutrition & Food Research, 59(7), 1339–1352. https://doi.org/10.1002/mnfr.201400922

Scholz, B., Wocheslander, S., Lander, V., & Engel, K.-H. (2015). On-line liquid chromatography–gas chromatography: A novel approach for the analysis of phytosterol oxidation products in enriched foods. Journal of Chromatography A, 1396, 98–108. https://doi.org/10.1016/j.chroma.2015.03.087

Shahidi, F., & Hossain, A. (2022). Role of Lipids in Food Flavor Generation. Molecules, 27(15). https://doi.org/10.3390/molecules27155014

Shahidi, F., & Zhong, Y. (2010). Lipid oxidation and improving the oxidative stability. Chemical Society Reviews, 39(11), 4067. https://doi.org/10.1039/b922183m

Shen, M., Yuan, L., Zhang, J., Wang, X., Zhang, M., Li, H., Jing, Y., Zeng, F., & Xie, J. (2024). Phytosterols: Physiological Functions and Potential Application. Foods, 13(11), 1754. https://doi.org/10.3390/foods13111754

Sieniawska, E., & Baj, T. (2017). Tannins. In Pharmacognosy (pp. 199–232). Elsevier. https://doi.org/10.1016/B978-0-12-802104-0.00010-X

Silbernagel, G., Schottker, B., Appelbaum, S., Scharnagl, H., Kleber, M. E., Grammer, T. B., Ritsch, A., Mons, U., Holleczek, B., Goliasch, G., Niessner, A., Boehm, B. O., Schnabel, R. B., Brenner, H., Blankenberg, S., Landmesser, U., & Marz, W. (2013). High-density lipoprotein cholesterol, coronary artery disease, and cardiovascular mortality. European Heart Journal, 34(46), 3563–3571. https://doi.org/10.1093/eurheartj/eht343

Sirk, T. W., Brown, E. F., Sum, A. K., & Friedman, M. (2008). Molecular Dynamics Study on the Biophysical Interactions of Seven Green Tea Catechins with Lipid Bilayers of Cell Membranes. Journal of Agricultural and Food Chemistry, 56(17), 7750–7758. https://doi.org/10.1021/jf8013298

Smeriglio, A., Barreca, D., Bellocco, E., & Trombetta, D. (2017). Proanthocyanidins and hydrolysable tannins: occurrence, dietary intake and pharmacological effects. British Journal of Pharmacology, 174(11), 1244–1262. https://doi.org/10.1111/bph.13630

Ștefănescu, R., Ciurea, C. N., Mare, A. D., Man, A., Nisca, A., Nicolescu, A., Mocan, A., Babotă, M., Coman, N.-A., & Tanase, C. (2022). Quercus robur Older Bark—A Source of Polyphenolic Extracts with Biological Activities. Applied Sciences, 12(22), 11738. https://doi.org/10.3390/app122211738

Tian, F., Li, B., Ji, B., Yang, J., Zhang, G., Chen, Y., & Luo, Y. (2009). Antioxidant and antimicrobial activities of consecutive extracts from Galla chinensis:The polarity affects the bioactivities. Food Chemistry, 113(1), 173–179. https://doi.org/10.1016/j.foodchem.2008.07.062

Tong, Z., He, W., Fan, X., & Guo, A. (2022). Biological Function of Plant Tannin and Its Application in Animal Health. Frontiers in Veterinary Science, 8. https://doi.org/10.3389/fvets.2021.803657

Turck, D., Castenmiller, J., De Henauw, S., Hirsch-Ernst, K. I., Kearney, J., Maciuk, A., Mangelsdorf, I., McArdle, H. J., Naska, A., Pelaez, C., Pentieva, K., Siani, A., Thies, F., Tsabouri, S., Vinceti, M., Cubadda, F., Frenzel, T., Heinonen, M., Marchelli, R., … Knutsen, H. K. (2020). Safety of the extension of use of plant sterol esters as a novel food pursuant to Regulation (EU) 2015/2283. EFSA Journal, 18(6). https://doi.org/10.2903/j.efsa.2020.6135

Valenzuela, A., Sanhueza, J., & Nieto, S. (2004). Cholesterol oxidized products in foods: potential health hazards and the role of antioxidants in prevention. Grasas y Aceites, 55(3). https://doi.org/10.3989/gya.2004.v55.i3.194

Venter, P. B., Sisa, M., van der Merwe, M. J., Bonnet, S. L., & van der Westhuizen, J. H. (2012). Analysis of commercial proanthocyanidins. Part 1: The chemical composition of quebracho (Schinopsis lorentzii and Schinopsis balansae) heartwood extract. Phytochemistry, 73, 95–105. https://doi.org/10.1016/j.phytochem.2011.10.006

Vigne, S., & Pot, C. (2024). Implication of Oxysterols and Phytosterols in Aging and Human Diseases. In Advances in Experimental Medicine and Biology (Vol. 1440). https://doi.org/10.1007/978-3-031-43883-7_12

Wang, Z., Liu, Z., Wu, C., Liu, S., Wang, D., Hu, C., Chen, T., Ran, Z., Gan, W., & Li, G. (2022). Computational Analysis on Antioxidant Activity of Four Characteristic Structural Units from Persimmon Tannin. Materials, 16(1), 320. https://doi.org/10.3390/ma16010320

Waraho, T., McClements, D. J., & Decker, E. A. (2011). Impact of free fatty acid concentration and structure on lipid oxidation in oil-in-water emulsions. Food Chemistry, 129(3), 854–859. https://doi.org/10.1016/j.foodchem.2011.05.034

Watrelot, A. A., Schulz, D. L., & Kennedy, J. A. (2017). Wine polysaccharides influence tannin-protein interactions. Food Hydrocolloids, 63, 571–579. https://doi.org/10.1016/j.foodhyd.2016.10.010

Zhang, R., Han, Y., McClements, D. J., Xu, D., & Chen, S. (2022). Production, Characterization, Delivery, and Cholesterol-Lowering Mechanism of Phytosterols: A Review. Journal of Agricultural and Food Chemistry, 70(8), 2483–2494. https://doi.org/10.1021/acs.jafc.1c07390

Chapter 2

Hypothesis, General and Specific Aims

The oxidation of sterols, including both phytosterols and cholesterol, is one of the main challenges in food science and human health. While phytosterols are recognized for their cholesterol-lowering effects, their oxidation leads to the formation of phytosterol oxidation products (POPs), whose health implications remain unclear. Similarly, cholesterol oxidation generates cholesterol oxidation products (COPs), which have been associated with negative health effects. Given the structural similarities between POPs and COPs, there is growing concern regarding the potential risks of sterol oxidation in food systems. Preventing sterol oxidation is critical for maintaining both the nutritional and functional quality of foods, despite the absence of validate analytical method for POPs. Moreover, due to their hydrophobic nature, sterols are particularly prone to oxidation when incorporated into emulsified food systems, where they tend to localize at the interface. This vulnerability necessitates effective stabilization strategies to minimize oxidative degradation. In response to the increasing demand for natural antioxidants, tannins have emerged as promising candidates due to their dual role as antioxidant and binding agents. Their capacity to interact with sterol molecules may provide a novel approach to mitigating oxidation while also influencing sterol solubility and bioaccessibility.

This Ph.D. project aims to investigate the antioxidant and binding properties of two types of tannins - chestnut tannins (representing hydrolysable tannins) and quebracho tannins (representing condensed tannins) - in emulsion systems containing sterols. The study will focus on assessing their impact on sterol oxidation and the formation of sterol oxidation products (SOPs). Furthermore, it will investigate how the interaction between tannins and sterols influences their oxidative stability.

The present work is structured in four parts:

i. The first part of the PhD project includes a preliminary study aimed at understanding the antioxidant activity of tannins in fresh egg pasta, demonstrating both a high antioxidant capacity and a potential surfactant activity (**Chapter 3**).

ii. In the second part, a comparative study on the determination of phytosterol oxidation products (POPs) is reported. Different analytical techniques including GC-MS and LC-Orbitrap-MS have been considered in order to determine POPs in high oleic sunflower oil by using commercial COPs or pure isolated POPs as reference material. The same samples were analyzed by two different laboratories (DISAFA-University of Turin and R&D Fats; Oils Department, Soremartec srl) using the same reference materials (**Chapter 4**).

iii. The third part of the project is focused on evaluating the antioxidant activity of tannins (**Chapter 5**) in a 10% oil-in-water emulsion model system containing cholesterol or phytosterols. The concentration of tannins and pH of emulsion were investigated as factors affecting their antioxidant capacity.

iv. The final part of the project aimed to investigate the interaction between sterols and tannin molecules, particularly in the formation of complexes and aggregates (**Chapter 6**).

Chapter 3

Effect of tannins on cholesterol content and its oxidation in egg pasta as related to different pasta shape

Published as:
Bonciolini A., Cantele, C., Salgarella, N.I., Zeppa, G., Bertolino, M., Cardenia, V. (2023). Effect of Tannins on Cholesterol Content and Its Oxidation in Egg Pasta as Related to Different Pasta Shapes. *Food and Bioprocess Technology,* 16, 1541–1554. https://doi.org/10.1007/s11947-023-03016-1

3.1 Abstract

Egg pasta contains high amount of cholesterol, which, upon oxidation, generates oxysterols (COPs), which play a key role in the onset of several human diseases. In this study, the effect of two tannins (esters of ellagic acid, A; esters of gallic acid, B) at three different concentrations (0.25%, 0.50%, 1.00%), were tested in egg pasta considering two different pasta shapes (squared, S; rectangular, F). When tannin B was added, the total phenolic content (TPC) in fresh pasta increased (p<0.01) and after cooking its content was greater than those obtained with tannin A. The pasta shape affected the presence of cholesterol, its amount in uncooked F shape samples (27.67 ± 0.28 mg/g pasta) was higher than that found in S shape (21.18 ± 0.49 mg/g pasta). In addition, tannin B significantly (p<0.01) increased the presence of cholesterol in the cooking water (up to 1.06 ± 3.13 μg/mL), in particular in S pasta shape. Tannin B was also greater than tannin A to reduce the content of COPs in fresh egg pasta, while the cooking process did not impact (p>0.05) the oxidation of cholesterol. The results suggest that tannin B could be applied in the formulation of egg pasta as strategy for reducing the content of cholesterol and its oxidation products.

3.2 Introduction

Egg pasta represents a typical Italian food product rich in eggs (at least four hens' eggs or 200 g of hens' eggs per kg of semolina (Presidential Decree, 2001)) and with a higher cholesterol content than traditional pasta. However, it might be highlighted that cholesterol, due to different reactions occurring during the processing and storage, in a similar way to monounsaturated fatty acids, may be oxidized generating cholesterol oxidation products (oxysterols, COPs), which negatively impact human health (Ansorena et al., 2013). COPs play a key role in the development of atherosclerotic plaques and in the onset of major chronic inflammatory processes (Cardenia et al., 2017; Gooding & de Ferranti, 2010; Mortensen & Nordestgaard, 2020; Nelson, 2013). Moreover, Malaguti et al. (2019) explained the role of COPs in altering the brain cholesterol homeostasis underlining their role in different neurodegenerative diseases (e.g., Alzheimer's, Parkinson's, and Huntington's diseases). Others (de Oliveira et al., 2018) reported the potential mutagenic and genotoxic effects of oxysterols. Thus, the correlation between COPs and human pathophysiology has been receiving increased attention (Kloudova et al., 2017). On the other hand, the COPs' functional groups including hydroxyl, hydroperoxyl, epoxy and keto, increase the intestinal absorption of COPs more than cholesterol impacting the cholesterol/lipid metabolism and membrane's function (Poli et al., 2022).

Thus, the COPs were largely determined in egg products as related to processing and storage conditions. As reported by Chudy and Teichert (2021) eggs and egg-derived products represent the main dietary sources of COPs. The pasta processing consists of steps such as mixing, extrusion, drying and also cooking that can promote the initiation of oxidative reactions, caused by high temperature, presence of metals, oxygen, and exposure to light in presence of photosensitizers (photooxidation), which lead to high production of COPs. For instance, Verardo et al. (2017) described a drastic increase in COPs content when a high temperature was applied to drying egg pasta. Again, food products formulated with pasteurized eggs displayed higher amount of COPs than those with spray-dried eggs (Verardo et al., 2020).

It is also well known that pasta shape is strictly related to macroscopic structural attributes, which could reflect different oxidative and retention behavior. As reported by literature, the pasta shape affects water absorption and solid loss; for instance, the penne shape absorbs less water than spaghetti, while both spaghetti and penne shapes lose fewer solids in cooking water than the risoni shape (Suo et al., 2021). The long pasta shape showed a higher glycaemic index than that of the short pasta shape (Pugnaloni et al., 2021); again, pasta shape together with gluten affects the texture, mastication behavior and retention of compounds as related to protein continuous network with embedded gelatinized starch (Suo et al., 2021).

To date, the interest in the development of novel or fortified food products with antioxidants drastically increased (de Oliveira et al., 2018; Sharma et al., 2022). Several natural compounds obtained from vegetal sources, or their processing by-products may represent interesting and promising alternatives to replace synthetic ones (Espinosa et al., 2015; Dutta et al., 2023; Sabaghi et al., 2022). The maqui berry powder was tested in fresh pasta for increasing the polyphenols content and antioxidant capacity and to reduce the glycemic index (Bianchi et al., 2022). An increased amount of phenol compounds, a boosted antioxidant activity and reduced digestible starch was also found in pasta fortified with olive pomace (Simonato et al., 2019). Similar results in terms of enhanced antioxidant properties were also found when mango peel dietary fiber concentrate was added at 5% in macaroni pasta (Garcia-Amezquita et al., 2018). Moreover, antioxidant properties of parboiled wheat noodles were improved by fortification with pomegranate peel extract (Kazemi et al., 2017).

Tannins have been receiving rising interest (Al-Hijazeen et al., 2016; Fruet et al., 2020; Gülçin et al., 2010). The tannins, water-soluble polyphenols, are a heterogeneous group of high molecular weight, plant bioactive compounds, that can be found in fruits, vegetables (in particular leaves, peels or seeds), certain grains, cocoa/chocolate and beverages such as coffee, tea and wine (Fraga-Corral et al., 2021; Lamy et al., 2016). They contribute to exert positive health effects due to their anti-inflammatory, anti-diabetic, cardioprotective, healing and antimicrobial (antiviral and antibacterial)

activity, since they may act as antioxidants, scavenging free radicals inhibiting lipid peroxidation and gut microbiota modulating (Lamy et al., 2016; Fraga-Corral et al., 2021; Smeriglio et al., 2017). Recently, tannins were also investigated as wall material in microencapsulated sacha inchi oil (da Silva Soares et al., 2021), origanum onites L. essential oil (Karagozlu et la., 2021) and as natural preservative in cooked chicken meat (Al-Hijazeen et al., 2016). Moreover, tannins are extensively investigated since they bind biological macromolecules such as proteins, polysaccharides, and in particular lipids and cholesterol impacting liposomes and lipid vesicles fluidity (Lamy et al., 2016). As reported by Sewoski et al. (2022) tannins interact with lipids in a similar manner and magnitude observed for proteins revealing a possible competition between lipids and proteins. On the other hand, Zeng et al. (2020) explained that apple condensed tannins directly interact with cholesterol leading to co-precipitation and cholesterol lowering effect.

Hence, these beneficial properties together with consolidated extraction techniques from natural sources make tannins promising compounds to be integrated into egg pasta formulation for increasing the content of the bioactive compounds, reducing cholesterol and oxysterols amounts.

Thus, the aim of the present study was to evaluate the ability of two different types of condensed tannins to impact the retention of cholesterol and its oxidation products in fresh and cooked egg pasta as related to two different pasta shapes.

3.3 Materials and methods

3.3.1 Chemical and Materials

All chemicals and solvents were of analytical grade. Millipore membrane filters (0.45 μm and 0.20 μm), chloroform, n-hexane, methanol, water (≥99.8%) and ethanol were purchased from Merck (Darmstadt, Germany). N° 1 filters (70 mm diameter) were provided from Whatmann (Maidstone, England). The standard mixtures of free fatty acids (GLC 469) were purchased from Nu-Chek

(Elysian, MN, USA). Folin–Ciocalteu's phenol reagent, triolein (≥99.0%), tripalmitin (≥99.0%), tristearin (≥99.0%), 1,3-diolein (≥99.0%), 1,2(3)-dipalmitin (≥99.0%), cholesteryl palmitate (≥97%), 1-oleoyl-rac-glycerol (≥99.0%), methyl tridecanoate (≥99.5%), 5-cholesten-3β-ol (cholesterol, ≥99%), 5α-cholestane (≥97%), anhydrous pyridine (99.8%) and N,O-Bis(trimethylsilyl)trifluoroacetamide with trimethylchlorosilane (BSTFA:TMCS, 99:1, v/v) were purchased from Sigma (St. Louis, MO, USA). 2-2′-diphenyl-1-picrylhydrazyl (DPPH•), gallic acid (≥98%) were provided by Fluka (Milan, Italy). Sodium carbonate and potassium hydroxide were purchased from Carlo Erba (Milan, Italy). Tannins with ellagic acid esters of glucose, from oak wood extract (A); gallic acid esters of quinic acid, from purified and deodorized tara pods extract (B) were kindly provided by a local company.

3.3.2 Pasta sampling

The pasta dough was prepared by mixing and kneading 160 g of wheat flour (type 00), 80 g of durum wheat semolina flour, 100 g of pasteurized egg product, tannins, and 40 mL of water in a mixer bowl (Dolly, Imperia & Monferrina S.p.A., Moncalieri, Italy) until a compact and homogeneous mixture was obtained. Tannins (powder) were added in different percentages of the total flour amount namely 0.25 % (w/w), 0.50 % (w/w), and 1.00 % (w/w). Afterward, two different pasta shapes, squared shape (S) and rectangular shape (F) were obtained from the same dough by using a bronze die-extruder in order to produce pasta characterized by the same volume but a different shape (Figure 1). Control without the addition of the tannins was also prepared for both S and F shapes. The pasta samples obtained were left to air dry on traditional hangers. Lastly, the samples were cooked in ultrapure water at 1:10 pasta/water ratio (w/w) (Cappa & Alamprese, 2017) for 4 minutes until the white center core of the pasta disappeared. Three independent experiments (n=3) were conducted. All pasta samples were freeze-dried (Lio 5P, 5 Pascal, Italy), ground immediately before to be analyzed.

3.3.3 Extraction of antioxidant compounds

The extraction of the antioxidant compounds from both uncooked and cooked pasta was performed according to Fares et al. (2010) with a modified weight/solvent ratio (1:20, w/v). In brief, 20 mL of a methanol:water solution (80:20; v/v) acidified with formic acid (to reach a pH equal to 2.5) was added to 1 g of ground pasta and stirred in darkness for 2 hours. Subsequently, the sample was centrifuged (12,900 × g, 15 min, 5 °C) and the supernatant was collected. The extraction was then repeated two times and the supernatants were pooled, filtered through a Millipore filter (PTFE; 0.45 μm) and stored in amber glass vials at 4 °C until subsequent analyses.

3.3.4 Total phenolic content

The determination of the total phenolic content (TPC) was carried out by Folin-Ciocalteu colorimetric method described by Singleton & Rossi (1965) with slight modifications as reported by Cantele et al. (2020), for adapting it to a BioTek Synergy HT spectrophotometric multi-detection 96-well microplate reader (BioTek Instruments, Milan, Italy). The analysis was run in triplicate. Results were expressed as milligrams of gallic acid equivalents (GAE) per gram of dry pasta.

3.3.5 Radical scavenging activity

The radical scavenging activity (RSA) was determined through the inhibition of the 2,2-diphenyl-1-picrylhydrazyl (DPPH•) free radical according to the method described by Gadow et al. (1997) with some modifications to adapt it to a BioTek Synergy HT microplate reader (Barbosa-Pereira et al., 2018). Results were expressed as μmol of Trolox equivalents (TE) per gram of dry pasta.

3.3.6 Determination of total cholesterol

The total cholesterol was extracted according to Kuczyńska et al. (2019) with some modifications. Briefly, 3 mL of KOH (4M) in methanol were added to 100 mg of ground lyophilized sample, together with 1 mg of 5α-cholestane (internal standard 1; IS1) and 0.5 mg of 19-hydroxycholesterol (internal standard 2; IS2), used as internal standards to quantify cholesterol and cholesterol oxidation products, respectively. Samples were stirred in darkness for 18 hours at room temperature (25 °C) and then 10 mL of chloroform and 10 mL of a citric acid solution (0.1%; w/v) were added. After centrifugation (3,600 × g for 15 minutes at 10 °C), the organic phase (subnatant), containing the cholesterol, was collected. The extraction was then repeated, and the two organic phases were combined. The solvent was removed by flushing nitrogen and the unsaponifiable fraction solubilized with an *n*-hexane:isopropanol solution (3:2; v/v) and stored at -18 °C. Once extracted, the cholesterol-containing fraction was subjected to silylation in order to obtain the trimethylsilyl ethers (TMS). In detail, 200 µL of the unsaponifiable matter were dried under nitrogen flow, then 200 µL of pyridine and 180 µL of BSTFA (with 1% TMCS) were added; the reaction was carried out for 30 min at 60 °C under stirring. Lastly, the solvent was evaporated and TMS derivatives were dissolved in 100 µL of n-hexane. One microliter was injected into a Shimadzu QP2010 Plus GC/MS (Shimadzu, Kyoto, Japan) equipped with a fused silica capillary column (RXi-5ms, 10 m x 0.1 mm i.d. x 0.1 µm film thickness; Restek, Bellefonte, PA). The oven temperature ramped from 220 °C to 330 °C (at 10 °C/min) and then maintained at 350 °C for 2 min. The temperature of injector and the interface were set at 325 °C and 330 °C, respectively. The injection was performed in split mode (1:30 ratio) using an autosampler AOC-5000 Pal (Shimadzu, Kyoto, Japan). Helium was chosen as carrier gas with a linear velocity of 47.0 cm/sec. Acquisitions and peak integrations were performed in TIC (Total Ion Current) and SIM (Single Ion Monitoring), respectively.

3.3.7 Determination of lipids in cooking water

After cooking pasta, the water was collected, weighed, and transferred into a separating funnel. Afterwards, the lipid extraction was performed as suggested by Folch et al. (1957). The extraction was performed twice, and the organic phases were pooled and filtered through a Whatman filter paper to remove any solid suspensions. The solvent was then evaporated and the lipid matter was dissolved in 200 µL of n-hexane:isopropanol (3:2; v/v) containing 10 µg of 5α-cholestane (internal standard, IS). According to Luise et al. (2018) 1 µL of sample was injected in a GC-FID system (GC-2010 Plus, Shimadzu, Kyoto, Japan) equipped with a Rtx®-5 fused silica capillary column (20 m x 0.10 mm i.d. x thickness 0.10 µm; Restek, Bellefonte, PA) in split mode (1:50 ratio). The oven temperature was programmed from 100 to 350 °C at a rate of 5 °C/min. The final temperature was maintained for 20 minutes. The injector and FID temperature was set at 348 °C and 350 °C, respectively. Helium was chosen as the carrier gas with a linear velocity of 47.0 cm/sec. The free fatty acids, free and esterified cholesterol, monoacylglycerols, diacylglycerols and triacylglycerols were recognized by injection of pure commercial standards under the same analytical conditions.

3.3.8 Determination of cholesterol oxidation products

Cholesterol oxidized products (COPs) were isolated from the unsaponifiable matter according to Rose-Sallin et al. (1995). Briefly, an SPE-NH2 cartridge, containing 3 mm of anhydrous sodium sulfate, was activated with 3 mL of n-hexane. Then, the 9/10 of the unsaponifiable fraction was loaded and eluted with 6 mL of n-hexane:ethylacetate (95:5; v/v) and 10 mL of n-hexane:ethylacetate (9:1; v/v). Once purified, COPs were eluted through the column with 10 mL of acetone and collected. Subsequently, the acetone was removed under nitrogen flow and the COPs were derivatized as described in Section 2.6. Samples were dissolved in 100 µL of n-hexane and injected into a Shimadzu QP2010 Plus GC/MS (Shimadzu, Kyoto, Japan) equipped with a RXi-5ms fused silica capillary column (10 m x 0.10 mm i.d. x thickness 0.10 µm; Restek, Bellafonte, PA) as reported by Cardenia

et al. (2012). The injection (1 µL) was performed in splitless mode. The temperature was programmed from 250 to 325 °C at 20 °C/min. The injector temperature was set at 325 °C and the ion source temperature was set at 200 °C. Helium was used as the carrier gas with a linear velocity of 43.0 cm/sec. The COPs were recognized by their mass spectra (TIC) and quantified by single ion monitoring (SIM). The quantifier ion and the three qualifier ions are shown in Supplementary Table S1 (Supplementary material section). The acquisition and integration modes were in TIC (Total Ion Current) and SIM (Single Ion Monitoring), respectively, using the qualifier and quantifier ions.

The oxidation factor was calculated according to the following equation:

$$F_{ox} = \frac{COPs}{Cholesterol} * 100$$

where cholesterol represents the cholesterol content in pasta sample and COPs the cholesterol oxidation products content.

3.3.9 Statistical analysis

Results were reported as means and standard deviation of three independent replicates and were statistically processed using SPSS Statistics software (version 25.0; IBM, Chicago, USA). Analysis of variance (ANOVA) and Tukey's post-hoc test, with 95% confidence level, were used to identify significant differences between the mean values of the groups as related to the different tannins, their concentrations, the pasta shapes and the cooking effect. To further understand the data variability, principal component analysis (PCA) was carried out.

3.4 Results

3.4.1 Total phenolic content

The effect of two tannins on the phenolic content (TPC) in cooked pasta as related to different shapes is depicted in Figure 3.1. In uncooked pasta, the pasta without tannins (control) exhibited a TPC equal

to 1.21 ± 0.00 mg GAE/g and the addition of tannins in the formulation increased the TPC. The S pasta shape fortified with tannin A showed a TPC ranging from 1.56 to 2.46 mg GAE/g, while F shape displayed a TPC ranged between 1.55 and 2.49 mg GAE/g. In S pasta shape the presence of tannin A at both 0.5 and 1.0 % led to the highest value of TPC, while in F shape only with 1.0% of tannin A the greatest value was reached. The tannin B displayed greater TPC than tannin A, in fact, the content of phenols increased at least twice; the TPC ranged between 2.76 and 6.31 mg GAE/g in S pasta shape and in a similar way ranged from 2.73 to 6.10 mg GAE/g in F pasta shape.

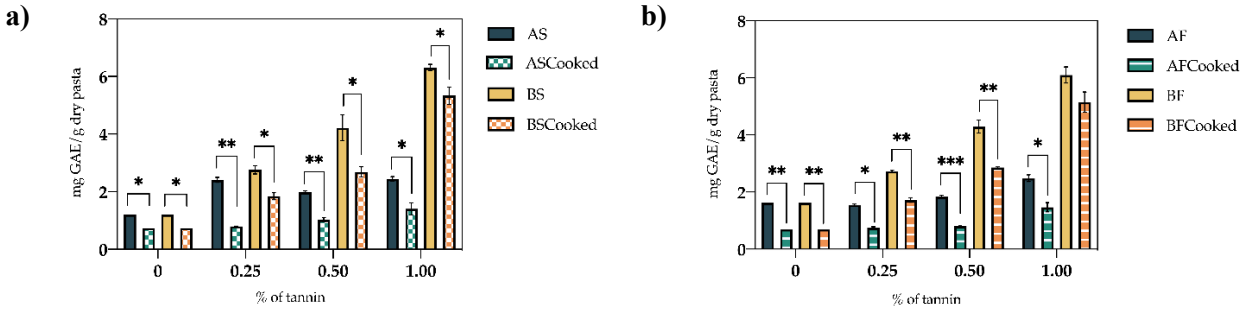

Figure 3.1. Total phenolic content (TPC) (mg GAE/g dry pasta) of pasta added with tannins before (filled bars) and after (dot patterned bars) cooking in: **a)** squared shape (S); **b)** rectangular shape (F) for both tannins (A and B). Each bar represents the mean ± standard deviation of three independent experiments (n=3). Each sample is named with the combination of two letters indicating the shape (S; F) and added tannin (A; B). Results were analyzed trough the Tukey's post hoc test. Significance: * = $p<0.05$; ** = $p<0.01$; *** = $p<0.001$.

To evaluate the possible losses of the bioactive compounds due to the cooking process, the TPC was also evaluated in cooked samples (Table 3.1). The TPC loss was more marked when tannin A was used; both F and S shapes pasta with 1% of tannin A shown the highest loss (by 41% and 42 % of TPC, respectively). On the other hand, pasta with tannin B lost less phenolic compounds since the loss was less than 15% (at 1.0% of tannin concentration).

Table 3.1 Total phenolic content (TPC) (mg GAE/g of dry pasta) and radical scavenging activity (RSA) (µmol TE/g of dry pasta) in cooked squared (S) and rectangular (F) shape added with tannins A and B.

		TPC (mg GAE[1]/g dry pasta)			RSA (µmol TE[2]/g dry pasta)		
Tannin	**concentration**	**S shape**	**F shape**	*Sig.*	**S shape**	**F shape**	*Sig.*
A	0%	0.74 ± 0.00 ^{d}	0.70 ± 0.01 ^{d}	n.s.	0.52 ± 0.04 ^{c}	0.84 ± 0.00 ^{b}	n.s.
	0.25%	0.80 ± 0.06 ^{bc}	0.75 ± 0.01 ^{b}	n.s.	3.43 ± 0.36 ^{b}	6.47 ± 0.14 ^{a}	***
	0.50%	1.03 ± 003 ^{b}	0.80 ± 0.02 ^{b}	n.s.	3.69 ± 0.17 ^{b}	7.09 ± 0.15 ^{a}	n.s.
	1.00%	1.41 ± 0.10 ^{a}	1.47 ± 0.02 ^{a}	n.s.	12.00 ± 0.35 ^{a}	10.72 ± 0.31 ^{a}	n.s.
	Sig.	**	**		***	*	
B	0%	0.74 ± 0.00 ^{d}	0.70 ± 0.01 ^{d}	n.s.	0.52 ± 0.04 ^{d}	0.84 ± 0.00 ^{d}	n.s.
	0.25%	1.84 ± 0.01 ^{c}	1.72 ± 0.03 ^{c}	n.s.	26.80 ± 0.58 ^{c}	24.63 ± 0.39 ^{c}	n.s.
	0.50%	2.69 ± 0.05 ^{b}	2.86 ± 0.01 ^{b}	n.s.	38.43 ± 1.13 ^{b}	38.66 ± 1.62 ^{b}	n.s.
	1.00%	5.33 ± 0.07 ^{a}	5.15 ± 0.06 ^{a}	n.s.	96.29 ± 3.11 ^{a}	91.07 ± 3.56 ^{a}	n.s.
	Sig.	***	***		***	***	

Each value represents the mean ± standard deviation of three independent experiments (n=3). Value with different letters within a column are significantly different (Tukey's test; $p<0.05$).
[1]GAE = gallic acid equivalents.
[2]TE = Trolox equivalent.
Abbreviations: A, esters of ellagic acid; B, esters of gallic acid B; S, squared pasta shape; F, rectangular pasta shape. Sig., statistical significance; n.s., not significant
asterisks denote the level of significance: *, $p<0.05$; **, $p<0.01$; *** $p<0.001$.

3.4.2 Radical scavenging activity (RSA)

The antiradical activity determined in both uncooked and cooked pasta with and without tannins for both S and F shapes is reported in Fig. 3.2.

In general, RSA significantly increased with increasing concentrations of tannins. However, no significant differences ($p > 0.05$) were observed between the two pasta shapes. A distinct behavior was observed between the two tannins. At all tested concentrations, in both uncooked and cooked samples, pasta fortified with tannin B exhibited higher RSA values than that with tannin A. Notably, pasta enriched with tannin B at 1.0% (S shape) showed an RSA increase from 81.27 ± 1.03 µmol TE/g to 96.29 ± 3.11 µmol TE/g (an 18.5% increase) after cooking. Similarly, in pasta containing 0.25% of tannin A (F shape), RSA increased from 3.55 ± 0.14 µmol TE/g to 6.47 ± 0.14 µmol TE/g following cooking.

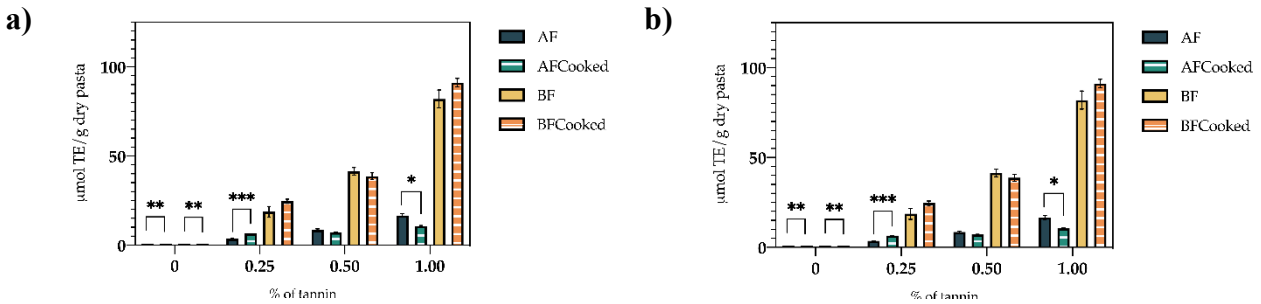

Figure 3.2. Radical scavenging activity (RSA) (µmol TE/g dry pasta) of pasta added with tannins before (filled bars) and after (dot patterned bars) cooking in: a) squared shape (S); b) rectangular shape (F) for both tannins. Each bar represents the mean ± standard deviation of three independent experiments (n=3). Results were analyzed through the Tukey's post hoc test. Significance: * = p<0.05; ** = p<0.01; *** = p<0.001. Each sample is named with the combination of two letters indicating the shape (S; F) and added tannin (A; B).

3.4.3 Cholesterol content in pasta

The cholesterol content in pasta samples (with and without tannins) was evaluated in relation to shape, cooking treatment, and tannin type. As shown in Table 3.2, the pasta shape affected cholesterol concentrations: in uncooked control samples, the F shape showed significantly higher cholesterol content compared to the S shape (p<0.05). Since natural extracts may contain lipid compounds, the quality control of tannins was assessed by extraction of potential lipid matter and analysis by GC-FID. The results confirmed that no lipids were in powder tannins (data not shown).

Tannin addition influenced cholesterol levels differently depending on the type and concentration. In the S shape, both tannins significantly (p<0.05) affected cholesterol content, whereas in the F shape no significant changes were observed (p>0.05). Specifically, tannin A increased cholesterol levels only in uncooked pasta, while tannin B caused a significant increment (p<0.01) in both uncooked and cooked samples. As stated above, the cooking process did not significantly (p>0.05) affect the content of cholesterol in pasta except for tannin B added in S shape; in fact, cooked samples added by 0.50 and 1.00 % of tannin B displayed a cholesterol decrease by 18 % and 33 %, respectively (Supplementary Table S2).

Table 3.2. Total cholesterol content (mg/g dry pasta) in uncooked and cooked squared (S) and rectangular (F) shapes added with tannins A and B.

			Cholesterol content (mg/dry g)		
Tannin	**Thermal treatment**	**Concentration tannins**	**S shape**	**F shape**	*Sig.*
A	*Uncooked*	0%	21.18 ± 0.49 [b]	27.67 ± 0.28	**
		0.25%	32.50 ± 6.10 [a]	31.61 ± 3.97	n.s.
		0.50%	30.57 ± 2.67 [a]	32.08 ± 4.46	n.s.
		1.00%	36.08 ± 0.62 [a]	33.41 ± 0.55	**
		Sig.	*	n.s.	
	Cooked	0%	19.72 ± 2.15	29.15 ± 5.50	n.s.
		0.25%	30.56 ± 1.96	32.24 ± 0.04	n.s.
		0.50%	25.69 ± 6.34	28.22 ± 2.60	n.s.
		1.00%	30.37 ± 7.11	32.74 ± 4.90	n.s.
		Sig.	n.s.	n.s.	
B	*Uncooked*	0%	21.18 ± 0.49 [c]	27.67 ± 0.28	**
		0.25%	23.30 ±3.99 [bc]	39.97 ± 7.95	n.s.
		0.50%	30.34 ± 0.89 [b]	31.20 ± 1.44	n.s.
		1.00%	53.59 ± 10.27 [a]	33.72 ± 1.83	**
		Sig.	***	n.s.	
	Cooked	0%	19.72 ± 2.15 [c]	29.15 ± 5.50	n.s.
		0.25%	27.61 ±4.53 [bc]	34.02 ± 4.99	n.s.
		0.50%	24.66 ± 1.72 [b]	30.59 ± 2.57	n.s.
		1.00%	35.69 ± 0.04 [a]	32.04 ± 3.56	**
		Sig.	**	n.s.	

Each value represents the mean ± standard deviation of three independent experiments (n=3). Value with different letters within a column are significantly different (Tukey's test; $p<0.05$).
Abbreviations: A, esters of ellagic acid; B, esters of gallic acid B; S, squared pasta shape; F, rectangular pasta shape. Sig., statistical significance; n.s., not significant
Asterisks denote the level of significance: *, $p<0.05$; **, $p<0.01$; *** $p<0.001$.

3.4.4 Cholesterol content in cooking water

To confirm the hypothesis of cholesterol transfer from the pasta to the cooking water, the latter was analyzed in terms of total cholesterol content. As reported in Table 3.3, the cooking water of S pasta

shape containing tannin B displayed an increased amount of cholesterol as related to the tannin concentration.

Table 3.3. Total cholesterol content (µg/g dry pasta) in cooking water as related to squared (S) and rectangular (F) shapes added with tannins A and B

Tannin	Concentration	Cholesterol content (µg/g)		
		S shape	**F shape**	*Sig.*
A	0%	0.35 ± 0.01	0.35 ± 0.01	n.s.
	0.25%	0.33 ± 0.00	0.38 ± 0.14	n.s.
	0.50%	0.30 ± 0.16	0.25 ± 0.16	n.s.
	1.00%	0.32 ± 0.05	0.41 ± 0.04	n.s.
	Sig.	n.s.	n.s.	
B	0%	0.35 ± 0.01 ^{c}	0.35 ± 0.01	n.s.
	0.25%	0.45 ± 0.03 ^{c}	0.48 ± 0.09	n.s.
	0.50%	0.56 ± 0.03 ^{b}	0.36 ± 0.02	n.s.
	1.00%	1.04 ± 0.05 ^{a}	0.32 ± 0.01	**
	Sig.	***	n.s.	

Each value represents the mean ± standard deviation of three independent experiments (n=3). Value with different letters within a column are significantly different (Tukey's test; $p<0.05$).
Abbreviations: A, esters of ellagic acid; B, esters of gallic acid B; S, squared pasta shape; F, rectangular pasta shape. Sig., statistical significance; n.s., not significant. The asterisks denote the level of significance: *, $p<0.05$; **, $p<0.01$; *** $p<0.001$.

The formulation of pasta containing at least 0.50 % of tannin B in S shape increased the solubility of cholesterol in the cooking water. The cooking water of control samples displayed a cholesterol content about 0.35 µg/mL of water for both shapes and then remained constant when tannin A was tested ($p>0.05$). In contrast, in the case of tannin B in the S shape, a significant rise in cholesterol content was observed as the percentage of fortification increased, reaching a value of 0.56 ± 0.03 and 1.04 ± 0.05 µg/mL when tannin was added at 0.50 and 1.00 %, respectively.

3.4.5 Cholesterol oxidation products (COPs)

Finally, the antioxidant activity of tannins has been verified in reduction or inhibition of cholesterol oxidation, representing a suitable valid solution to be applied in processed foods containing ingredients with a high content of cholesterol.

Table 3.4. Total cholesterol oxidation products (COPs; µg/g dry pasta) in uncooked and cooked squared (S) and rectangular (F) shapes added with tannins A and B.

			COPs (µg/g)		
Tannin	**Thermal treatment**	**Concentration tannins**	**S shape**	**F shape**	*Sig.*
A	*Uncooked*	0%	0.37 ± 0.06 ^{b}	0.41 ± 0.01 ^{b}	n.s.
		0.25%	0.50 ± 0.02 ^{ab}	0.66 ± 0.11 ^{a}	n.s.
		0.50%	0.45 ± 0.03 ^{ab}	0.53 ± 0.08 ^{ab}	n.s.
		1.00%	0.56 ± 0.17 ^{a}	0.43 ± 0.03 ^{b}	n.s.
		Sig.	*	*	
	Cooked	0%	0.33 ± 0.00	0.35 ± 0.01	*
		0.25%	0.46 ± 0.02	0.39 ± 0.11	n.s.
		0.50%	0.45 ± 0.01	0.43 ± 0.02	n.s.
		1.00%	0.53 ± 0.21	0.53 ± 0.15	n.s.
		Sig.	n.s.	n.s.	
B	*Uncooked*	0%	0.37 ± 0.06 ^{a}	0.41 ± 0.00 ^{a}	n.s.
		0.25%	0.41 ± 0.12 ^{ab}	0.33 ± 0.01 ^{ab}	n.s.
		0.50%	0.40 ± 0.02 ^{ab}	0.26 ± 0.08 ^{bc}	n.s.
		1.00%	0.31 ± 0.04 ^{b}	0.16 ± 0.01 ^{c}	*
		Sig.	*	*	
	Cooked	0%	0.33 ± 0.00	0.35 ± 0.01	*
		0.25%	0.36 ± 0.02	0.34 ± 0.14	n.s.
		0.50%	0.32 ± 0.07	0.26 ± 0.01	n.s.
		1.00%	0.32 ± 0.01	0.32 ± 0.05	n.s.
		Sig.	n.s.	n.s.	

Each value represents the mean ± standard deviation of three independent experiments (n=3). Value with different letters within a column are significantly different (Tukey's test; $p<0.05$).
Abbreviations: A, esters of ellagic acid; B, esters of gallic acid B; S, squared pasta shape; F, rectangular pasta shape. Sig., statistical significance; n.s., not significant. The asterisks denote the level of significance: *, $p<0.05$; **, $p<0.01$; *** $p<0.001$.

The COPs determined in the pasta samples were 7α-hydroxycholesterol (0.0722 – 0.1890 µg/g of pasta; 7α-HC), 7β-hydroxycholesterol (0.0491 - 0.2183 µg/g of pasta; 7β-HC), and 7-ketocholesterol

(0.1030 – 0.4432 µg/g of pasta; 7-KC). In addition, 5,6 α/β-epoxycholesterol isomers, triol, and 25-hydroxycholesterol were detected in trace amounts. The total amount of COPs was ranged from 0.16 ± 0.01 to 0.66 ± 0.11 µg/g of pasta (**Errore. L'origine riferimento non è stata trovata.**3.4).

Figure 3.3 shows the content of COPs in the pasta samples. Significant differences (p<0.05) were found in uncooked pasta as related to the type of tannin.

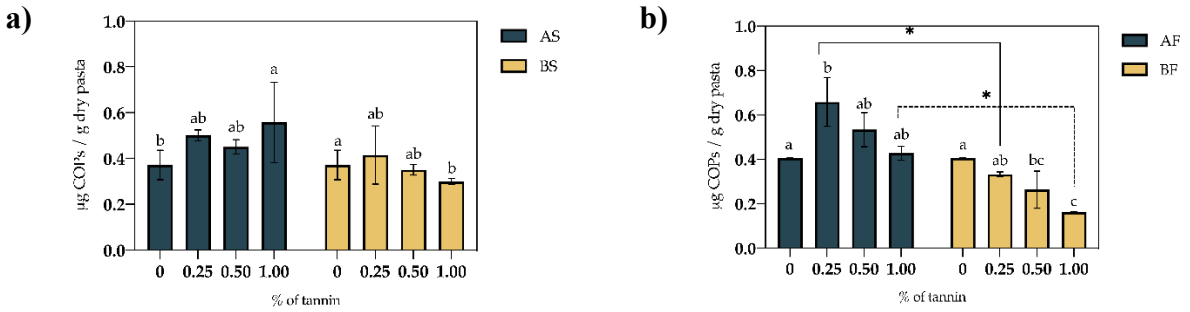

Figure 3.3. Total cholesterol oxidation products (COPs; µg/g dry pasta) in cooked squared (S) and rectangular shape (F) added with tannin A and B. Each bar represents the mean ± standard deviation of three independent experiments (n=3). Different letters denote statistically different means (Tukey's test p<0.05). Significance: * = p<0.05.

Within F shape, as the amount of tannin B increased up to 1.00 % as COPs content decreased up to 60 %. On the other hand, in S pasta shape only 1.00 % of tannin B significantly reduced the amount of COPs. On the contrary, tannin A led to a significant increase of COPs in both shapes. In F shape a significant COPs increment was found (p<0.05) rising from 0.41 µg/g (control) to 0.66 µg/g (0.25% tannin concentration), while in the S shape an increase was observed with respect to control as the concentration of tannin increased (p<0.05). However, in order to better define the extent of cholesterol oxidation with respect to the total cholesterol the oxidation factor (Fox; %) was calculated. The tannin B added at 1.00 % shown the lowest Fox on both pasta shapes F (0.5 %) and S (0.7 %) confirming the tannin B as greater antioxidant tannin. On the other hand, F pasta shape samples with tannin A displayed higher value of Fox (2.1 %) with respect to control (1.8 %).

3.4.6. Principal component analysis (PCA) of all data

All data for phenolic compounds, radical scavenging activity, cholesterol and COPs content of raw and cooked egg pasta were submitted to PCA to better understand which parameters were the most significant for analyzing the impact of tannins, their concentration and pasta shape on egg pasta.

The total variability for the first two principal components was estimated to be 73.02%. As reported in Figure 3.4 the 7α-HC, 7β-HC, 7-KC and total COPs were more correlated to PC1, which explained the 49.20% of total variance and fully separated from TPC and RSA. Moreover, the total cholesterol found in egg pasta as well as in cooking water was mostly correlated with PC2, with a variance of 23.82%. The PCA score plot is shown in Fig. 3.5. Tannin A and B used at high concentrations were fully recognized. Specifically, tannin A added in both pasta shapes resulted more characterized by all COPs, while egg pasta formulated with the highest concentration level of tannin B was located in the same cluster with TPC, RSA and total cholesterol found in both egg pasta and cooking water. These results confirm the antioxidant effect of gallotannin and its impact on cholesterol water solubility.

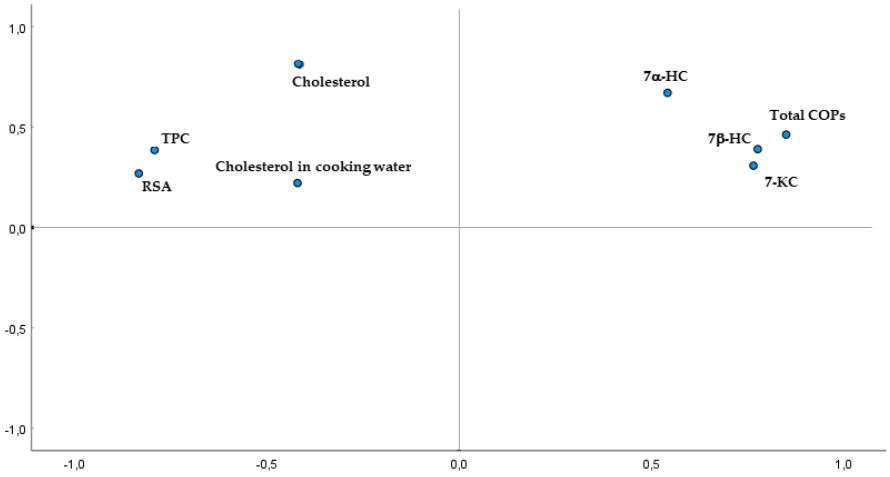

Figure 3.4. PCA loadings' plot of all COPs, cholesterol detected in egg pasta and water cooking, TPC and RSA.

Figure 3.5. PCA score plot of COPs, cholesterol detected in egg pasta and water cooking, TPC and RSA (circles) and samples (triangles).

3.5 Discussion

The present study aimed to explore the functional role of tannins in fresh egg pasta, with particular attention to their antioxidant properties and their potential influence on cholesterol behavior during processing.

The significant decrease of TPC value (Figure 3.1) during cooking process was in accordance with the literature (Lisiecka et al., 2019). The reduction in TPC was more pronounced in samples containing tannin A, with both F and S shapes at 1.0% showing the greatest losses (41% and 42%, respectively). In contrast, samples enriched with tannin B exhibited a more limited decrease, with TPC losses remaining below 15% at the same concentration. That decrease can be attributed to the thermal degradation of phenolic compounds during boiling and to their solubilization in cooking water (Alide et al., 2020; Gunathilake et al., 2018; Simonato et al., 2019). Furthermore, as reported

by Tanaka et al. (2018), the solubility of tannins in water is additionally influenced by their molecular structure and flexibility. However, the TPC found in the samples containing tannin B at each concentration and with tannin A at 0.5 and 1% was higher than that observed by Tolve et al. (2020), where pasta fortified with 5% grape pomace powder displayed a TPC equal to 1.28 and 1.05 mg/g GAE before and after cooking, respectively. Moreover, lower values were also found by Simonato et al. (2019) when olive pomace powder was integrated at 5% in pasta, obtaining a TPC of 1.29 and 0.38 mg/g GAE for uncooked and cooked pasta, respectively.

In line with the trends observed for total phenolic content (TPC), the radical scavenging activity (RSA) increased with the higher tannin concentrations, particularly in samples enriched with tannin B. This consistency further supports the close correlation between phenolic content and antioxidant capacity. The significant higher RSA observed in pasta containing tannin B, compared to tannin A, reflects the greater phenolic content previously recorded in those samples. This suggests that the gallic acid ester tannin not only contributed more phenolic compounds but also retained greater functional activity, likely due to its molecular structure and higher stability during processing. The great gap observed between the two tannins can be again ascribed to their different chemical structures and also reflects the results obtained for TPC. In fact, the ability of phenolic compounds to exert antioxidant activities, including scavenging free radicals, is mainly based on the number of hydroxyl groups and their position on the aromatic ring characteristic of polyphenols (Kumar & Goel, 2019). Moreover, potential interactions between tannins and macromolecules present in the dough (such as proteins and carbohydrates) may partially modulate the antioxidant potential by limiting the availability of free phenolic groups (Sęczyk et al., 2021). The ability of tannins to form stable complexes can attenuate their bioactivity (Fraga-Corral et al., 2020; Minatel et al., 2017) and may differ depending on tannin type and concentration.

Interestingly, cooking led to an increase in RSA in some cases, particularly in pasta fortified with 1.0% tannin B and 0.25% tannin A. That phenomenon may be attributed to structural modifications

induced by heat, such as partial hydrolysis or degradation of tannins, which could enhance their availability or activity in the food matrix (Karim et al., 2017; Moreno et al., 2018; Parada & Aguilera, 2007). Those results align with other findings on heat-treated products enriched with phenolic sources like maqui (Bianchi et al. 2022) or olive pomace (Simonato et al., 2019).

In agree with the results obtained for total phenolic content (TPC) and radical scavenging activity (RSA), the data on cholesterol reinforce the multifunctional role of tannins in egg pasta. Beyond their antioxidant properties, tannins also appear to affect the retention and distribution of cholesterol within the food matrix. It is well known that egg pasta contains a high amount of cholesterol and the processing as well as ingredients could affect its content in significant way (Verardo et al., 2017). On the other hand, different strategies were tested for developing egg-products with reduced amount of cholesterol (Lamas et al., 2016). In general, pasta shape affected cholesterol content, with significantly higher levels (p<0.05) observed in uncooked control samples of the F shape. In agree with the literature, the larger surface area of the F shape could contribute to a higher moisture transfer by diffusion (Srikiatden & Roberts, 2007), resulting in a higher concentration of macro- and micro-nutrients within the food, including cholesterol. However, as reported in Table 3.2 the tannins significantly (p<0.05) affected the content of cholesterol in the S pasta shape, while no significant differences (p>0.05) were found in the F pasta shape. Moreover, while tannin A impacted the cholesterol content only in uncooked pasta, tannin B significantly (p<0.01) affected cholesterol occurrence in both uncooked and cooked pasta. Thus, the pasta shape as well as the kind of tannin seems to influence the retention of cholesterol in pasta. The latter is not unexpected, as it is well known that the success of adding bioactive compounds into food products in terms of not only antioxidant activity but also of food quality and safety depends on both the type of bioactive compound (and specifically its molecular structure) and the food matrix (Sabaghi et al., 2022). On the other hand, cholesterol complexing activity was in deep investigated in egg yolk. For instance, Lamas et al. (2016) suggested the use of chitosan as promising strategy to reduce the presence of

cholesterol in egg-derived foods. However, no data about cholesterol complexing activity with tannins has been reported before. The results reported in the present paper, for the first time demonstrated how the use of appropriate tannin could contribute to reduce the presence of cholesterol in egg pasta. That phenomenon could be ascribed to tannin and cholesterol coprecipitation through ionic and hydrophobic interactions as well as intermolecular hydrogen bonds (Zeng et al., 2020). However, since coprecipitation may impact on cholesterol water solubility, the cholesterol content in pasta cooking water was also investigated. As stated above, the cooking process did not significantly (p>0.05) affect the content of cholesterol in pasta except for tannin B added in S shape; in fact, cooked samples added by 0.50 and 1.00 % of tannin B displayed a cholesterol decrease by 18 % and 33 %, respectively (Supplementary Table S2). Probably, that behavior could be due to a migration phenomenon of tannin-sterol complex from pasta to cooking water as the hydrophilicity of tannin tends to prevail. Specifically, the presence of tannin B in S shape led to a significant rise in cholesterol content in cooking water as the percentage of fortification increased. In order to better explain that phenomenon, two hypotheses have been considered. Firstly, a synergistic effect between the type of tannin and the shape of pasta, which is distinguished by a specific and characteristic microstructure, could be involved in the mechanism of cholesterol loss during cooking. Food microstructure can be defined as the organization, spatial arrangement and interaction of food constituents resulting in a particular microscopically visible spatial partition of different material phases (Verboven et al., 2018). The microscopic organization of food products has a great impact on their nutritional value, since it contributes both to the binding of food macromolecules and to the protection of easily degradable components from structural changes during processing (Parada & Aguilera, 2007). According to the literature, S and F pasta shapes own different microstructures (Aravind et al., 2012; Martín-Esparza et al., 2018), since S shape is reported to be much more outlined and developed than F shape. Thus, the interaction between the components inside the pasta could be different, leading to a link between cholesterol and tannin more or less encouraged. In addition, the greater solubilization of cholesterol

within the cooking water could be ascribed to the greater capacity of the water to penetrate into S shape for higher interspace volume, combined with potential surfactant activity, particularly by gallic acid; however, a more in deep investigation is required to better understand how the tannins are able to conjugate or complex cholesterol molecules related to its different forms (free vs esterified). Another explanation may be related to the formation of a surface crust during dry processing due to excessive moisture loss (Migliori et al., 2005). In fact, during the drying phase, a preliminary dehydration of the surface of the dough takes place with the formation of a thin crust with the aim of preventing pasta from sticking or becoming deformed. However, the shape and dimension are parameters that determine a different transfer of moisture from pasta to the air (Conte et al., 2021). Consequently, due to the greater surface exposure of F shape to air, the transfer of moisture to the outside could be faster and the formation of the crust easier than for the S shape, where moisture is better retained inside. Thus, the penetration of water inside the F shape pasta during the cooking step could be reduced resulting in a lower cholesterol solubility.

Finally, the antioxidant activity of tannins and the oxidation factor were evaluated on cholesterol content. Oxidation factors define the extent of cholesterol oxidation with respect to the total cholesterol. Tannin B was confirmed as a greater antioxidant. Surprisingly, F shape with tannin A displayed higher value of oxidation factor respect to the control sample. From the results obtained, it seems that tannin A showed a pro-oxidant activity. As reported by Salminen et al. (2011) there are several studies reporting controversial results regarding the activities of tannins, referring that the type, dosage, and matrix into which they are added, may be determining factors in the balance between beneficial and deleterious effects. In that case, the pasteurized egg product affects the pH of the dough. In fact, as reported by Atilgan & Unluturk (2008) the pH values of the egg product vary with temperature, due to the nature of the chemical composition and the ionic mobility in the liquid. Thus, the pH decreases because ionic mobility increases with increasing temperature. In formulating the dough, the egg product was stored at refrigeration temperature and used at room temperature, thus

estimating a pH between 7.96 and 8.00 (Atilgan & Unluturk, 2008). The high pH value and co-presence of tannin A, based on ellagitannis, probably resulted in a pro-oxidant activity. Direct pro-oxidant activities are based on the generation of a phenoxyl radical or a redox complex with a transition metal ion. Phenoxyl radicals can react with oxygen to generate O_2^-, H_2O_2, and a complex combination of semiquinones and quinones, leading to an increase in free radicals present in the environment, increasing the oxidation reactions (Barbehenn et al., 2006; Moilanen et al., 2016). On the other hand, authors reported a superior pro-oxidant activity of ellagitannin with respect to simple gallic acid derivatives, gallotannins or proanthocyanidins (Eghbaliferiz & Iranshahi, 2016). Finally, the effect of cooking on the generation of COPs was evaluated (Supplementary Table S3) and no significant differences were found (p>0.05), indicating that, despite the exposure to high temperatures, 4 minutes of cooking are not sufficient to trigger the oxidation of cholesterol in a significant way.

3.6 Conclusion

In the present study, the effect of ellagic acid esters of glucose (ellagitannins) and gallic acid esters of quinic acid (gallotannins) on the content of cholesterol and oxysterols in egg pasta was investigated also considering the contribute of pasta shape. The results demonstrated that tannin based on gallic acid ester was the most performing in egg pasta, with a substantial increase in both TPC and RSA without significant differences due to different pasta shapes considered. Again, the high antiradical activity of gallotannins suggests its use as a natural antioxidant able to reduce cholesterol oxidation. In general, the results highlighted that tannins interacted with cholesterol affecting its content in egg pasta. However, without the use of tannins F pasta shape collected higher cholesterol than S pasta shape. Furthermore, due to coprecipitation or surfactant properties of tannins, the gallotannins in the S pasta shape improved the solubility of cholesterol in water cooking revealing interesting activity to be in deep investigated. To our knowledge, no results were reported before about the

hypocholesterolemic effect of gallotannins, suggesting its use as promising technological strategy for the development of more healthy foods.

In terms of cholesterol oxidative behavior, as shown for TPC and RSA, gallotannin was more effective than ellagitannin in reducing the occurrence of COPs in both egg pasta shapes. The current study confirms that gallotannins may be a promising alternative to synthetic antioxidants for developing fresh egg pasta with a low content of COPs; however, further research is needed to better understand how tannins can bind or interact with cholesterol, impacting its water solubility also taking into account both free and esterified forms.

References

Al-Hijazeen, M., Lee, E., Mendonca, A., & Ahn, D. (2016). Effects of tannic acid on lipid and protein oxidation, color, and volatiles of raw and cooked chicken breast meat during storage. *Antioxidants*, *5*(2), 19. https://doi.org/10.3390/antiox5020019

Alide, T., Wangila, P., & Kiprop, A. (2020). Effect of cooking temperature and time on total phenolic content, total flavonoid content and total in vitro antioxidant activity of garlic. *BMC Research Notes*, *13*(1), 564. https://doi.org/10.1186/s13104-020-05404-8

Ansorena, D., Barriuso, B., Cardenia, V., Astiasarán, I., Lercker, G., & Rodriguez-Estrada, M. T. (2013). Thermo-oxidation of cholesterol: effect of the unsaturation degree of the lipid matrix. *Food Chemistry*, *141*(3), 2757–2764. https://doi.org/10.1016/j.foodchem.2013.04.1298

Aravind, N., Sissons, M. J., Fellows, C. M., Blazek, J., & Gilbert, E. P. (2012). Effect of inulin soluble dietary fibre addition on technological, sensory, and structural properties of durum wheat spaghetti. *Food Chemistry*, *132*(2), 993–1002. https://doi.org/10.1016/j.foodchem.2011.11.085

Atilgan, M. R., & Unluturk, S. (2008). Rheological properties of liquid egg products (LEPS). *International Journal of Food Properties*, *11*(2), 296–309. https://doi.org/10.1080/10942910701329658

Barbehenn, R. V., Jones, C. P., Hagerman, A. E., Karonen, M., & Salminen, J. P. (2006). Ellagitannins have greater oxidative activities than condensed tannins and galloyl glucoses at high ph: potential impact on caterpillars. *Journal of Chemical Ecology*, *32*(10), 2253-2267. https://doi.org/10.1007/s10886-006-9143-7

Barbieri, S., Mercatante, D., Balzan, S., Esposto, S., Cardenia, V., Servili, M., Novelli, E., Taticchi, A., & Rodriguez-Estrada, M. T. (2021). Improved oxidative stability and sensory quality of beef hamburgers enriched with a phenolic extract from olive vegetation water. *Antioxidants*, 10, 1969. https://doi.org/10.3390/antiox10121969

Barbosa-Pereira, L., Guglielmetti, A., & Zeppa, G. (2018). Pulsed electric field assisted extraction of bioactive compounds from cocoa bean shell and coffee silverskin. *Food and Bioprocess Technology*, *11*(4), 818-835. https://doi.org/10.1007/s11947-017-2045-6

Bianchi, F., Giuberti, G., Cervini, M., & Simonato, B. (2022). Fortification of durum wheat fresh pasta with maqui (Aristotelia chilensis) and its effects on technological, nutritional, sensory properties, and predicted glycemic index. *Food and Bioprocess Technology, 15(7)*, 1563-1572. https://doi.org/10.1007/s11947-022-02838-9

Cantele, C., Rojo-Poveda, O., Bertolino, M., Ghirardello, D., Cardenia, V., Barbosa-Pereira, L., & Zeppa, G. (2020). In vitro bioaccessibility and functional properties of phenolic compounds from enriched beverages based on cocoa bean shell. *Foods*, *9*(6), 715. https://doi.org/10.3390/foods9060715

Cappa, C., & Alamprese, C. (2017). Brewer's spent grain valorization in fiber-enriched fresh egg pasta production: Modelling and optimization study. *Lwt*, *82*, 464–470. https://doi.org/10.1016/j.lwt.2017.04.068

Cardenia, V., Massimini, M., Poerio, A., Venturini, M. C., Rodriguez-Estrada, M. T., Vecchia, P., & Lercker, G. (2015). Effect of dietary supplementation on lipid photooxidation in beef meat, during storage under commercial retail conditions. *Meat Science*, *105*, 126–135. https://doi.org/10.1016/j.meatsci.2015.02.010

Cardenia, V., Rodriguez-Estrada, M. T., Baldacci, E., Savioli, S., & Lercker, G. (2012). Analysis of cholesterol oxidation products by fast gas chromatography/mass spectrometry. *Journal of Separation Science*, *35*(3), 424–430. https://doi.org/10.1002/jssc.201100660

Cardenia, V., Rodriguez-Estrada, M. T., Lorenzini, A., Bandini, E., Angeloni, C., Hrelia, S., & Malaguti, M. (2017). Effect of broccoli extract enriched diet on liver cholesterol oxidation in rats subjected to exhaustive exercise. *Journal of Steroid Biochemistry & Molecular Biology, 169,* 137-144. http://dx.doi.org/10.1016/j.jsbmb.2016.04.005

Chudy S., & Teichert J. (2021). Oxysterols in stored powders as potential health hazards. *Scientific Reports, 11 (1)*, 21192. https://doi.otg/10.1038/s41598-021-00636-5

Conte, P., Piga, A., Del Caro, A., Urgeghe, P. P., & Fadda, C. (2021). Italian dried pasta; conventional and innovative ingredients and processing. In F. Boukid (ed.), *Cereal-Based Foodstuffs: The Backbone of Mediterranean Cuisine* (pp. 89-110). Springer Nature.

da Silva Soares, B., de Carvalho, C. W. P., & Garcia-Rojas, E. (2021). Microencapsulation of Sacha Inchi Oil by Complex Coacervates using Ovalbumin-Tannic Acid and Pectin as Wall Materials. *Food and Bioprocess Technology, 14(5)*, 817-830. https://doi.org/10.1007/s11947-021-02594-2

de Oliveira, V. S., Ferreira, F. S., Cople, M. C. R., Labre, T. da S., Augusta, I. M., Gamallo, O. D., & Saldanha, T. (2018). Use of natural antioxidants in the inhibition of cholesterol oxidation: a review. *Comprehensive Reviews in Food Science and Food Safety*, *17*(6), 1465–1483. https://doi.org/10.1111/1541-4337.12386

Dutta, D., Nayak, A., Dutta, D. (2022). Reconnoitring the Usage of Agroindustrial Waste in Carotenoid Production for Food Fortification: a Sustainable Approach to Tackle Vitamin A Deficiency. *Food and Bioprocess Technology*. https://doi.org/10.1007/s11947-022-02888-z

Eghbaliferiz, S., & Iranshahi, M. (2016). Prooxidant Activity of Polyphenols, Flavonoids, Anthocyanins and Carotenoids: Updated Review of mechanisms and catalyzing metals. *Phytotherapy Research*, *30*, 1379–1391. https://doi.org/10.1002/ptr.5643

Espinosa, R. R., Inchingolo, R., Alencar, S. M., Rodriguez-Estrada, M. T., & Castro, I. A. (2015). Antioxidant activity of phenolic compounds added to a functional emulsion containing omega-3 fatty acids and plant sterol esters. *Food Chemistry*, *182*, 95–104. https://doi.org/10.1016/j.foodchem.2015.02.130

Fares, C., Platani, C., Baiano, A., & Menga, V. (2010). Effect of processing and cooking on phenolic acid profile and antioxidant capacity of durum wheat pasta enriched with debranning fractions of wheat. *Food Chemistry*, *119*(3), 1023–1029. https://doi.org/10.1016/j.foodchem.2009.08.006

Folch, J., Lees, M., & Sloane Stanley, G. H. (1957). A simple method for the isolation and purification of total lipides from animal tissues. *The Journal of Biological Chemistry*, *226*(1), 497–509. https://doi.org/10.1016/s0021-9258(18)64849-5

Fraga-Corral, Maria, García-Oliveira, P., Pereira, A. G., Lourenço-Lopes, C., Jimenez-Lopez, C., Prieto, M. A., & Simal-Gandara, J. (2020). Technological application of tannin-based extracts. *Molecules, 25*(3), 614. https://doi.org/10.3390/molecules25030614

Fraga-Corral, María, Otero, P., Echave, J., Garcia-Oliveira, P., Carpena, M., Jarboui, A., Nuñez-Estevez, B., Simal-Gandara, J., & Prieto, M. A. (2021). By-products of agri-food industry as tannin-rich sources: a review of tannins' biological activities and their potential for valorization. *Foods*, *10*(1), 137. https://doi.org/10.3390/foods10010137

Fruet, A. P. B., Giotto, F. M., Fonseca, M. A., Nörnberg, J. L., & De Mello, A. S. (2020). Effects of the incorporation of tannin extract from quebracho colorado wood on color parameters, lipid oxidation, and sensory attributes of beef patties. *Foods*, *9*(5), 667. https://doi.org/10.3390/foods9050667

Gadow, A. V., Joubert, E., & Hansmann, C. F. (1997). Comparison of the antioxidant activity of rooibos tea (*Aspalathus linearis*) with green, oolong and black tea. *Food Chemistry*, *60*(1), 73-77. https://doi.org/10.1016/S0308-8146(96)00312-3

Garcia-Amezquita, L. E., Tejada-Ortigoza, V., Serna-Saldivar, S. O., & Welti-Chanes, J. (2018). Dietary fiber concentrates from fruit and vegetable by-products: processing, modification, and application as functional ingredients. *Food and Bioprocess Technology*, 11(8), 1439-1463. https://doi.org/10.1007/s11947-018-2117-2

Gooding, H. C., & de Ferranti, S. D. (2010). Cardiovascular risk assessment and cholesterol management in adolescents: getting to the heart of the matter. *Current Opinion in Pediatrics*, *22*(4), 398–404. https://doi.org/10.1097/MOP.0b013e32833a6e22

Gülçin, I., Huyut, Z., Elmastaş, M., & Aboul-Enein, H. Y. (2010). Radical scavenging and antioxidant activity of tannic acid. *Arabian Journal of Chemistry*, *3*(1), 43–53. https://doi.org/10.1016/j.arabjc.2009.12.008

Gunathilake, K. D. P. P., Somathilaka Ranaweera, K. K. D., & Vasantha Rupasinghe, H. P. (2018). Effect of different cooking methods on polyphenols, carotenoids and antioxidant activities of selected edible leaves. *Antioxidants*, *7*(9), 117. https://doi.org/10.3390/antiox70901178

Karim, M. A., Rahman, M. M., Pham, N. D., & Fawzia, S. (2017). Food microstructure as affected by processing and its effect on quality and stability. In S. Devahastin (Ed.), *Food Microstructure and Its Relationship with Quality and Stability* (pp. 43–57). Elsevier. https://doi.org/10.1016/B978-0-08-100764-8.00003-4

Karagozlu, M., Ocak, B., & Ocak, Ö. (2021). Effect of Tannic Acid Concentration on the Physicochemical, Thermal, and Antioxidant Properties of Gelatin/Gum Arabic–Walled Microcapsules Containing Origanum onites L. Essential Oil. *Food and Bioprocess Technology, 14(7)*, 1231-1243. https://doi.org/10.1007/s11947-021-02633-y

Kazemi, M., Karim, R., Mirhosseini, H., Hamid, A. A., & Tamnak, S. (2017). Processing of Parboiled Wheat Noodles Fortified with Pulsed Ultrasound Pomegranate (Punica granatum L. var. Malas) Peel Extract. *Food and Bioprocess Technology, 10(2)*, 379-393. https://doi.org/10.1007/s11947-016-1825-8

Kloudova, A., Guengerich, F. P., & Soucek, P. (2017). The Role of oxysterols in human cancer. *Trends in Endocrinology & Metabolism*, *28*(7), 485-496. https://doi.org/10.1016/j.tem.2017.03.002

Kuczyńska, A., Cardenia, V., Ogrodowicz, P., Kempa, M., Rodriguez-Estrada, M. T., & Mikołajczak, K. (2019). Effects of multiple abiotic stresses on lipids and sterols profile in barley leaves (*Hordeum vulgare* L.). *Plant Physiology and Biochemistry*, *141*, 215–224. https://doi.org/10.1016/j.plaphy.2019.05.033

Kumar, N., & Goel, N. (2019). Phenolic acids: Natural versatile molecules with promising therapeutic applications. *Biotechnology Reports*, *24*, e00370. https://doi.org/10.1016/j.btre.2019.e00370

Lamas, A., Anton, X., Miranda, J.M., Roca-Saavedra, P., Cardelle-Cobas, A., Ibarra, I. S., Franco, C. M., Cepeda, A. (2016). Technological Strategies for the Development of Egg-Derived Products with Reduced Content of Cholesterol. *Food and Bioprocess Technology, 9*(1), *81-90.* https://doi.org/10.1007/s11947-015-1599-4.

Lamy, E., Pinheiro, C., Rodrigues, L., Capela e Silva, F., Lopes, O. S., Tavares, S., & Gaspar, R. (2016). Determinants of tannin-rich food and beverage consumption: Oral perception vs. psychosocial aspects. In C.A. Combs (Ed.), *Tannins: Biochemistry, Food Sources and Nutritional Properties*, *(*pp. 29–58). Nova Science Publishers.

Lisiecka, K., Wójtowicz, A., Dziki, D., & Gawlik-Dziki, U. (2019). The influence of *Cistus incanus* L. leaves on wheat pasta quality. *Journal of Food Science and Technology*, *56*(9), 4311–4322. https://doi.org/10.1007/s13197-019-03900-9

Luise, D., Cardenia, V., Zappaterra, M., Motta, V., Bosi, P., Rodriguez-Estrada, M. T., & Trevisi, P. (2018). Evaluation of breed and parity order effects on the lipid composition of porcine colostrum. *Journal of Agricultural and Food Chemistry*, *66*(49), 12911–12920. https://doi.org/10.1021/acs.jafc.8b03097

Malaguti, M., Cardenia, V., Rodriguez-Estrada, M. T., & Hrelia, S. (2019). Nutraceuticals and physical activity: their role on oxysterols-mediated neurodegeneration. *Journal of Steroid Biochemistry and Molecular Biology*, *193*, 105430. https://doi.org/10.1016/j.jsbmb.2019.105430

Martín-Esparza, M., Raga, A., González-Martínez, C., & Albors, A. (2018). Micronised bran-enriched fresh egg tagliatelle: significance of gums addition on pasta technological features. *Food Science and Technology International*, *24*(4), 309-320. https://doi.org/10.1177/1082013217750683

Migliori, M., Gabriele, D., de Cindio, B., & Pollini, C. M. (2005). Modelling of high quality pasta drying: quality indices and industrial application. *Journal of Food Engineering*, *71*(3), 242-251. https://doi.org/10.1016/j.jfoodeng.2004.11.004

Minatel, I. O., Borges, C. V., Ferreira, M. I., Gomez, H. A. G., Chen, C.-Y. O., & Lima, G. P. P. (2017). Phenolic compounds: functional properties, impact of processing and bioavailability. In M.S. Hernandez (Ed.), *Phenolic Compounds - Biological Activity*. InTech. https://doi.org/10.5772/66368

Moilanen, J., Karonen, M., Tähtinen, P., Jacquet, R., Quideau, S., & Salminen, J. P. (2016). Biological activity of ellagitannins: effects as anti-oxidants, pro-oxidants and metal chelators. *Phytochemistry*, *125*, 65–72. https://doi.org/10.1016/j.phytochem.2016.02.008

Moreno, C. R., Fernández, P. C. R., Rodríguez, E. O. C., Carrillo, J. M., & Rochín, S. M. (2018). Changes in nutritional properties and bioactive compounds. In S. Z. Qamar (Ed.), *Cereals During Extrusion Cooking in Extrusion of Metals, Polymers and Food Products*. (pp. 103-124) InTechOpen. https://doi.org/10.5772/intechopen.68753

Mortensen, M. B., & Nordestgaard, B. G. (2020). Elevated LDL cholesterol and increased risk of myocardial infarction and atherosclerotic cardiovascular disease in individuals aged 70–100 years: a contemporary primary prevention cohort. *The Lancet*, *396*(10263), 1644–1652. https://doi.org/10.1016/S0140-6736(20)32233-9

Nelson, R. H. (2013). Hyperlipidemia as a risk factor for cardiovascular disease. *Primary Care - Clinics in Office Practice*, *40*(1), 195–211. https://doi.org/10.1016/j.pop.2012.11.003

Parada, J., & Aguilera, J. M. (2007). Food microstructure affects the bioavailability of several nutrients. *Journal of Food Science*, *72*(2), 21–32. https://doi.org/10.1111/j.1750-3841.2007.00274.x

Poli, G., Leoni, V., Biasi, F., Canzoneri, F., Risso, D., & Menta, R. (2022). Oxysterols: from redox bench to industry. *Redox Biology, 49,* 102220. https://doi.org/10.1016/j.redox.2021.102220

Presidential Decree 9 Febbraio 2001, n. 187, Regolamento per la revisione della normativa sulla produzione e commercializzazione di sfarinati e paste alimentari, a norma dell'articolo 50 della legge 22 febbraio 1994, n. 146. *Gazzetta Ufficiale della Repubblica Italiana*, n. 117 of 05-22-2001.

Pugnaloni, S., Alia, S., Gabrielli, M., Di Paolo, A., Turco, I., Mazzanti, L., Orsini, R., Vignini, A., & Ferretti, G. (2021). Senatore cappelli (Triticum turgidum spp. durum) pasta: a study on the nutritional quality of whole grains and its physical form. *International Journal of Food Sciences and Nutrition, 73(4)*, 451-459. https://doi.org/10.1080/09637486.2021.2025212

Rose-Sallin, C., Huggett, A. C., Bosset, J. O., Tabacchi, R., & Fay, L. B. (1995). Quantification of cholesterol oxidation products in milk powders using [$^2H_7$] cholesterol to monitor cholesterol autoxidation artifacts. *Journal of Agricultural and Food Chemistry*, *43*(4), 935-941. https://doi.org/10.1021/jf00052a017

Sabaghi, M., Tavasoli, S., Jamali, S. N., Katouzian, I., & Faridi Esfanjani, A. (2022). The pros and cons of incorporating bioactive compounds within food networks and food contact materials: a review. *Food and Bioprocess Technology*, *15*, 2422–2455. https://doi.org/10.1007/s11947-022-02837-w

Salminen, J. P., Karonen, M., & Sinkkonen, J. (2011). Chemical ecology of tannins: Recent developments in tannin chemistry reveal new structures and structure-activity patterns. *Chemistry - A European Journal*, *17*(10), 2806–2816. https://doi.org/10.1002/chem.201002662

Sęczyk, Ł., Gawlik-Dziki, U., & Świeca, M. (2021). Influence of phenolic-food matrix interactions on in vitro bioaccessibility of selected phenolic compounds and nutrients digestibility in fortified white bean paste. *Antioxidants*, *10*(11), 1825. https://doi.org/10.3390/antiox10111825

Sewoski, S., Veiko, A., Olchowik-Grabarek, E., Dubis, A., Wilczewska, A. Z., Markiewicz, K. H., Zavodnik, I. B., Lapshina, E., Dobrzynska, I., Abdulladjanova, N., & Zamaraeva, M. (2022). Hydrolysable tannins change physicochemical parameters of lipid nano-vesicles and reduce DPPH radical – experimental studies and quantum chemical analysis. *BBA – Biomembranes, 1864*, 183778

Sharma, K., Babaei, A., Oberoi, K., Aayush, K., Sharma, R., & Sharma, S. (2022). Essential oil nanoemulison edible coating in food industry: a review. *Food and Bioprocess Technology, 15*, 2375-2395. https://doi.org/10.1007/s11947-022-02811-6.

Simonato, B., Trevisan, S., Tolve, R., Favati, F., & Pasini, G. (2019). Pasta fortification with olive pomace: Effects on the technological characteristics and nutritional properties. *Lwt*, *114,* 108368. https://doi.org/10.1016/j.lwt.2019.108368

Singleton, V.L. & Rossi, J., (1965). Colorimetry of Total Phenolics with Phosphomolybdic-phosphotungstic acid reagents. *American Journal of Enology and Viticulture*, *16*, 144–158.

Smeriglio, A., Barreca, D., Bellocco, E., & Trombetta, D. (2017). Proanthocyanidins and hydrolysable tannins: occurrence, dietary intake and pharmacological effects. *British Journal of Pharmacology*, *174*(11), 1244-1262. https://doi.org/10.1111/bph.136308

Srikiatden, J., & Roberts, J. S. (2007). Moisture transfer in solid food materials: a review of mechanisms, models, and measurements. *International Journal of Food Properties*, *10*(4), 739-777. https://doi.org/10.1080/10942910601161672

Suo, X., Mosca, A. C., Pellegrini, N., & Vittadini, E. (2021). Effect of pasta shape and gluten on pasta cooking quality and structural breakdown during mastication. *Food and Function*, *12*(22), 11577–11585. https://doi.org/10.1039/d1fo02339j

Tanaka, T., Matsuo, Y., & Saito, Y. (2018). Solubility of tannins and preparation of oil-soluble derivatives. *Journal of Oleo Science*, *67*(10), 1179–1187. https://doi.org/10.5650/jos.ess18164

Tolve, R., Pasini, G., Vignale, F., Favati, F., & Simonato, B. (2020). Effect of grape pomace addition on the technological, sensory, and nutritional properties of durum wheat pasta. *Foods*, *9*(3), 354. https://doi.org/10.3390/foods9030354

Verardo, V., Riciputi, Y., Messia, M. C., Marconi, E., & Caboni, M. F. (2017). Influence of drying temperatures on the quality of pasta formulated with different egg products. *European Food Research and Technology*, *243*(5), 817-825. https://doi.org/10.1007/s00217-016-2795-9

Verardo., V., Messia, M., Marconi., E., & Caboni, M. F. (2020). Effect of different egg products on lipid oxidation of biscuits. Foods, 9(11), 1714. https://doi.org/10.3390/foods9111714

Verboven, P., Defraeye, T., & Nicolai, B. (2018). Measurement and visualization of food microstructure. In S. Devahastin (Ed.), *Food Microstructure and Its Relationship with Quality and Stability* (pp.3-28). Woodhead Publishing. https://doi.org/10.1016/B978-0-08-100764-8.00001-0

Zeng, X., Du, Z., Ding, X., & Jiang, W. (2020). Characterization of the direct interaction between apple condensed tannins and cholesterol in vitro. *Food Chemistry*, *309*, 125762. https://doi.org/10.1016/j.foodchem.2019.125762

Chapter 4

Comparative study on phytosterol oxidation products determination in high oleic sunflower oil by using cholesterol oxidation products or purified phytosterol oxidation products as reference materials

Published as:
Bonciolini A., Vissio, A., Calaminici, R., Forte, E., Cardenia, V. (2025). Comparative study on phytosterol oxidation products determination in high oleic sunflower oil by using cholesterol oxidation products or purified phytosterol oxidation products as reference materials. *Journal of Agriculture and Food Research,* 21, 101961. https://doi.org/10.1016/j.jafr.2025.101961.

4.1 Abstract

Phytosterols received great interest over the last decade due to their capacity to compete with cholesterol absorption during digestion. However, phytosterols can be oxidized resulting in oxidation products (phytosterol oxidation products, POPs), which could be associated with negative effects on human health. Thus, different studies were focused on their determination in foods and biological systems. Since no POPs commercial standards are available, except for 7-keto sitosterol, the cholesterol oxidation products (COPs) are often used as reference material (RM) for analytical purposes. However, up to date, no data confirmed the suitability of that approach. In the present study, two different laboratories were enrolled, and commercial standard COPs with pure isolated POPs, obtained by a validated semi-preparative HPLC method, were compared to determine the content of POPs in refined high oleic sunflower oil. Two technologies were also considered LC-Orbitrap-HRMS (LC-MS) and GC-MS. Except for 7-keto derivatives, the use of COPs as RM led to an overestimation of the POPs content by both tested systems LC-MS and GC-MS. Again, the Orbitrap technique was more sensitive than GC-MS, and significant differences (p<0.05) in the quantitation were also found

between LC-MS and GC-MS when identical stock solutions were used. The results demonstrated that the analysis of POPs is challenging, and the use of pure POPs leads to reduce the risk of a poor determination of POPs in vegetable oils and the use of COPs as RM for detecting and quantifying POPs should be reconsidered.

4.2 Introduction

The phytosterols represent one of the main fractions of unsaponifiable matter of vegetable fats and oils and could be found in free form or as steryl-fatty acid esters (where the 3β-OH group is esterified) (Winkler et al., 2007). The main detected phytosterols in plants are β-sitosterol, brassicasterol, campesterol and stigmasterol, and vegetable oils such as sunflower oil, canola oil, and soybean oil represent a good source of phytosterols. In the last decade, phytosterols received great interest due to their ability to compete with cholesterol absorption during the digestion process, lowering the blood cholesterol level, in particular the low-density lipoproteins (Poudel et al., 2022). However, phytosterols can be oxidized through auto-oxidation or photo-induced oxidation, and in a similar way to cholesterol, they can generate hazardous compounds such as phytosterol oxidation products (POPs), of which the 7α-hydroxy, 7β-hydroxy, 5,6α-epoxy, 5,6β-epoxy, triol and 7-keto represent the main isomers determined for each phytosterol (Bonciolini et al., 2024; Calaminici et al., 2024; Gachumi et al., 2021; Menéndez-Carreño et al., 2008). Authors suggested a significant correlation between the absorption of POPs and an increased risk of the formation of lesions (Rudzińska et al., 2022); again, cytotoxicity, as well as pro-atherogenic and pro-inflammatory effects of POPs were also reported (Wang & Lu, 2018). Moreover, the significant frequency of POPs in phytosterol-enriched meals highlights the health hazards associated with the continuous use of these products (Islam et al., 2024; Poudel et al., 2019; Scholz et al., 2015; Vanmierlo et al., 2013; Wani er al., 2023). Thus, a sensitive and reproducible analytical method able to better determine the content of POPs in foods or ingredients is highly required. It might be pointed out that since no commercial reference

standards of POPs are available, except for 7-ketositosterol, up to now the quantitation of POPs is mostly carried out using the cholesterol oxidation products (COPs) as reference material (Gachumi et al., 2021). Poudel and co-authors determined POPs in vegetable oils and liposomal formulations by LC-MS/MS using COPs as reference standards for optimizing the ionization parameters and calibration curves. Gallina Toschi et al. determined POPs in silverskin through GC-MS based on COPs calibration curves. Others determined POPs in oil-in-water emulsions by GC-MS using COPs response factors (Yang et al., 2023). Again, the COPs response factors achieved by GC-MS were used to determine POPs as related to photo-induced oxidation of phytosterols (Yang et al., 2020); and other authors applied the same approach in cooked and baked food products (Menéndez-Carreño et al., 2016).

Considering the actual literature, it might be highlighted that few studies reported the use of chemically synthesized or purified POPs for quantitative purposes. For instance, Plat and co-authors chemically synthesized deuterated and non-deuterated POPs for determining POPs in human serum and lipid emulsions (Plat et al., 2001). Others attempted to add chemical synthesis of triol to thermo-oxidize phytosterols (Menéndez-Carreño et al., 2008). Again, authors thermo-oxidized pure β-sitosterol, campesterol and stigmasterol to generate POPs, which were purified by semi-preparative HPLC and used to build calibration curves for determining POPs in different vegetable oils (Calaminici et al., 2024).

To our knowledge, even if different studies investigated POPs using COPs as reference material or someone tried purified POPs, no data about the comparison between the use of pure POPs and COPs as reference material for analytical purposes were published. The aim of the present work was to assess whether pure isolated POPs and commercial standard COPs exhibit comparable analytical behavior with regard to mass spectrometry detection (GC-MS and LC-Orbitrap-HRMS). The analysis of POPs is challenging, and the present study may contribute to overcoming the limitations associated

with the unavailability of reference standards improving the knowledge about using COPs as reference material for POPs detection.

4.3 Material and Methods

4.3.1 Chemicals and Materials

All chemicals and solvents were of analytical grade. Millipore membrane filters (0.45 μm and 0.20 μm), chloroform, n-hexane, methanol, water (≥ 99.8%), and ethanol were purchased from Merck (Darmstadt, Germany). β-Sitosterol (purity >95%; sitosterol), anhydrous pyridine (99.8%), and N,O-Bis(trimethylsilyl)trifluoroacetamide with trimethylchlorosilane (BSTFA:TMCS, 99:1, v/v) were purchased from Sigma (St. Louis, MO, USA). Campesterol (purity >95%), stigmasterol (purity >95%), and 19-hydroxycholesterol (19-HC; purity >99%; internal standard (IS)) were purchased by Larodan (Larodan AB - Retzius, SE). Hyper grade solvent for LC/GC analysis, n-heptane, 2-propanol, and formic acid were purchased by VWR (VWR International - Radnor, US). Acetone, pyridine, hexamethyldisilazane and trimethylchlorosilane were purchased from Sigma-Aldrich (Sigma-Aldrich—St. Louis, US). The 7-ketocholesterol (7-KC; purity: 99%), 7α-hydroxycholesterol (7α-HC; purity: 90%), 7β-hydroxycholesterol (7β-HC; purity: 95%), 5,6α-epoxycholesterol (α-EC; purity: 87%), 5,6β-epoxycholesterol (β-EC; purity: 80%) were supplied by Steraloids (Wilton, NH, USA). Silica solid-phase extraction (SPE) cartridges (500 mg/3 mL) from Phenomenex (Bologna, Italy) were utilized for POPs purification.

4.3.2 Preparation of phytosterol oxidation products (POPs) reference material.

Pure phytosterols oxidation products (POPs) were obtained according to our validated method (Calaminici et al., 2024). In brief, 5 mg of pure β-sitosterol, campesterol and stigmasterol each dissolved in 5 mL of acetone were individually put in glass petri dishes, dried under a stream of

nitrogen and thermo-oxidized in a static oven at 180 °C for 90 min. Then, the samples were dissolved in 4 mL of *n*-heptane/2-propanol (98:2, *v/v*) mixture and the different isomers of POPs were collected through injection into a semi-preparative liquid chromatography system LC 20AR (Shimadzu - Kyoto, Japan) equipped with shim-pack UC-Diol II Core Focus as preparative column (250 mm, 10 mm ID, 5 μm; Shimadzu, Kyoto, Japan). From pure phytosterols each single isomer POP was isolated, in particular 7α-hydroxycampesterol (7α-HCam), 7α-hydroxystigmasterol (7α-HStig), 7α-hydroxysitosterol (7α-HS), 7β-hydroxycampesterol (7β-HCam), 7β-hydroxystigmasterol (7β-HStig), 7β-hydroxysitosterol (7β-HS), 5,6α-epoxysitosterol (α-ES), 5,6β-epoxysitosterol (β-ES), 5,6α-epoxystigmasterol (α-EStig), 5,6β-epoxystigmasterol (β-EStig), 5,6α-epoxycampesterol (α-ECam), 5,6β-epoxycampesterol (β-ECam), 7-ketocampesterol (7-KCam), 7-ketostigmasterol (7-KStig), 7-ketositosterol (7-KS).

4.3.3 Quality control of POPs reference material

To ascertain the amount and purity of each collected POP, 100 μL each were added of 19-HC (12 μg dissolved in 50 μL of methanol) dried under nitrogen flow (40 °C), silylated (Leal-Castañeda et al., 2015) and 1 μL of TMS-derivatives were injected (split mode, 1:30) into a GC-MS and GC-FID (Shimadzu GC 2010; Kyoto, Japan). A capillary column Restek RTX-5 MS (50 m, 0.25 mm I.D., 0.1 μm film thickness; Bellefonte, PA), coated with 95% dimethyl and 5% diphenyl-polysiloxane was considered. The injector and FID temperatures were set at 325°C and 340°C, respectively; while in the case of GC-MS a temperature of 325 °C and 200 °C was set for transfer line and ion source, respectively. Helium at a constant linear velocity of 37.7 cm/s was employed as the carrier gas. For qualitative purposes, the POPs were recognized by comparing the mass spectra with those reported in literature, whereas the FID was used to determine the purity of recognized POPs. Due to the linear response of FID, the purity of POPs in each collected fraction was obtained by comparing the FID response of each POP isomer to that of the internal standard (19-hydroxycholesterols, 19-HC).

4.3.4 Determination of POPs by LC-Orbitrap-HRMS

The determination of POPs was carried out according to literature (Calaminici et al., 2024). Using an HPLC Ultimate 3000 system coupled to a Orbitrap high-resolution mass spectrometer (HRMS) Exploris 120 (Thermoscientific, USA) equipped with APCI ion source, 10 µL of filtered sample (0.22 µm, nylon filter) were injected. The elution was carried out using *n*-heptane (A) and 2-propanol (B) with the following gradient: 0 - 15 min 2 % B; at 35 min and up to 40 min 20 % B; 40 - 85 min 2 % B. The separation was carried out on a Shim-pack UC-Diol II (250 mm, 2.1 mm ID, 3 µm, 100 Å; Shimadzu, Kyoto) maintained at 40 °C. The acquisition was in positive and full scan mode (190 - 450 m/z) with a resolution of 120,000 at 300 °C. Parallel reaction monitoring (PRM) was used to do the MS^2 analysis.

4.3.5 Determination of POPs by GC-MS

The TMS derivatives of POPs were determined in agree with Gallina Toschi et al. using a GC-MS (Shimadzu GC 2010; Kyoto, Japan) equipped with a capillary column Restek Rxi - 5 MS (60 m, 0.25 mm I.D., 0.25 µm film thickness; Bellefonte, PA) coated with 95 % dimethyl and 5 % diphenyl-polysiloxane. The injector, transfer line and ion source temperatures were set at 325 °C, 325 °C and 200 °C, respectively. The injection was carried out in splitless mode (2 min) and the separation of analytes was achieved by programming the oven temperature from 220 °C to 330 °C with a rate of 7 °C/min using a 35.3 cm/s linear velocity of helium. A filament emission current of 70 eV was used to generate ions scanned at a rate of 1500 amu/s in a range from 50 to 600 m/z. For qualitative purposes the mass spectra were acquired in full scan (total ion current, TIC), whereas the characteristic and most abundant ions were used (single ion monitoring, SIM) for quantification: *m/z* 353 (19-HC); *m/z* 456 (7α/7β-HC); *m/z* 384 (α/β-EC); *m/z* 403 (triol); *m/z* 472 (7-KC); *m/z* 470 (7α/7β-HCam); m/z 482 (7α/7β-HStig); *m/z* 484 (7α/7β-HS); m/z 410 (α/β-EStig); *m/z* 398 (α/β-ECam); *m/z* 412 (α/β-ES); m/z 486 (7-KCam); m/z 498 (7-KStig); and m/z 500 (7-KS) [20].

4.3.6 Validation of GC-MS method

Since the validation of the LC-MS-orbitrap method was reported in our recently published study (Calaminici et al., 2024), in the present work the validation of the analytical method for determining POPs by GC-MS is described. Commercial COPs and purified POPs were used to validate the method considering specificity, linearity, limit of detection, precision and recovery. The linearity of the method was determined using commercial COPs or purified POPs in the range of 0.001 μg/mL – 5.060 μg/mL. The calibration curves were built at seven different concentration levels in triplicates by the internal standard method, where the POP or COP concentration / IS concentration ratio was plotted as related to POP or COP area / IS area ratio. The lowest concentrations that generated signals at least three times and ten times greater than the noise signal were used to determine the LOD and LOQ, respectively. Intraday and interday precision reported as relative standard deviation (%, RSD) was calculated by injecting (n=3) the identical sample on the same day for three consecutive days (n=3), respectively. Recovery was determined in refined high oleic sunflower oil (HOSO) by standard addition method at a concentration of 2.000 μg/g.

4.3.7 Determination of POPs in refined high oleic sunflower oil

In an amber flask containing 10 μL of IS (0.5 mg/mL) and 300 mg of refined high oleic sunflower oil were weighed and then 10 mL of 4N KOH in methanol containing BHT (5 mg/mL) were added. The cold saponification was carried out at room temperature (25 °C) in the dark for 18h. Then, the unsaponifiable matter was extracted with diethyl ether and neutralized with double-distilled water until pH 7. After being filtered with anhydrous sodium sulfate (Na_2SO_4) the neutralized organic layer was dried at 38 °C using a rotary evaporator. To carry on the LC-Orbitrap-HRMS determination, the unsaponifiable matter was dissolved in 1 mL of *n*-heptane/2-propanol (98:2, v/v), filtered (0.22 μm, nylon filter) and 10 μL were injected and analyzed as reported above (section 2.4). On the other hand, when GC-MS analysis was considered, the POPs fraction was isolated from unsaponifiable matter by

SPE (Hu et al., 2015), silylated (Leal-Castañeda et al., 2015) and then the TMS derivatives were dissolved in 100 µL of *n*-hexane. One µL was injected into a GC and evaluated as reported in section 2.5.

4.3.8 Statistical analysis

In order to confirm if pure COPs can be used as reference material to quantify POPs, statistical analysis of results was carried out. The results are reported as the mean of at least three independent replicates (n=3) and standard deviation; a t-test with a 95% confidence level (p<0.05) was used to recognize differences between the two groups (COPs *vs* POPs) as related to the two laboratories involved in the study.

4.4 Results

4.4.1 Isolation of POPs

The thermo-oxidative conditions tested led to the formation of 7-hydroxy, 5,6-epoxy and 7-keto oxidative derivatives of sitosterol, campesterol and stigmasterol. Figure 4.1 reports the rate of formation estimated by GC-FID.

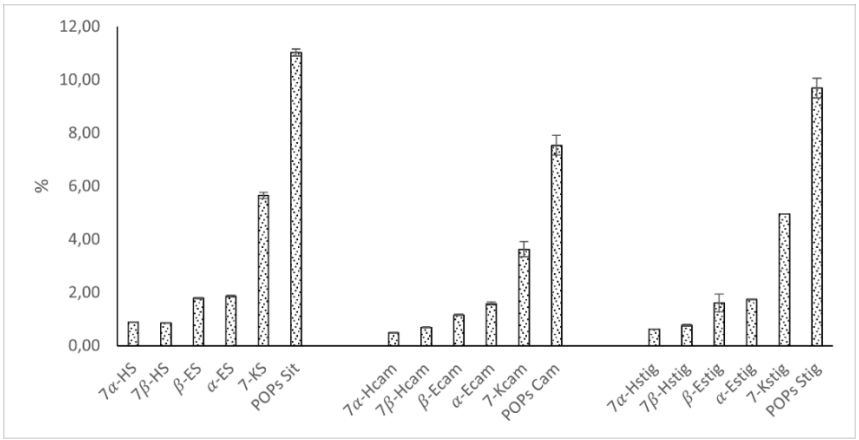

Figure 4.1. Thermo-oxidative formation of POPs from pure phytosterols

The highest amount of POPs was obtained from β-sitosterol followed by stigmasterol and campesterol. In particular, under the tested conditions an oxidation rate of 11.03 %, 9.68 % and 7.53 % was found for β-sitosterol, stigmasterol and campesterol, respectively.

Under the tested conditions, the 7-keto derivatives were the most abundant isomers followed by epoxy-isomers and 7-hydroxy derivatives and the purity for each isolated compound was > 90 %.

4.4.2 GC-MS Validation method

Table 4.1 reports the validation parameters. The method's sensitivity was determined by establishing the limits of detection (LOD) and quantification (LOQ). These parameters were determined for each compound to ensure accurate quantification across matrices. Linearity was evaluated by calculating the correlation coefficient (r^2) using the least squares method and confirming that its value was equal to or greater than 0.99 for all the analytes examined. As reported in Table 4.1, all the isolated compounds displayed a good linearity ($R^2 > 0.99$) in the range considered. The LOD for COPs ranged between 0.0128 and 0.0512 µg/mL, while a range of 0.0163 - 0.0415 µg/mL, 0.0212 - 0.0941 µg/mL, and 0.0206 – 0.1340 µg/mL was assessed for sitosterol, campesterol and stigmasterol POPs derivatives, respectively.

Table 4.1. Linearity of calibration Curves (R^2), limit of detection (LOD), and limit of quantification (LOQ) of sterol oxidation products by GC-MS.

Sterol Oxidation Products	**Calibration curve**	**R^2**	**LOD** (µg/mL)	**LOQ** (µg/mL)
Cholesterol				
7α-HC	$y = 2.51\,x - 4.00^{-2}$	0.998	0.0132	0.0418
7β-HC	$y = 3.81\,x - 4.61^{-2}$	0.999	0.0128	0.0426
α-EC	$y = 0.22\,x - 6.33^{-3}$	0.997	0.0485	0.1615
β-EC	$y = 8.15\,x - 3.15^{-3}$	0.994	0.0512	0.1705
7-KC	$y = 0.79\,x - 2.09^{-2}$	0.998	0.0168	0.0560
β-Sitosterol				
7α-HS	$y = 3.43\,x - 5.87^{-2}$	0.995	0.0170	0.0547
7β-HS	$y = 3.47\,x - 6.00^{-2}$	0.992	0.0163	0.0543
α-ES	$y = 0.12\,x - 4.00^{-4}$	0.994	0.0310	0.1033
β-ES	$y = 0.10\,x - 4.00^{-4}$	0.990	0.0199	0.0663
7-KS	$y = 0.67\,x - 3.00^{-5}$	0.996	0.0415	0.1383
Campesterol				
7α-HCam	$y = 1.04\,x - 2.96^{-4}$	0.993	0.0261	0.0860
7β-HCam	$y = 1.06\,x - 3.00^{-4}$	0.993	0.0257	0.0857
α-ECam	$y = 9.00^{-5}\,x - 7.00^{-4}$	0.992	0.0212	0.0707
β-ECam	$y = 0.06\,x - 3.00^{-4}$	0.991	0.0941	0.3137
7-KCam	$y = 0.51\,x - 7.00^{-4}$	0.992	0.0392	0.1307
Stigmasterol				
7α-HStig	$y = 5.35\,x - 5.06^{-5}$	0.996	0.0641	0.2131
7β-HStig	$y = 5.32\,x - 5.00^{-5}$	0.991	0.0638	0.2127
α-EStig	$y = 0.07\,x - 1.00^{-4}$	0.994	0.0206	0.0687
β-EStig	$y = 0.08\,x - 2.00^{-4}$	0.993	0.0274	0.0913
7-KStig	$y = 0.50\,x - 1.20^{-3}$	0.990	0.1340	0.4467

The recoveries were determined using both COPs and pure POPs as reference material. As reported in Table 4.2, using POPs as reference the recoveries ranged 90 – 97 %, whereas when pure COPs were considered, the recoveries ranged from 86 % to 102 % displaying a larger variability.

Table 4.2. Recovery (%), intraday and interday repeatability (%) determined on spiked refined high oleic sunflower oil by GC-MS as related to reference material (pure COPs (*C*); isolated POPs (*P*)).

POPs	**Recovery *C***	**Recovery *P***	*Sig. Recovery C x P*	**Intraday *C***	**Intraday *P***	*Sig. Intraday C x P*	**Interday *C***	**Interday *P***	*Sig. Interday C x P*
β-Sitosterol									
7α-HS	99.8	94.4	*	2.1	2.4	n.s.	2.5	3.3	n.s.
7β-HS	100.1	96.2	*	3.3	2.2	n.s.	2.4	3.8	n.s.
α-ES	101.2	95.2	*	4.2	3.5	n.s.	3.8	4.0	n.s.
β-ES	100.7	92.3	*	4.8	4.1	n.s.	3.4	2.6	n.s.
7-KS	86.4	90.1	*	2.6	3.5	n.s.	4.1	5.2	n.s.
Campesterol									
7α-HCam	77.8	96.7	*	3.7	2.6	n.s.	4.5	5.3	n.s.
7β-HCam	81.7	97.3	*	2.6	3.2	n.s.	3.3	3.6	n.s.
α-ECam	92.5	96.1	*	6.3	5.2	n.s.	3.4	5.1	n.s.
β-ECam	100.7	94.6	*	4.1	5.0	n.s.	4.2	5.2	n.s.
7-KCam	98.0	93.2	*	5.2	4.1	n.s.	4.9	3.5	n.s.
Stigmasterol									
7α-HStig	102.2	93.2	*	2.1	2.8	n.s.	2.5	3.1	n.s.
7β-HStig	92.1	94.1	*	3.6	2.6	n.s.	2.2	4.6	n.s.
α-EStig	98.6	92.5	*	4.1	3.3	n.s.	4.1	3.5	n.s.
β-EStig	99.7	93.6	*	3.4	5.3	n.s.	3.5	2.6	n.s.
7-KStig	100.5	91.7	*	2.1	3.8	n.s.	2.2	4.3	n.s.

Abbreviations: Sig., statistical significance; n.s., not significant; the asterisks denote the level of significance: *, $p<0.05$

Again, the present study showed how the choice of reference material significantly ($p<0.05$) impacted the recoveries. The β-sitosterol derivatives showed better recovery values, ranging from 99.8 % to 101.2 % (based on COPs) and from 90.1 % to 95.2 % (based on purified POPs). On the other hand,

campesterol displayed the worst performance in terms of recovery based on COPs (77.8 – 100.7 %) while it significantly improved when pure POPs were considered (93.2 – 97.3 %). The stigmasterol oxidizes also exhibited higher recoveries (92.1 – 102.2 %) with COPs reference material than isolated pure POPs (91.7 – 94.1 %).

The intraday precision when COPs and POPs were used as reference material was lower than 6.3 % and 5.3 %, respectively. Again, the interday repeatability was lower than 4.9 % and 5.3 % as related to COPs and POPs, respectively. It may be pointed out, that no significant differences (p<0.05) were found on the repeatability as related to the reference material and results agree with the literature (Poudel et al., 2022; Menèndez-Carreño, 2012). Moreover, both intraday and interday confirmed an excellent precision of the method and β-sitosterol oxidized derivatives showed the best precision, with RSD values ranging from 2.1 % to 4.8 % (COPs based) and from 2.2 % to 4.1 % (POPs based) for intraday, and from 2.4 % to 4.1 % (COPs-based) and from 2.6 % to 5.2 % (POPs based) for interday precision.

4.4.3 Determination of POPs in refined high oleic sunflower oil

Table 4.3 presents the quantification of POPs in HOSO. The total POPs determined by LC-MS based on isolated POPs in HOSO were from 1.88 to 2.83 mg/kg oil, while using COPs as standard a content ranged between 10.56 mg/kg oil and 15.33 mg/kg oil was found. On the other hand, by GC-MS the content was 1.29 – 1.61 mg/kg oil and 4.20 – 5.12 mg/kg oil as related to pure COPs and POPs as reference material, respectively. Significant differences (p>0.05) were found in the content of total POPs between LC-MS-Orbitrap and GC-MS using POPs as chemical standards.

Table 4.3. Content of POPs in HOSO (mg/kg oil) determined by LC-Orbitrap-HRMS and GC-MS based on the different reference material (isolated POPs (*P*) and pure COPs (*C*)).

POPs	**LC-Orbitrap-MS**			**GC-MS**			**LC-Orbitrap-MS (*P*) *x* GC-MS (*P*)**
	Calibration P	*Calibration C*	*Sig.*	*Calibration P*	*Calibration C*	*Sig.*	*Sig.*
β-Sitosterol							
7α-HS	0.024 ± 0.003	0.126 ± 0.012	***	0.021 ± 0.001	0.115 ± 0.010	***	n.s
7β-HS	0.024 ± 0.003	0.136 ± 0.009	***	0.039 ± 0.005	0.132 ± 0.012	***	*
α-ES	0.647 ± 0.027	0.786 ± 0.035	**	0.542 ± 0.054	1.047 ± 0.094	***	*
β-ES	0.194 ± 0.034	7.175 ± 1.296	***	0.092 ± 0.004	1.475 ± 0.152	**	*
7-KS	0.946 ± 0.350	0.671 ± 0.226	n.s.	0.594 ± 0.072	0.515 ± 0.069	n.s.	*
Total	1.845 ± 0.590	8.894 ± 1.232	***	1.188 ± 0.192	3.284 ± 0.477	***	n.s.
Campesterol							
7α-HCam	0.004 ± 0.001	0.032 ± 0.002	***	nd	nd	-	
7β-HCam	0.018 ± 0.001	0.049 ± 0.002	***	0.008 ± 0.001	0.035 ± 0.004	***	*
α-ECam	0.068 ± 0.011	0.168 ± 0.027	**	0.037 ± 0.004	0.104 ± 0.009	**	*
β-ECam	0.004 ± 0.001	1.643 ± 0.242	***	nd	nd	-	-
7-KCam	0.187 ± 0.016	0.146 ± 0.019	n.s.	0.041 ± 0.005	0.053 ± 0.008	n.s.	*
Total	0.281 ± 0.042	2.038 ± 0.413	***	0.086 ± 0.014	0.192 ± 0.030	*	*
Stigmasterol							
7α-HStig	0.009 ± 0.001	0.032 ± 0.005	**	0.007 ± 0.000	0.029 ± 0.002	**	n.s.
7β-HStig	0.005 ± 0.002	0.085 ± 0.035	*	nd	nd	-	-
α-EStig	0.078 ± 0.003	0.199 ± 0.012	***	0.063 ± 0.005	0.177 ± 0.014	**	*
β-EStig	0.026 ± 0.007	1.522 ± 0.440	**	0.015 ± 0.002	0.837 ± 0.074	***	n.s.
7-KStig	0.118 ± 0.015	0.176 ± 0.023	n.s.	0.092 ± 0.007	0.139 ± 0.012	n.s.	n.s.
Total	0.236 ± 0.040	2.014 ± 0.728	***	0.177 ± 0.020	1.182 ± 0.144	***	n.s.
ΣTotal POPs	2.352 ± 0.672	12.946 ± 3.373	***	1.451 ± 0.226	4.658 ± 0.651	***	n.s.

Abbreviations: Sig., statistical significance; n.s., not significant; the asterisks denote the level of significance: *, $p<0.05$; **, $p<0.01$; *** $p<0.001$; nd, not detected.

4.5 Discussion

The accurate quantification of phytosterol oxidation products (POPs) is essential for evaluating the oxidative stability and nutritional quality of foods. However, POPs analysis is still often carried out using cholesterol oxidation products (COPs) as reference standard, based on the unverified assumption that structural similarities between cholesterol and phytosterol oxidation derivatives, translate into comparable analytical behavior. The present study challenges this assumption by addressing both chemical and instrumental variables that influence POPs quantification.

As first step, POPs standards were prepared by subjecting pure phytosterol standards to controlled oxidation followed by purification. The resulting oxidation rates for each phytosterol differed from those reported in the literature. Notably, the values obtained in the present study were higher than the oxidation rate typically reported for cholesterol, which is around 6.0% (Ansorena et al., 2013). Under the tested conditions, the 7-keto derivatives were the most abundant isomers followed by epoxy-isomers and 7-hydroxy derivatives and the purity for each isolated compound was > 90 %. Authors (Kmiecik et al., 2020) found that 7-KS and 7β-HStig were the main isomers detected when free stigmasterol was thermo-oxidized. Others (Kmiecik et al., 2020) found the 5,6β-epoxy derivatives as the main POPs in heated rapeseed oil. Moreover, Rudzinska et al. (2022), detected the 7-KStig, 7β-HStig and β-EStig as the main POPs when stigmasterol was stored at 60 °C. However, as well reported by literature, the different results could be ascribed to many different factors. In fact, the composition of the environment system where phytosterols are dissolved (such as bulk oils and emulsions), their form such as free or esters as well as the nature of esterified groups (e.g., fatty acids, phenols, glycoside, etc.) significantly impacts the kinetics of sterol oxidation (Ansorena et al., 2013; Kasprzak et al., 2020; Rudzińska et al., 2009; Yang et al., 2023).

The purified POPs obtained were employed to validate the analytical method, ensuring its suitability for accurate and compounds specific quantification. All isolated compounds reported a good linearity in the considered range. However, it might be pointed out that the highest sensitivity for 7β-HC was

detected while the 7-KStig displayed the worst one. Thus, it might be hypothesized that considered POPs own different fragmentation behavior with respect to COPs when electronic ionization was considered. On the other hand, when Orbitrap® technology was considered the 7β-HCam exhibited the relatively lowest sensitivity (Calaminici et al., 2024). That hypothesis was also established by the ionic abundance ratios calculated for each analyte (COP or purified POP) injected at the same concentration. The response factor determined as COP_{area} / IS_{area} or POP_{area} / IS_{area} ratio was estimated for both GC-MS and LC-MS-Orbitrap (Tables S4.1 and S4.2). The oxidative cholesterol derivatives (COPs) displayed a significant different (p<0.05) response with respect to the POPs for both techniques. When GC-MS was considered the α/β-EC and 7-KC displayed a greater response than relative phytosterol derivatives, whereas the 7α/7β-HStig exhibited the highest response (Tables S4.1). However, it might be pointed out that no significant differences (p>0.05) were found between 7-KC, 7α/7β-HC and 7-KStig, 7α/7β-HStig, respectively. Again, COPs response determined by LC-MS-Orbitrap was significantly (p<0.05) lower than POPs and the β-ECam displayed the highest response (Table S4.2). The validation results clearly demonstrated that the choice of reference material has a significant impact on recovery values, particularly for certain phytosterol oxidation products. While β-sitosterol and stigmasterol derivatives yielded high and consistent recoveries regardless of the reference used, campesterol derivatives showed notably lower recoveries when quantified using COPs, highlighting the limitations of applying cholesterol-based standards across structurally distinct sterols. Those results agree with Menéndez-Carreño et al. (2012) except for 7-KStig, which showed a recovery of 104 %.

These findings reinforce the need for compound-specific calibration whenever feasible. Despite these differences in recovery, the method showed excellent precision considering intraday and interday RSD values, especially as concern β-sitosterol. It might be pointed out, that no significant differences (p>0.05) were found on the repeatability as related to the reference material and results agree with literature (Poudel et al., 2022; Menéndez-Carreño, 2012).

Finally, in order to compare the response of the two methods, both LC-MS-Orbitrap and GC-MS were compared using pure commercial COPs and isolated POPs as reference material for quantification of POPs in refined high oleic sunflower oil (HOSO). As reported in Table 4.3, significant differences (p>0.05) were found in the content of total POPs between LC-MS-Orbitrap and GC-MS using POPs as chemical standards (Table 4.3). The β-sitosterol being the main sterol detected in HOSO generated the highest amount of POPs followed by campesterol and stigmasterol. Both LC-MS and GC-MS methods based on pure POPs confirmed the 7-KS and α-ES as the main oxidized sterols, whereas COPs led β-ES as the greatest POP. The observed differences between the results based on the two calibration curve systems highlight a potential issue in the quantification of POPs. That divergence raises questions about the consistency and reliability of the use of COPs for determining POPs. When pure COPs were used as reference material, a general overestimation was observed by both LC-MS and GC-MS, except for 7-keto derivatives, which displayed similar results. These results suggest that even if POPs and COPs could have similar pattern fragmentation (Alemany et al., 2013; Gallina Toschi et al., 2014; Jiang et al., 2019) a different ion abundance is generated as related to the ion source. In the EI-MS, as reported for COPs, the characteristic ions of TMS ethers of POPs were $[M]^+$, $[M - 90]^+$ or $[M - 180]^+$, which corresponds to the loss of 1 or 2 TMSOH groups. As expected, $[M]^+$ was the base peak for the 7-keto derivatives; while the $[M - 90]^+$ was the most abundant fragment for hydroxy derivatives. However, in the case of β-sitosterol epoxy derivates $[M]^+$ and $[M - 90]^+$ was about 30 % and 42 %, respectively, of total ions; whereas about 20 % and 14 % for campesterol; 18 % and 16 % for stigmasterol were found. Considering the obtained results, the main differences observed in the quantification of POPs are related to the fragmentation of POPs. In fact, when $[M]^+$ was the base peak and used as quantifier ion not significant differences (p>0.05) were observed with respect to the reference material. As reported by literature (Louter, 2004) the different groups in the side chains of phytosterols (such as methyl, ethyl substituent, or double bound) could affect the abundance of characteristic ions; explaining the different responses. When POPs were

determined by LC-MS the derivatization procedure as well as SPE isolation can be avoided leading to a simplified analytical determination (Calaminici et al., 2024; Gachumi et al., 2021). Considering the polarity of POPs, the APCI permits an efficient ionization of POPs; generally, the 7-keto derivatives generate ion $[M + H]^+$ whereas the 7-hydroxy and epoxy sterol derivatives produce characteristic ions $[M + H - H_2O]^+$ or $[M + H – 2H_2O]^+$ due to the loss of one or two water molecules, respectively. Since the 7-keto sterol derivatives content did not display significant differences (p>0.05) as related to reference material, it can be hypothesized that different responses of unstable polar POPs could be ascribed to the energy required to lose water during the fragmentation. On the other hand, even though β-sitosterol, campesterol and stigmasterol share the same central sterol nucleus of cholesterol (four hydrocarbon rings, a hydroxyl group in C3, and a double bond in C5-C6) differences are in the side chain: β-sitosterol displays an ethyl substituent in C24; campesterol shows a methyl substituent in C24 and stigmasterol exhibits an ethyl substituent and additional double bound in C22-C23.

In the present work, two different laboratories (DISAFA - University of Turin; and R&D Fats and Oils Department, Soremartec srl) were enrolled for the determination of POPs in HOSO using the same standard solutions. Based on these results, for the first time, it was demonstrated that the use of COPs for determining POPs has to be reconsidered, in particular for quantitative scope. In fact, the present work confirms the suitability of 7-KC to be used as reference material for the determination of 7-keto phytosterol derivatives. However, it might be highlighted that significant differences (p<0.05) in the POPs content were observed as related to the considered equipment, since GC-MS displayed a lower value than those obtained by LC-Orbitrap-HRMS. Furthermore, a similar behavior was reported about COPs by Lutjohann et al., (2018) where eleven laboratories were involved in the determination of COPs in lyophilized pooled sera using the same standard stock solutions. However, higher sensitivity was confirmed by LC-Orbitrap-HRMS, since 7a-HCam, β-ECam, and 7β-HStig (not detected by GC-MS) were at level < 0.004 mg/kg of oil.

4.6 Conclusion

Over the past decade, there has been a significant increase in interest in phytosterol oxidation products due to their potential involvement in the development of various diseases. Accordingly, there is a pressing need for the development of a sensitive and reproducible analytical method that can more accurately determine the content of POPs in foods or ingredients. However, as no commercial pure standards for POPs are currently available, except for 7-ketositosterol, the use of COPs as reference material has been the prevailing applied approach. Recently, the isolation of pure POPs was reported through the use of a semi-preparative HPLC. Based on that, the primary purified POPs isomers (7-hydroxy; 5,6-epoxy and 7-keto derivatives of sitosterol, campesterol and stigmasterol) were employed to build calibration curves and utilized for the determination of POPs in refined high oleic sunflower oil. The results were then compared with those obtained using pure COPs. In the present study, liquid chromatography and gas chromatography were employed coupled with high-resolution mass spectrometry (Orbitrap® technology) and low-resolution mass spectrometry (single quadrupole), respectively. The use of COPs or POPs as reference material resulted in significant differences in the quantification of POPs. In particular, the use of COPs led to a general overestimation of POPs content, except for the 7-keto derivatives of sitosterol, campesterol, and stigmasterol. However, the LC-Orbitrap-HRMS displayed greater sensitivity than the GC-MS, as some isomers were not detected in HOSO. Once more, the results were significantly affected by the preparative procedure. Indeed, when GC-MS was considered, in addition to the saponification, also the isolation of POPs by SPE and their derivatization were carried out, which affected the final results. The present study for the first time compared the two approaches to quantify POPs. It demonstrated that the choice of the right reference material plays a crucial role in order to reach robust and reproducible results and the use of pure COPs as chemical standards for POPs quantification in vegetable oil such as HOSO has to be reconsidered.

Appendix

Table S1. Response factor of sterol oxidation products determined by GC/MS

	Cholesterol	Sitosterol	Campesterol	Stigmasterol	*Sign.*
α-E	0.22 ± 0.01[a]	0.12 ± 0.00[b]	0.09 ± 0.00[b]	0.07 ± 0.00[b]	**
β-E	0.18 ± 0.00[a]	0.10 ± 0.01[b]	0.06 ± 0.00[b]	0.08 ± 0.00[b]	**
7-K	0.79 ± 0.02[a]	0.68 ± 0.02[ab]	0.52 ± 0.02[b]	0.51 ± 0.01[b]	*
7α-H	3.81 ± 0.12[b]	3.44 ± 0.10[b]	1.06 ± 0.03[c]	5.46 ± 0.16[a]	**
7β-H	3.84 ± 0.11[b]	3.48 ± 0.10[b]	1.08 ± 0.03[c]	5.43 ± 0.14[a]	**

The results are expressed as mean ± standard deviation (n=3). Sign., statistical significance. Means followed by different letter (row) are significantly different at $p<0.05$ (*), $p<0.01$ (**); α-E = α-epoxy isomers, β-E = β-epoxy isomers, 7-K= 7-keto isomers, 7α-H= 7α-hydroxy isomers, 7β-H = 7β-hydroxy isomers.

Table S2. Response factor of sterol oxidation products determined by LC-MS-Orbitrap

	Cholesterol	Sitosterol	Campesterol	Stigmasterol	Sign.
α-E	0.75 ± 0.16[b]	1.00 ± 0.02[b]	1.81 ± 0.24[a]	1.84 ± 0.18[a]	***
β-E	0.44 ± 0.01[c]	2.97 ± 0.09[b]	30.63 ± 2.24[a]	3.80 ± 0.25[b]	***
7-K	1.40 ± 0.01[b]	2.68 ± 0.18[a]	2.33 ± 0.54[a]	1.25 ± 0.24[b]	***
7α-H	0.79 ± 0.23[b]	2.85 ± 0.12[a]	2.55 ± 0.27[a]	2.36 ± 0.13[a]	***
7β-H	0.32 ± 0.03[c]	2.33 ± 0.09[b]	0.33 ± 0.02[c]	9.80 ± 0.14[a]	***

The results are expressed as mean ± standard deviation (n=3). Sign., statistical significance. Means followed by different letter (row) are significantly different at $p<0.05$ (*), $p<0.01$ (**), $p<0.001$(***); α-E = α-epoxy isomers, β-E = β-epoxy isomers, 7-K= 7-keto isomers, 7α-H= 7α-hydroxy isomers, 7β-H = 7β-hydroxy isomers.

References

Alemany, L., Cilla, A., Garcia-Llatas, G., Rodriguez-Estrada, M.T., Cardenia, V., Alegría, A. Effect of simulated gastrointestinal digestion on plant sterols and their oxides in enriched beverages, Food Res. Int. 52 (2013) 1–7. https://doi.org/10.1016/j.foodres.2013.02.024.

Ansorena, D., Barriuso, B., Cardenia, V., Astiasarán, I., Lercker, G., Rodriguez-Estrada, M.T. Thermo-oxidation of cholesterol: effect of the unsaturation degree of the lipid matrix, Food Chem, 141 (2013) 2757–2764. https://doi.org/10.1016/j.foodchem.2013.04.129.

Bonciolini, A., Cantele, C., Piochi, M., Di Lecce, G., Risso, D., Cardenia, V. New insights on phytocannabinoids role in antioxidant activity of hemp inflorescences extract in high-oleic sunflower oil. LWT. 194 (2024), 115807. https://doi.org/10.1016/j.lwt.2024.115807.

Calaminici, R., Salgarella, N.I., Cardenia, V., Forte, E. Optimization and validation of an HPLC-HRMS method through semi-preparative HPLC system for determining phytosterol oxidation products during refining processing and storage of vegetable oils, J. Am. Oil Chem. Soc. 101 (2024) 735–751. https://doi.org/10.1002/aocs.12826.

Cardenia, V., Rodriguez-Estrada, M.T., Baldacci, E., Savioli, S., Lercker, G. Analysis of cholesterol oxidation products by Fast gas chromatography/mass spectrometry, J. Sep. Sci. 35 (2012), 424–430. https://doi.org/10.1002/jssc.201100660.

Gachumi, G., Poudel, A., Wasan, K.M., El-Aneed, A. Analytical Strategies to Analyze the Oxidation Products of Phytosterols, and Formulation-Based Approaches to Reduce Their Generation. Pharmaceutics, 13 (2021), 268. https://doi.org/10.3390/pharmaceutics13020268.

Gallina Toschi, T., Cardenia, V., Bonaga, G., Mandrioli, M., Rodriguez-Estrada, M.T. Coffee Silverskin: Characterization, Possible Uses, and Safety Aspects, J. Agric. Food Chem. 62 (2014), 10836–10844. https://doi.org/10.1021/jf503200z.

Hu, Y., Yang, G., Huang, W., Lai, S., Ren, Y., Huang, B., Zhang, L., Li, P., Lu, B. Development and validation of a gas chromatography-mass spectrometry method for determination of sterol oxidation products in edible oils, RSC Adv. 5 (2015), 41259–41268. https://doi.org/10.1039/c5ra02795k.

Islam, J., Mahmud, N., Oyom, W., Aminzare, M., Tahergorabi, R. Effects of B-sitosterol oleogel on fat uptake reduction, physicochemical properties, oxidative stability, and sensory characteristics of fried surimi fish balls, J. Agric Food Res. 17 (2024). https://doi.org/10.1016/j.jafr.2024.101240.

Jiang, K., Gachumi, G., Poudel, A., Shurmer, B., Bashi, Z., El-Aneed, A. The Establishment of Tandem Mass Spectrometric Fingerprints of Phytosterols and Tocopherols and the Development of Targeted Profiling

Strategies in Vegetable Oils. J. Am. Soc. Mass Spectrom 30 (2019) 1700–1712. https://doi.org/10.1007/s13361-019-02242-2.

Kasprzak, M., Rudzińska, M., Kmiecik, D., Przybylski, R., Olejnik, A. Acyl moiety and temperature affects thermo-oxidative degradation of steryl esters. Cytotoxicity of the degradation products. Food Chem. Toxicol. 136 (2020), 111074. https://doi.org/10.1016/j.fct.2019.111074.

Kmiecik, D., Fedko, M., Rudzińska, M., Siger, A., Gramza-Michałowska, A., Kobus-Cisowska, J. Thermo-Oxidation of Phytosterol Molecules in Rapeseed Oil during Heating: The Impact of Unsaturation Level of the Oil. Foods 10 (2020), 50. https://doi.org/10.3390/foods10010050.

Leal-Castañeda, E.J., Inchingolo, R., Cardenia, V., Hernandez-Becerra, J.A., Romani, S., Rodriguez-Estrada, M.T., Garcia Galindo, H.S. Effect of Microwave Heating on Phytosterol Oxidation, J. Agric. Food Chem. 63 (2015), 5539–5547. https://doi.org/10.1021/acs.jafc.5b00961.

Lütjohann, D., Björkhem, I., Friedrichs, S., Kerksiek, A., Geilenkeuser, W.J., Lövgren-Sandblom, A., Ansorena, D., Astiasar´an, I., Baila-Rueda, L., Barriuso, B., Bretillon, L., Browne, R.W., Caccia, C., Cenarro, A., Crick, P.J., Fauler, G., García- Llatas, G., Griggiths, W.J., Iuliano, L., Lagarda, M.J., Leoni, V., Lottenberg, A.M., Matysik, S., McDonald, J., Rideout, T.C., Schmitz, G., Nunes, V.S., Wang, Y., Zerbinati, C., Diczfalusy, U., Schött, H.F. International descriptive and interventional survey for oxycholesterol determination by gas- and liquid- chromatographic methods, Biochimie 153 (2018) 26–32, https://doi.org/10.1016/ j.biochi.2018.07.016.

Menéndez-Carreño, M., Ansorena, D., Astiasarán, I. Stability of Sterols in Phytosterol-Enriched Milk under Different Heating Conditions, J. Agric. Food. Chem. 56 (2008) 9997–10002. https://doi.org/10.1021/jf802000m.

Menéndez-Carreño, M., Knol, D., Janssen, H.G. Development and validation of methodologies for the quantification of phytosterols and phytosterol oxidation products in cooked and baked food products. J. Chromatogr. A 1428 (2016) 316–325. https://doi.org/10.1016/j.chroma.2015.09.073.

Menéndez-Carreño, M., Steenbergen, H., Janssen, H.G. Development and validation of a comprehensive two-dimensional gas chromatography–mass spectrometry method for the analysis of phytosterol oxidation products in human plasma. Anal. Bioanal. Chem. 402 (2012) 2023–2032. https://doi.org/10.1007/s00216-011-5432-2.

Plat, J., Brzezinka, H., Lütjohann, D., Mensink, R.P., von Bergmann, K. Oxidized plant sterols in human serum and lipid infusions as measured by combined gas-liquid chromatography-mass spectrometry, J. Lipid Res. 42 (2001), 2030–2038. https://doi.org/10.1016/S0022-2275(20)31532-7.

Poudel, A., Gachumi, G., Purves, R., Badea, I., El-Aneed A. Determination of phytosterol oxidation products in pharmaceutical liposomal formulations and plant vegetable oil extracts using novel fast liquid chromatography - Tandem mass spectrometric methods. Anal. Chim. Acta. 1194 (2022), 339404. https://doi.org/10.1016/j.aca.2021.339404.

Poudel, A., Gachumi, G., Wasan, K.M., Dallal Bashi, Z., El-Aneed, A., Badea, I. Development and Characterization of Liposomal Formulations Containing Phytosterols Extracted from Canola Oil Deodorizer Distillate along with Tocopherols as Food Additives. Pharmaceutics, 11 (2019), 185. https://doi.org/10.3390/pharmaceutics11040185.

Rudzińska, M., Olejnik, A., Grygier, A., Kowalska, K., Kmiecik, D., Grudniewska, A., Chojnacka, A., Gòdkowski, W., Maciejewska, G., Przybylski, R. Thermo-oxidative stability of asymmetric distigmasterol-modified acylglycerols as novel derivatives of plant sterols. Food Chem. 390 (2022), 133150. https://doi.org/10.1016/j.foodchem.2022.133150.

Rudzińska, M., Przybylski, R., Wąsowicz, E. Products formed during thermo-oxidative degradation of phytosterols, J. Am. Oil Chem. Soc. 86 (2009) 651–662. https://doi.org/10.1007/s11746-009-1397-0.

Scholz, B., Guth, S., Engel, K.H., Steinberg, P. Phytosterol oxidation products in enriched foods: Occurrence, exposure, and biological effects, Mol. Nutr. Food. Res. 59 (2015) 1339–1352. https://doi.org/10.1002/mnfr.201400922.

Vanmierlo, T., Husche, C., Schött, H.F., Pettersson, H., Lütjohann, D. Plant sterol oxidation products-Analogs to cholesterol oxidation products from plant origin? Biochimie 995 (2013) 464–472. https://doi.org/10.1016/j.biochi.2012.09.021.

Wang, M., Lu, B. How do oxyphytosterols affect human health? Trends Food Sci. Technol. 79 (2018) 148–159. https://doi.org/10.1016/j.tifs.2018.07.002.

Wani, A.K., Rahayu, F., Fauziah, L., Suhara, C. Advances in safe processing of sugarcane and bagasse for the generation of biofuels and bioactive compounds. J. Agric. Food Res. 12 (2023). https://doi.org/10.1016/j.jafr.2023.100549.

Winkler, J.K.,Warner, K., Glynn, M.T. Effect of deep-fat frying on phytosterol content in oils with differing fatty acid composition, J. Am. Oil Chem. Soc. 84 (2007) 1023–1030. https://doi.org/10.1007/s11746-007-1138-1.

Yang, B., Zhao, T., Liu, Y., Lu, B. Guidelines for extraction and quantitative analysis of phytosterols and oxidation products. EFood 4 (2023). https://doi.org/10.1002/efd2.108.

Yang, B.W., Ji, S.Y., Zhao, T., Wang, Z.T., Zhang, Y.S., Pan, Q.N., Huang, W.S., Lu, B.Y. Phytosterols photooxidation in O/W emulsion: Influence of emulsifier composition and interfacial properties. Food Hydrocoll. 142 (2023), 108698. https://doi.org/10.1016/j.foodhyd.2023.108698.

Yang, B.W., Lu, B.Y., Zhao, Y.J., Luo, J.Y., Hong, X. Formation of phytosterol photooxidation products: A chemical reaction mechanism for light-induced oxidation. Food Chem. 333 (2020), 127430. https://doi.org/10.1016/j.foodchem.2020.127430.

Chapter 5

Tannins as natural emulsifiers: enhancing oxidative stability in oil-in-water emulsions and their potential synergistic effect

5.1 Abstract

Lipid oxidation represents a major challenge in the preservation of food quality, particularly in lipid-rich and emulsified systems where the large oil–water interface accelerates oxidative reactions. Due to their structure properties, tannins can localize at the oil–water interface, where they act both as physical stabilizers and potent antioxidants. This study investigates the efficacy of two plant-derived tannins, extracted from chestnut (C) and quebracho (Q) in improving the oxidative and physical stability of O/W emulsions. Emulsions were formulated with 10% of stripped sunflower oil (SF) or lipid fraction of egg yolk (EY) with tannins incorporated at concentration of 0.1% and 0.2% (*w/v*). Tween-20 was used as surfactant and partially replaced by tannins. Throughout 14 days of storage at 40 °C, and at two pH levels (3.5 and 7.0), the evolution of peroxide values, aldehydes, sterol oxidation products (SOPs), particle size, and ζ-potential was monitored. Tannins markedly reduced the formation of primary and secondary oxidation products. Notably, quebracho tannins increased the negative surface charge of emulsion droplets, contributing to improved physical stability. In EY-based emulsions, pH 7.0 proved more effective, potentially due to a synergistic effect between chestnut tannins and lutein. These findings highlight the potential of tannins as multifunctional, natural ingredients for improving the shelf life and stability of emulsified food systems.

5.2 Introduction

Lipid oxidation represents a critical factor in the food quality deterioration, adversely affecting both the nutritional profile and sensory attributes of products, while also generating compounds that pose risks to human health. This complex process is triggered and accelerated by exposure to oxygen, elevated temperatures, light, and transition metals, leading to the formation of reactive species such as hydroperoxides, aldehydes, and ketones (McClements & Decker, 2018). Particularly, in lipid-rich food matrices, such as fatty acids and sterols, oxidation leads to the generation of primary (hydroperoxides) and secondary oxidation products, such as volatile and non-volatile compounds as sterol oxidation products (SOPs) that severely compromise safety and palatability. This challenge becomes even more pronounced in emulsified food systems, notably in oil-in-water (O/W) emulsions. The latter are the backbone of numerous everyday food products such as sauces, dressings, mayonnaise, and dairy-based beverages, each characterized by a diverse composition in lipid content. The large surface area between the dispersed oil droplets and the continuous aqueous phase provides a highly reactive interface, where lipids are exposed to aqueous-phase prooxidants such as metal ions, photosensitizers, and enzymes, thereby accelerating oxidation processes (Cercaci et al., 2007; Waraho et al., 2011a). Furthermore, beyond chemical deterioration, O/W emulsions are thermodynamically unstable systems prone to physical destabilization phenomena such as coalescence, flocculation, and Ostwald ripening, which, if left unchecked, ultimately lead to phase separation (Vratsanos & Gianneschi, 2022). The widespread use of emulsions in foods rich in lipid matrices underscores the urgent need for effective strategies to combat both oxidation and physical instability. Conventional approaches typically rely on the incorporation of antioxidants, which act through mechanisms including free radical scavenging, metal chelation, and singlet oxygen quenching. However, in emulsified systems, the effectiveness of these antioxidants is often limited by their inadequate partitioning at the oil-water interface (McClements & Decker, 2018). Simultaneously, growingly

consumer demand for natural, health-promoting ingredients has intensified the search for clean-label solutions capable of stabilizing emulsions without synthetic additives.

In this context, a promising avenue lies in the use of amphiphilic plant-derived molecules capable of performing dual functions. While proteins and phospholipids have long been recognized as effective emulsion stabilizers (McClements et al., 2017; McClements & Decker, 2018) recent studies have increasingly focused on lipophilized phenolic compounds, whose intrinsic amphiphilicity enables them to localize at the oil-water interface and directly counteract lipid oxidation (Cantele et al., 2025; Delfanian et al., 2023). Among these, tannins could be promising candidates. Tannins are polyphenolic compounds abundantly present in various plant tissues, including bark, leaves, and fruits. Structurally, they encompass both hydrolysable tannins and condensed tannins (proanthocyanidins), which possess multiple hydroxyl groups and aromatic rings that confer amphiphilic characteristics (Molino et al., 2023). This structural duality enables tannins to localize effectively at the oil-water interface, where they can act as emulsifiers and antioxidants suggesting that they could improve the physical stability of the emulsion, making them attractive candidates for natural stabilization strategies (Figueroa-Espinoza et al., 2015). The antioxidant efficacy of tannins is well-documented, encompassing free radical scavenging, metal ion chelation, and inhibition of prooxidative pathways. Beyond their antioxidant capacity, tannins also exhibit a wide range of bioactivities, including antimicrobial, anti-inflammatory, antiviral, and prebiotic effects, enhancing their appeal as multifunctional food ingredients (Liu et al., 2024; Molino et al., 2024).

The current work aims to investigate the potential of two specific tannins, derived from chestnut and quebracho, to enhance both the oxidative and physical stability of oil-in-water emulsions. The present work has studied the impact of tannin concentration (0.1% and 0.2% w/v) and pH (3.5 and 7.0) on their functional performance, considering the established impact of these parameters on tannin activity and interfacial behavior.

5.3 Material and Methods

5.3.1 Chemicals and Materials

All solvents and reagents were of analytical grade. Tween 20, activated charcoal, BHT, and iron chloride were purchase from Sigma-Aldrich (St. Louis, MO, USA). Diethyl ether, n-hexane (99.0%), ethyl acetate, iso-octane, and potassium hydroxy were obtained from Carlo Erba (Milan, Italy). Ethanol, methanol, acetone, and methanol + 0.1% formic acid were purchased from Honeywell (Morristown, NJ, USA). Butanol was purchased from Alfa Aesar (Haverhill, MA, USA). Propan-2-ol and formic acid were obtained from Merck (Burlington, MA, USA). Ammonium thiocyanate was purchased from Thermo Fisher (Waltham, MA, USA). Milli-Q filter system (Millipore, Milan, Italy) was used to prepare double distilled water. N° 1 filter papers were purchased from Whatman (Maidstone, England). Solid-phase extraction (SPE) cartridges (Strata® NH2, 55 µm, 70 Å, 500 mg/3 mL) were provided by Phenomenex (Torrence, CA, USA). Quebracho tannin and Chestnut tannins extract were supplied by SILVATEAM (Mondovì, Italy). Sunflower oil and egg yolk were purchased from local market.

5.3.2 Stripping of sunflower oil

In order to avoid bias in evaluating the antioxidant activity of tannins, the natural tocopherols present in the sunflower oil were removed according to Abad & Shahidi, (2020) with slight modification. Sixty grams of sunflower oil were mixed with 60 mL of *n*-hexane and stirred with 45 g of activated charcoal for 2 hours at room temperature (25 °C). Then, the oil was filtered by Buchner funnel with filter paper (Whatman no. 1) and the solvent was removed using a rotary evaporator at 35 °C, followed by nitrogen flushing. Quality control before and after the stripping of the oil was performed with GC-FID (GC-2010 Plus, Shimadzu, Kyoto, Japan) in order to verify the efficacy remotion of natural antioxidant (supplementary material 6.3).

5.3.3 Lipid extraction from egg yolk

The lipid fraction from egg yolk was obtained following the method reported by Kovalcuks (2014). Liquid egg yolk was mixed with ethanol (2:1, *v/v*) and stirred for 30 minutes. The solution was then vacuum-filtered, and the solid residue was washed twice with *n*-hexane. Solvent was subsequently removed using a rotary evaporator (Rotavapor ® R-210, Büchi, Flawil, Switzerland). The free cholesterol content of the obtained lipid fraction was determined using gas chromatography coupled with a flame ionization detector (Shimadzu, Kyoto, Japan), equipped with UltiMetal capillary column (25 m × 0.25 mm × 0.10 µm; Agilent, Santa Clara, CA, US), under the following parameters: oven temperature was set from 100°C to 360 °C with rate of 15°C/min. The injector and detector temperatures were set at 355 °C and 340 °C, respectively. Helium was chosen as carrier gas with linear velocity of 40.4 cm/sec. The injection was performed in split mode (ratio 1:30).

5.3.4 Emulsion preparation

O/W emulsions were prepared according to Figueroa-Espinoza et al., (2015). Twenty-four hours prior to preparation, tannins (chestnut, C; Quebracho, Q) were dissolved in phosphate buffer solution (10 mmol/L, pH 7.0 or pH 3.5) at two concentrations (0.1 % and 0.2 % of the total volume of buffer, *w/v*) as a substitute for 1% of Tween 20. Subsequently, stripped sunflower oil (SF) or egg lipid yolk (EY) (10% of the total weight of the emulsion; *w/w*) was added to the aqueous solution and pre-emulsified using an IKA T25 digital Ultra-Turrax (IKA-Werke GmbH & Co. KG, Staufen, Germany) for 2 minutes at speed of 20,000 rpm. The pre-emulsion was further homogenized by ultrasound sonication for 3 minutes (cycles of 30 seconds of sonication alternated with 30 seconds off) at 40% of amplitude. The temperature was continuously monitored during the process and maintained lower than 30 °C. A control sample (C), prepared without tannins and with 1% of Tween 20, was also prepared in parallel. At the end, 2 mL of emulsion were transferred in 20 mL headspace vials previously pre-cleaned with 1N HCl solution to remove metal residues. The vials were sealed with aluminium caps with

PTFE/silicone septa and stored in darkness at 40°C for 14 days. Each experiment was repeated in triplicate.

5.3.5 Primary oxidation products

The peroxide value (PV) were analyzed using the method described by Shantha & Decker, (1994) in order to monitor the primary oxidation products. Three-hundred microliters of the emulsion were dissolved in an iso-octane/propan-2-ol solution (3:1, *v/v*) and vigorously shaken. The mixture was then centrifuged at 3,400 × *g* for 2 minutes, and the supernatant was added to a methanol/butanol solution (2:1, *v/v*). Ammonium thiocyanate (30%, *w/v*, 15 µL) and iron (II) chloride (15 µL) were then added and, after 20 minutes at room temperature in the dark, absorbance was measured at 510 nm. A standard calibration curve for cumene hydroperoxides (10–300 µmol/L) was used for quantification. Results from three separate replicates were expressed as millimoles of hydroperoxides per kilogram of oil (mmol/kg oil).

5.3.6 Secondary oxidation products

Hexanal was determined using headspace solid-phase microextraction (HS-SPME) combined with gas chromatography-mass spectrometry (GC-MS) (QP-2010 Plus, Shimadzu, Kyoto, Japan), following the method reported by Cantele et al., (2025) with some modifications. Sample vials were preheated at 40 °C for 10 minutes, after which a divinylbenzene/carboxen/polydimethylsiloxane (DVB/CAR/PDMS) fiber (df 50/30 µm; 1 cm; Supelco, Bellefonte, PA, USA) was exposed to the vial headspace for 5 min. The fiber was then desorbed in the GC injector at 260 °C for 3 min in split mode (1:50), using helium as the carrier gas at a constant linear velocity of 34.8 cm/s. The GC system was equipped with a Stabilwax-MS capillary column (30 m × 0.25 mm × 0.25 µm; Restek, Centre County, PA, USA). The oven temperature program was as follows: initial hold at 40°C for 1 min, ramp to 100 °C (5 °C/min), then increased to 240 °C at 10 °C/min, with a final hold time of 1 min.

The transfer line and ion source temperatures were set at 230 °C and 200 °C, respectively. Ions were acquired in scan mode within a 33–350 m/z range at a scan speed of 1666 amu/s. Hexanal was identified by comparing the mass spectra with those in the NIST08s library. The results are reported as absolute area of signal peak and represent the mean of three independent replicates.

5.3.7 Particle size and ξ-potential measurements

An aliquot of emulsion was diluted with a proper buffer solution at ratio 1:50 (*v/v*). After filling Folded Capillary Zeta Cell (DTS1070, Malvern Panalytical, UK) with the solution, particle size and zeta potential were determined using a Zetasizer Pro (Malvern Instruments, Worcestershire, UK) through dynamic light scattering. The results are reported as the mean of three independent replicates.

5.3.8 Sterols Oxidation Products (SOPs)

The oxidation of sterols in emulsion samples was monitored through the determination of COPs and POPs for EY and SF, respectively. Three mL of emulsion (namely, 300 mg of lipid matter) were saponified with 10 mL oh KOH 4N with BHT (0.5 mg/mL) for 18 hours, in dark at room temperature. Then, the extraction of the unsaponifiable fraction was obtained with 10 mL of diethyl ether and 10 mL of bi-distilled water. The organic phase was recovered and the water added of 10 mL of diethyl ether. The two organic phases were combined, and the solvent was removed with a rotary evaporator (Rotavapor® R-210, Büchi, Flawil, Switzerland). Purification and concentration of the COPs were obtained with NH_2- solid phase extraction (Phenomenex, Torrence, CA, USA) following the method reported by Rose-Sallin et al., (1995). Briefly, after activation of the stationary phase with 5 mL of *n*-hexane, the sample was inserted in a NH_2-cartridge and eluted with 6 mL of hexane-ethyl acetate (95:5 *v/v*) and 10 mL of hexane-ethyl acetate (90:10 *v/v*). The COPs fraction was collected with 10 mL of acetone. On the other side, the purification and concentration of POPs were obtained with Si-solid phase extraction following the method reported by Hu et al. (2015). Again, after activation of

stationary phase with 5 mL of *n*-hexane, 10 mL of hexane-diethyl ether (90:10, *v/v*) and 10 mL of hexane-diethyl ether (95:5, *v/v*) were eluted. The POPs fraction was collected with 10 mL of acetone, as for COPs.

The acetone of both SOPs was removed with a stream of nitrogen and the samples dissolved in 100 µL of methanol. Five µL were injected in Shimadzu Nexera X3 UHPLC, equipped with a Kinetex C18 column (2.6 µm, 100 Å, 100 × 2.1 mm, Phenomenex, Torrence, CA, USA) protected by a guard column. The mobile phase was composed of water with 0.1% formic acid (A) and methanol acidified with 0.1% formic acid (B). Separation of the SOPs was obtained with the gradient program reported by Wang et al. (2019): 0–0.5 min 80% B, linear gradient from 80% B to 100% B in 8 min, held for 4 min then switched back to 80% B and re-equilibrated for 4 min. The flow rate was 0.2 mL/min. The column temperature was set at 40 °C and the injection volume was 2 µL. The detection and quantification were performed using an AB Sciex 3200 QTRAP mass spectrometer (AB Sciex, Concord, ON, Canada) equipped with an atmospheric pressure chemical ionization (APCI) source. Tandem mass spectrometric analysis (MS/MS) was employed in positive ionization mode. Interface parameters were set as follows: source temperature 380 °C, curtain gas 35 psi, nebulizer current 3.0 µA. Direct infusion was performed to optimize the ion source and compound dependent parameters for peak intensity and signal stability. In addition, commercial standards of COPs, as well as isolated and purified POPs as described in Chapter 4 (Bonciolini et al., 2025), were used to build the calibration curves for each considered compound.

5.3.9 Statistical Analysis

To investigate the formation of tannins-sterols aggregate, one-way analysis of variance (one way ANOVA) and Tukey's post hoc test was used to determine any statistical difference between the samples at a confidence level of 95%. IBM SPSS statistical software (version 29; IBM, Chicago, USA) was used.

5.4 Results

5.4.1 Effect of tannin in lipid oxidation

The lipid oxidation rate in each O/W emulsion was evaluated by systematically monitoring the formation of lipid hydroperoxides and headspace hexanal, which serve as reliable indicators of primary and secondary lipid oxidation products, respectively. Since the tocopherol extraction plays a pivotal role in the initiation of lipid oxidation processes, the peroxide value (PV) in SF emulsion was immediately measured following the whole experiment to assess the lag phase of oxidation. The fresh oil exhibited a PV of 1.07 ± 0.02 mmol O_2/kg, indicating minimal oxidation, whereas the oil subjected to carbon treatment displayed a PV of 2.40 ± 0.12 mmol O_2/kg, reflecting a significant rise in oxidation levels (data not shown). Figure 5.1 reports the results related to PV in SF and EY emulsions throughout the 14 days of experiment. A different behavior was denoted as related to the lipid matter considered; SF reported higher amount than EY emulsion. In control SF emulsion, immediately after emulsions preparation, the PV was significantly higher (p<0.001) compared to the samples containing tannins. Throughout the experiment, it was evident that the presence of tannins significantly reduced (p<0.001) the generation of hydroperoxides. Again, the PV reduction was correlated to the concentration of tannins: the 0.1% of both tannins resulted in higher PV levels, particularly at pH 3.5 (110.04 ± 2.05 mmol/kg of oil for C and 110.79 ± 24.33 mmol/kg of oil for Q at day 14) compared to pH 7 (44.38 ± 11.04 mmol/kg of oil and 23.67 ± 4.17 mmol/kg of oil with, respectively, C and Q at day 14). The 0.2% reported a lower value in PV content in acidic environment, without significant (p>0.05) differences between them (p>0.05) (15.58 ± 0.94 mmol/kg of oil and 16.40 ± 6.63 mmol/kg of oil for, respectively, C and Q) respect to neutral conditions (0.2C, 43.00 ± 0.04 mmol/kg of oil; 0.2Q, 62.19 ± 5.17 mmol/kg of oil).

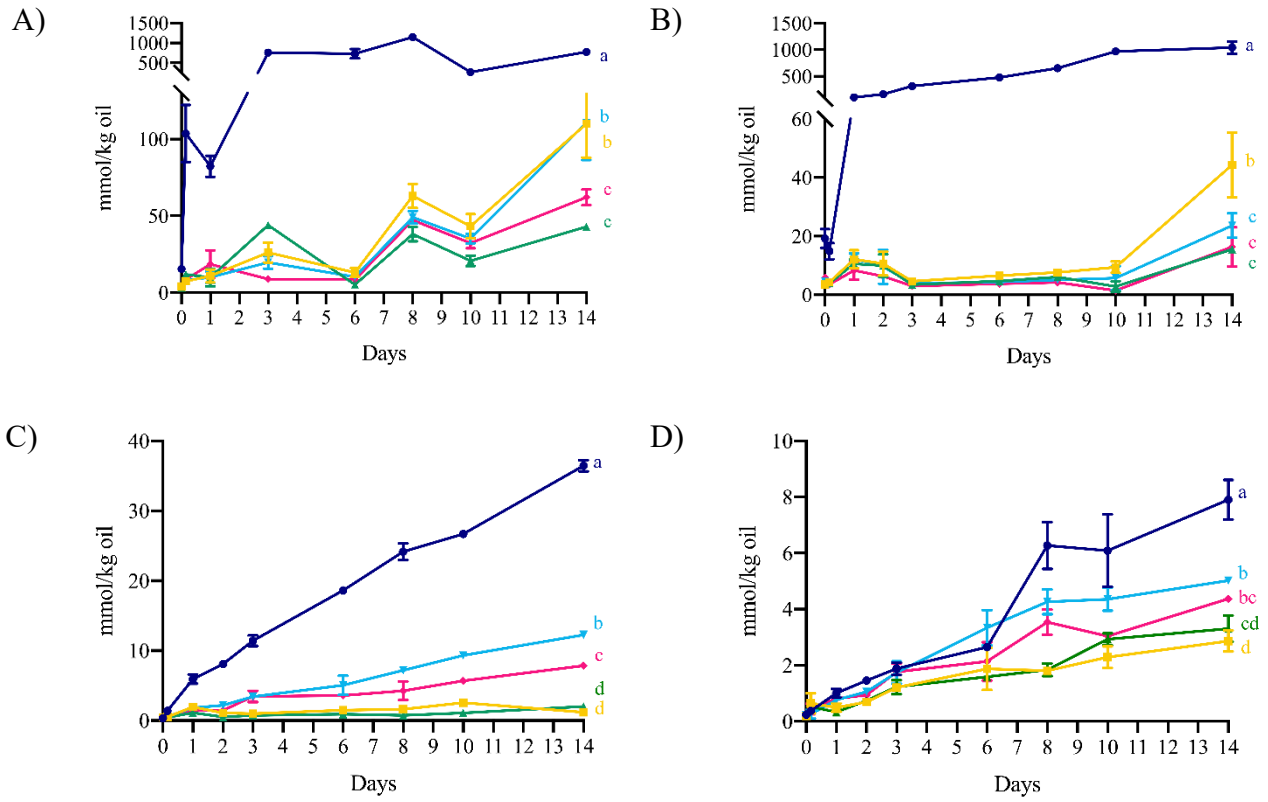

Figure 5.1. Hydroperoxides content in the O/W emulsions during 14 days of storage. A) SF at pH 3.5; B) SF at pH 7.0; C) EY at pH 3.5; D) EY at pH 7.0: (●) Control, (■) 01C, (▲) 02C, (▼) 01Q. (♦) 02Q. Each point represents the mean ± standard deviation of three independent replicates (n=3). Results of ANOVA with Tukey's post hoc test are reported; different letters indicate significantly different means (p<0.05) among the samples.

Again, in EY emulsions, acidic pH favored the peroxides production. The higher level of PV was observed in control samples at pH 3.5, reaching a content of 36.44 ± 0.81 mmol/Kg oil at day 14. At pH 7, C sample reached a PV of 7.90 ± 0.71 mmol/Kg oil at the same day, which corresponds to a reduction of 78% with respect that observed at acidic condition. The presence of tannins in both pHs significantly (p<0.05) counteracted the formation of hydroperoxides. The best antioxidants activity was obtained at pH 3.5 with chestnut tannin; after 14 days of storage no significant differences (p>0.05) were observed (1.17 ± 0.33 and 2.02 ± 0.28 related to concentration 0.1% and 0,2%, respectively). On the other hand, peroxides formation under neutral conditions was strongly reduced in control samples.

The results of hexanal content (Figure 5.2) in SF reflect a similar trend observed for peroxides.

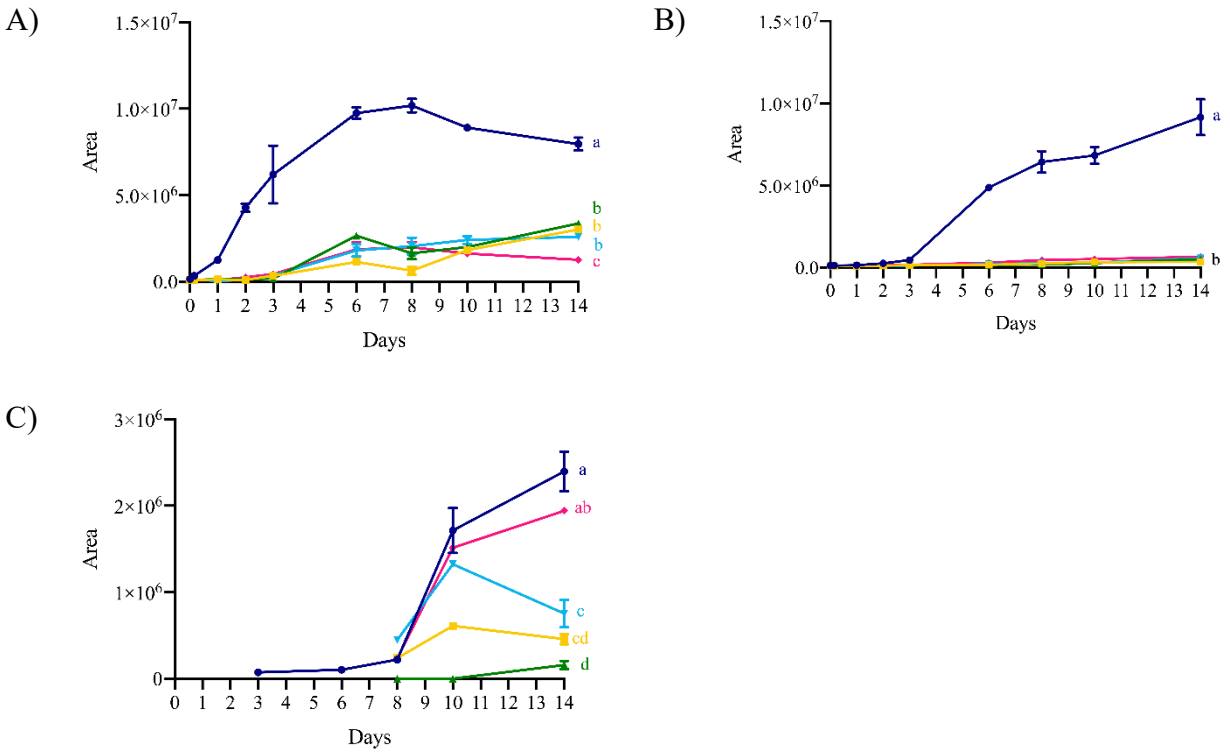

Figure 5.2. Hexanal content in the emulsions during 14 days of storage. A) SF at pH 7.0; B) SF at pH 3.5; C) EY at pH 3.5: (●) Control, (■) 01C, (▲) 02C, (▼) 01Q. (♦) 02Q. Each point represents the mean ± standard deviation of three independent replicates (n=3).

Tannins reduced the hexanal formation (p<0.001) compared to the control at both pH values. However, hexanal registered higher values under acidic conditions, where no differences (p>0.05) were observed between tannin-samples except for 02Q that reduced the formation of hexanal even more. Moreover, the increase in hexanal levels was observed only after the 3 days at pH 7.0, whereas at acidic condition, an increase (p<0.01) was already detectable after just 1 day. On the other hand, in EY emulsion hexanal was noticed only in control sample at pH 3.5 after 8 days, while in neutral environment no trace of aldehydes was observed throughout the whole experiment.

5.4.2 Particle size e ζ-potential

The droplets size was analyzed to evaluate the physical stability of the emulsified system over the storage time. Instabilities, such as flocculation, creaming and coalescence, involve the clustering of oil particles ultimately leading to the separation of the dispersed phase from the continuous phase and resulting in a loss of emulsion stability. The dimension of the particles is depicted in Figure 5.3.

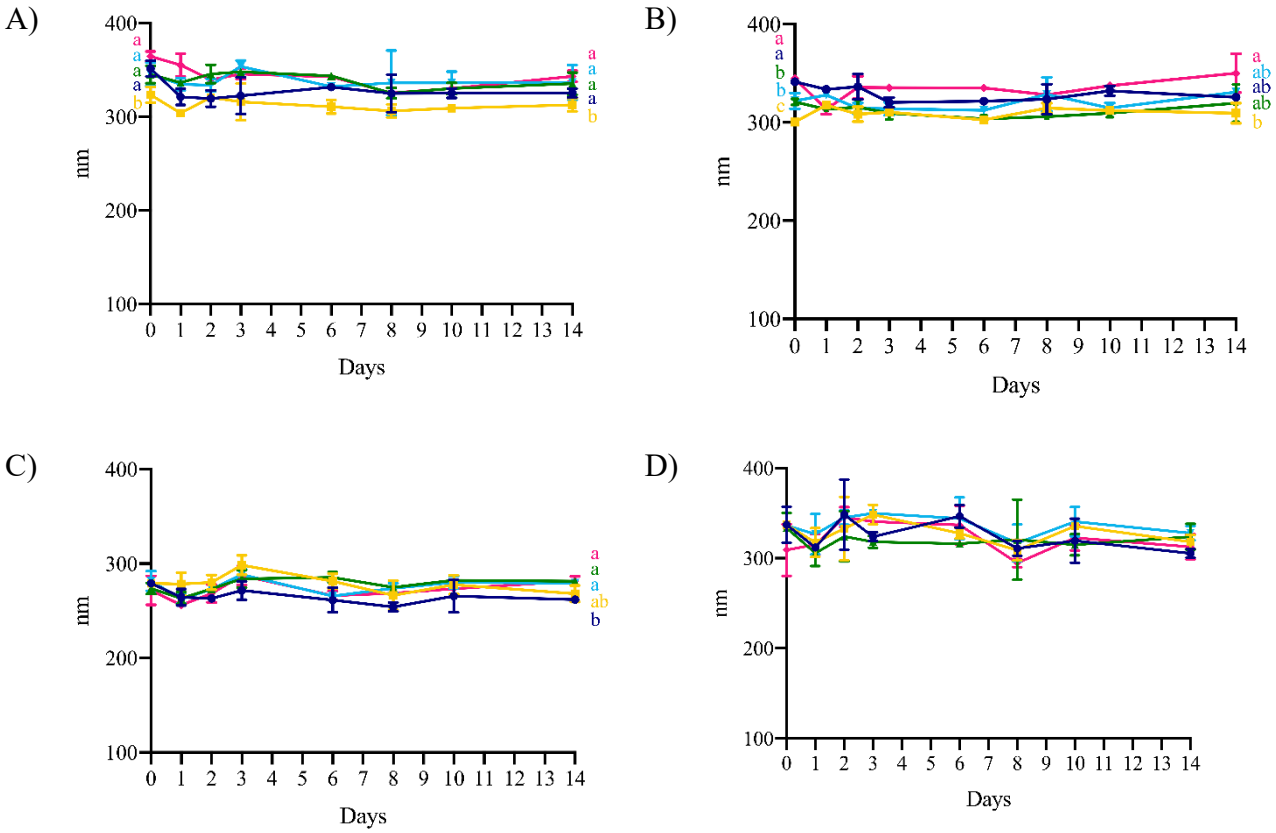

Figure 5.3. Particle size (nm) of the control emulsion and emulsion with tannin. A) SF at pH 7.0; B) SF pH 3.5; C) EY at pH 7.0; D) EY at pH 3.5: (●) control, (■) 01C, (▲) 02C, (▼) 01Q. (♦) 02Q. Each pc represents the mean ± standard deviation of three independent replicates (n=3)3). Results of ANOVA w Tukey's post hoc test are reported; different letters indicate significantly different means (p<0.05) among samples.

In general, particle size ranged between 300 and 360 nm, except for EY at pH 7.0 where smaller size was observed. In EY emulsion (Figure 3.C), the initial particle size of all samples ranged between 271 ± 15.15 nm and 281 ± 10.65 nm (day 0). No significant (p>0.05) differences were observed at

the beginning of the experiment. Over time, slight variations in particle size were observed but differences among the control sample and emulsion with tannins were not significant (p>0.05) until day 14. On the last day, however, control sample showed the smallest particle size (p<0.05) with respect to tannins-emulsions. The presence of Q led to larger particles, while 01C formed smaller particles at both pH conditions at the beginning and on the last day of experiment. A similar trend was observed using pH 7.0, but with slightly larger particle sizes value compared to the acidic condition (ranging from 309.23 ± 28.86 nm to 337.16 ± 19.94 nm at day 0). Throughout the experiment, no significant differences (p>0.05) were identified among all samples, especially for SF emulsions

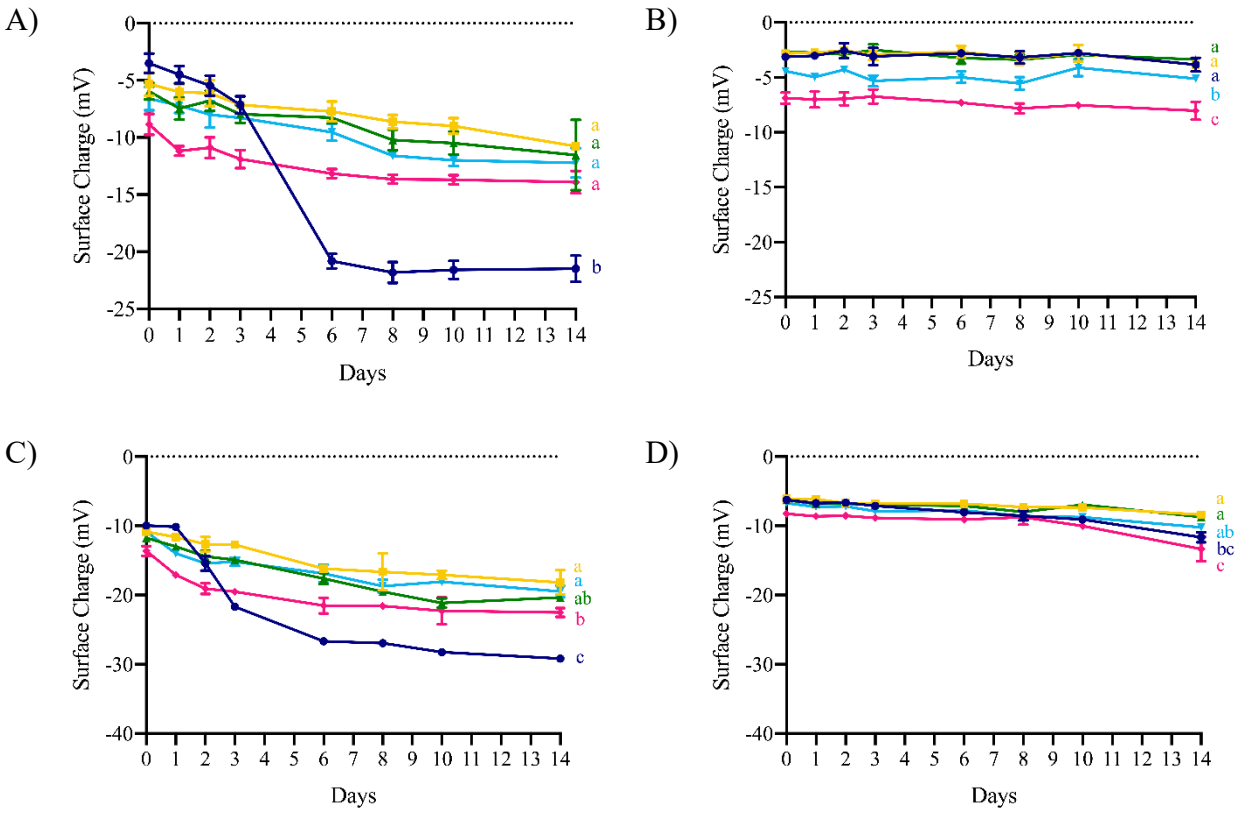

Figure 5.4. ξ-potential (mV) of the control emulsion and emulsion with tannin. A) SF at pH 7.0; B) SF at pH 3.5; C) EY at pH 7.0; D) EY at pH 3.5: (●) Control, (■) 01C, (▲) 02C, (▼) 01Q. (♦) 02Q. Each point represents the mean ± standard deviation of three independent replicates (n=3). Results of ANOVA with Tukey's post hoc test are reported; different letters indicate significantly different means (p<0.05) among the samples.

The measurement of ζ-potential provides valuable insights into the electrostatic stability of emulsions. It reflects the surface charge of the dispersed droplets and, consequently, the strength of repulsive forces between them. In oil-in-water emulsions, a high absolute ζ-potential (either positive or negative) typically indicates stronger inter-droplet repulsion, reducing the risk of coalescence and phase separation over time. Figure 5.4 shows the surface charge verified for all samples over 14 days of storage. Initially, control samples displayed a negative surface charge. In the SF, the ζ-potential was −3.14 ± 0.19 mV and −3.48 ± 0.86 mV at pH 3.5 and 7.0, respectively. In contrast, EY exhibited a more negative surface charge: −6.25 ± 0.42 mV at pH 3.5 and −9.94 ± 0.31 mV at pH 7.0. The addition of tannins increased the negative surface charge, particularly quebracho tannin, where the 0.2% concentration showed the highest negative value for all cases. The pH had a notable effect on ζ-potential: pH 7.0 consistently led to more negative charges across all samples, while acidic conditions (pH 3.5) attenuated this effect. In SF emulsions at pH 7.0, significant differences were observed between control and tannin-enriched emulsion for 02C, 01Q, and 02Q (p<0.01). At pH 3.5, chestnut tannin did not significantly differ from the control (p>0.05). In EY emulsions at pH 7.0, only quebracho tannins resulted in significant differences compared to the control (p<0.01), whereas at pH 3.5, no significant differences were observed among samples, except for 02Q. Overall, emulsions stored at pH 3.5 maintained more stable ζ-potential values throughout the 14-day period. Conversely, at neutral pH, the ζ-potential became progressively more negative over time. Notably, the control samples showed a sharp drop in surface charge after day 3 in SF (reaching −20.83 ± 0.66 mV) and after day 2 in EY (−21.70 ± 0.42 mV).

5.4.3 Sterol Oxidation Products (SOPs)

The most abundant POPs present in seeds oil are 7-hydroxy, 5,6α/β epoxy and keto isomers. In the present study, the POPs originated from the main phytosterols (β-sitosterol, campesterol, stigmasterol) were monitored during the whole experiment.

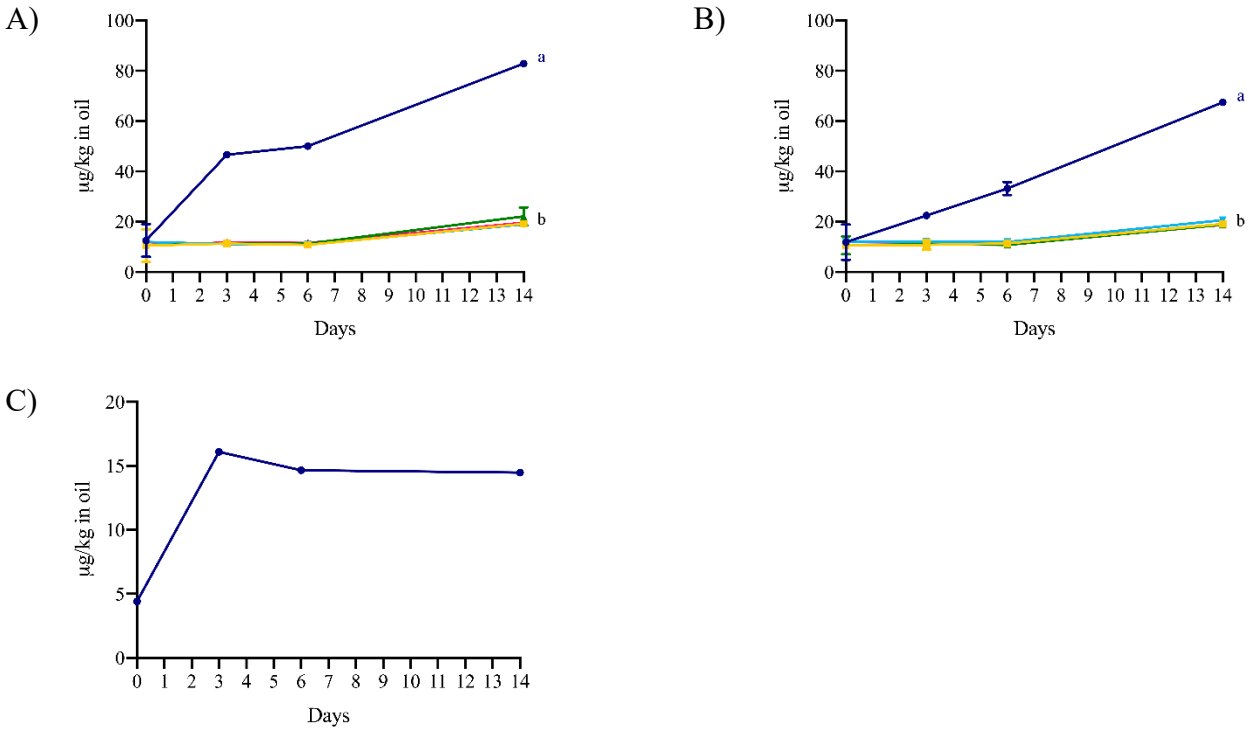

Figure 5.5. Total content of Phytosterol Oxidation Products (POPs) (ppb on oil in emulsion) of control and emulsion with tannin. a) pH 7.0; b) pH 3.5: Cholesterol Oxidation Products of control c) pH 3.5. (●) control, (■) 01C, (▲) 02C, (▼) 01Q. (♦) 02Q. Each point represents the mean ± standard deviation of three independent replicates (n=3). Results of ANOVA with Tukey's post hoc test are reported; different letters indicate significantly different means ($p< 0.05$) among the samples.

The total amount of POPs in each emulsion is depicted in Figure 5.5. Again, the antioxidant activity of tannins resulted in a significant reduction in POPs formation compared to the control ($p<0.001$). The acid environment represents a favorable condition for limiting oxidation in the control sample as well. However, after 6 days of storage, significant differences were observed in the control samples ($p<0.05$), where at pH 7 the POPs level (equal to 50.07 ± 4.05 µg/kg) was higher than that determined at pH 3.5 (33.20 ± 2.63 µg/kg). In contrast, the tannin-enriched emulsions did not differ from each other until the last day of sampling, and no differences ($p>0.05$) were observed comparing the pH conditions. Regarding the emulsions prepared with the lipid fraction extracted from egg yolk, COPs were only detected under acidic condition and in the control sample, whereas in the emulsions containing tannins COPs were present only in traces amount. At pH 7.0, COPs were found only in

traces amount even in control sample. Moreover, with respect to SF control, the concentration of COPs was, at least, 10 times lower considering the same conditions. Considering the individual molecules of POPs, the keto forms of sitosterol and campesterol were detected only in the control sample until day 6; after that, their presence was also observed in the tannin-enriched emulsions at both pH values considered (Appendix 5.6.1 and 5.6.2). Moreover, 7-ketostigmasterol was detected in control samples on the last day of the experiment. Additionally, no differences (p>0.05) were appreciated between control and other samples until day 6 with pH 3.5, in which control is well distinguished from tannin emulsion, while at pH 7.0 control started to differentiate at day 3. However, between samples with tannins no differences (p>0.05) were detected. Again, in EY (Appendix 5.6.3) 7-ketocholesterol was the last compounds formed in control emulsion. Surprisingly, while the sum of hydroxy, keto and β-epoxy did not show differences (p>0.05) during the experiment, α-epoxy cholesterol content increased after 3 days (p<0.01) of storage.

5.4 Discussion

The aim of this work was to investigate whether the use of two types of tannins could effectively enhance the oxidative stability of oil-in-water (O/W) emulsions, by exploiting their amphiphilic nature, which enables their partitioning at the droplet interface. Emulsions are complex systems consisting of two immiscible liquids, stabilized by emulsifiers. The size of the dispersed droplets plays a critical role in determining both the physical stability and the oxidative susceptibility of emulsions. Instabilities such as flocculation, creaming, and coalescence involve the aggregation of oil droplets, ultimately leading to phase separation and loss of emulsion stability. In food systems, droplet sizes can range from 0.2 μm to 100 μm, meaning that the surface area of lipid exposed to the aqueous phase can vary significantly across different studies (McClements & Decker, 2000), complicating direct comparisons. Generally, smaller droplet sizes result in a higher surface area, which increases lipid exposure at the oil–water interface and accelerates oxidation (Lethuaut et al.,

2002). However, smaller droplets may also promote a more efficient distribution of antioxidants, potentially counteracting oxidative degradation. Interestingly, Waraho et al. (2011) reported that the droplet size surface in emulsions has minimal impact on oxidation rates, suggesting that a large surface area is not the key point in limiting the reaction rates. Particle sizes achieved in the present study were larger compared to the values reported in other studies, where optimal droplet sizes are typically around 200 nm (Cantele et al., 2025; Inchingolo et al., 2021; Uluata et al., 2016). That results may be attributed to the concentration of Tween-20 used in this study (1% *v/v*). Given to the low critical micelle concentration (CMC) of Tween-20 (10-50 μM) only a small fraction is adsorbed at the oil–water interface, while the majority remains in the continuous phase, forming micelles capable of solubilizing components from the dispersed phase (Inchingolo et al., 2021). Teo et al. (2016) reported that increasing the concentration of Tween-20 from 0.75 % to 5 % (*w/w*), the particle size reached 120-450 nm, suggesting that unabsorbed micelles may induce flocculation through depletion interactions, leading to the formation of droplet aggregates with larger dimensions. Nevertheless, under the tested conditions, and despite the relatively large particle size, the emulsions exhibited good kinetic stability, with no visible marks of physical destabilization over 14 days of storage ($p<0.05$). That was confirmed by the consistent particle size distribution and unaltered visual appearance throughout the study period. Significant differences ($p<0.05$) observed among samples in the sunflower oil (SF) emulsions suggested that tannins may influence the interfacial properties of the emulsions. Notably, the 0.1% of chestnut tannin (01C) led to the smallest particle size compared to the quebracho tannin (Q) samples, under both pH conditions. In contrast, no significant differences ($p>0.05$) were observed between samples in the egg yolk lipid (EY) emulsions across both pH levels during the entire study period. Moreover, at pH 3.5, emulsions displayed smaller droplet sizes compared to other conditions. Similar results were obtained by Cantele et al. (2025), while Teo et al. (2016) reported that emulsions formulated with Tween-20 were also stable to pH change in a range between 2 and 10, due to its non-ionic nature characteristics.

A key characteristic of an effective emulsifier is its ability to establish strong repulsive interactions between droplets within an emulsion. Indeed, emulsion stability is governed by the balance between attractive forces (Van der Waals, hydrophobic interactions, electrostatic attractions, hydrogen bonding) and repulsive forces (electrostatic and steric repulsion) acting between dispersed droplets (Guzey & McClements, 2007). In oil-in-water emulsions, these interactions can be either electrostatic or steric. For electrostatic repulsion, the emulsifier must own sufficient charged groups to generate a high surface potential, whereas steric repulsion requires the presence of polymeric polar chains extending into the aqueous phase at high surface density (McClements & Decker, 2000). Results from the ζ-potential analysis suggest that tannins, particularly the quebracho type, tend to partition at the droplet interface alongside polysorbate, increasing the negative surface charge. Tannins are amphiphilic, often polymeric molecules characterized by a hydrophobic aromatic core surrounded by hydroxyl groups. The higher negative charge observed in emulsions containing tannins, compared to the control at the beginning of the experiment, indicates that tannins contribute to the electrostatic repulsion between droplets, thereby helping to maintain dispersion in the aqueous phase and enhancing system stability. Although, Tween 20 is typically classified as non-ionic and thus expected to confer no surface charge in control samples, the detection of a negative surface charge is not surprising. Similar observations have been reported by other authors (Cantele et al., 2025; Teo et al., 2016; Waraho et al., 2009). This phenomenon can be attributed to possible impurities in Tween 20, the presence of free fatty acids in the system, or the preferential adsorption of hydroxide ions (OH^-) over hydronium ions (H_3O^+) at the droplet interface (Vácha et al., 2011). When neutral conditions are considered, a progressive increase in negative charge was observed across all samples. Notably, in control emulsions, the surface charge dropped sharply after day 3 for the SF emulsions and after day 1 for the EY emulsions. Conversely, at pH 3.5, the surface charge remained stable over the storage period in SF emulsions and increased only on the last day in EY emulsions. Lipid oxidation produces compounds with distinct chemical properties, as previously investigated by other authors (Waraho et

al., 2009, 2011a). Molecules generated from lipid degradation with pKa below the operating pH can reach the interface and make the surface more negative. For instance, due to their amphiphilic nature, free fatty acids act as surface-active compounds, tending to accumulate at the droplet interface. At pH 7.0, which exceeds their pKa values (4.8–5.0 for fatty acid chains with >C10), the deprotonated forms predominate. The addition of chestnut tannin did not significantly affect the surface charge compared to the control (p>0.05) under acidic conditions. At neutral pH, only the higher concentration (0.2%) resulted in a significant difference from the control (p<0.05), making it challenging to confirm its effective partitioning at the interface. Chestnut tannins are primarily hydrolysable, rich in ellagic and gallic acid esterified on a glucose backbone (Khatib et al., 2023; Sanz et al., 2010). Gallic acid exhibits multiple acidic protons with distinct pKa values and can adopt different ionization states depending on the pH of the solution. Its three phenolic -OH groups remain largely protonated under the pH conditions tested, as their pKa values exceed 8 (Badhani & Kakkar, 2017; Eslami et al., 2010). Meanwhile, the carboxylic group (-COOH) has pKa of approximately 4, meaning that at pH 3.5 is only in partial deprotonation. In contrast, quebracho tannin significantly increased the negative charge (p<0.05) at both pH levels and across both lipid sources, suggesting an enhancement of emulsion stability compared to both the control and chestnut-tannin emulsions. Quebracho tannins are mainly composed of proanthocyanidins, consisting of catechin units linked to ent-fisetinidol extender units (Pasch et al., 2001; Venter et al., 2012), whose phenolic groups have pKa values exceeding 9. Consequently, under the experimental conditions tested, quebracho tannins were expected to remain predominantly protonated, despite the observed increase in negative surface charge. Venter et al. (2012) reported that commercial quebracho tannin extract is highly impure, containing around 20% tannins alongside low molecular weight phenolics (such as gallic acid), sugars and lignin which could modify interfacial properties. Further investigations into the detailed composition and interfacial behavior of quebracho tannins are needed to elucidate their impact on droplet surface characteristics. A reasonable hypothesis is that the negative charge increase arises

from the well-documented complexing and binding capacities of tannins (Bonciolini et al., 2023; Karonen, 2022; Molino et al., 2023) which could alter the structure of the interfacial layer and expose negatively charged functional groups. However, while a higher negative surface charge generally benefits emulsion stability, it may also accelerate lipid oxidation by attracting pro-oxidant metal cations to the interface.

Lipid oxidation is a radical chain reaction consisting of three phases: initiation, propagation, and termination. During the propagation phase, highly unstable alkyl radicals react with molecular oxygen to form peroxyl radicals, which in turn attack unsaturated fatty acids, generating new alkyl radicals and lipid hydroperoxides. These hydroperoxides are the first metastable oxidation products and are commonly referred to as primary oxidation products (Hennebelle et al., 2024).

The formation of hydroperoxides in SF emulsions was higher than in EY emulsions. Th difference can be attributed to the fatty acid composition of sunflower oil, which is particularly rich in polyunsaturated fatty acids, especially linoleic acid, making it highly susceptible to rapid and intense oxidative degradation. In contrast, the lipid fraction of egg yolk, predominantly composed of oleic acid (monounsaturated) and palmitic acid (saturated), provides greater intrinsic resistance to oxidation (Appendix, Figure 5.6.1). The addition of both types of tannins substantially reduced hydroperoxide formation. However, the effectiveness of the tannins varied depending on the type of emulsion. Chestnut tannins were more effective in the EY system at both pH conditions, while quebracho tannins significantly reduced peroxide formation in SF emulsions. The antioxidant activity of tannins is generally attributed to two main mechanisms. Firstly, the abundance of hydroxyl groups and the aromatic ring structure of tannins enables them to stabilize free radical intermediates by donating electrons and harboring unpaired electrons within their conjugated system (Molino et al., 2023). Secondly, their metal-chelating capacity allows tannins to bind iron ions, thereby inhibiting or reducing the intensity of Fenton-like reactions and consequently decreasing oxidative stress (Andrade et al., 2005).

In general, emulsions prepared at pH 3.5 exhibited higher hydroperoxide formation in both control and tannin-enriched systems. The pH plays a critical role in influencing charge, solubility, partitioning, redox state, and chemical stability of key actors in oxidative reactions, including metal ions and antioxidants. However, as reviewed by Berton-Carabin et al. (2014) the effect of pH on lipid oxidation in O/W emulsions displayed conflicting results. Some studies reported better oxidative stability at neutral pH than acidic conditions, partially due to the higher solubility of iron at lower pH levels. Additionally, at low pH, protonation of chelating agents can impair their ability to complex metal ions effectively. As a result, metal ions previously sequestered may be released in their active form, enhancing their catalytic contribution to oxidative processes. In the present study, quebracho tannins, rich in catechol groups, may have played a significant role in this context. Phenolic compounds containing catechol structures are known to chelate iron ions by forming iron–phenolic complexes (Sørensen et al., 2014). Deprotonation of the catechol group is essential for iron binding in this pH-dependent mechanism, as the complexing capacity of catechol increases at higher value of pH. Since the intrinsic pKa values of the first and second hydroxyl groups of catechol are 9.3 and 13, respectively; the presence of iron stabilizes the deprotonated state, lowering the apparent pKa to between 5 and 8 (Bijlsma et al., 2020). Conversely, other studies have suggested that neutral pH conditions may actually promote lipid oxidation, as the lower solubility of iron at pH 7 could lead to metal concentration at the droplet interface, depending on the nature of the antioxidant present (Berton-Carabin et al., 2014). The results obtained in the present study revealed contrasting antioxidant effects as related to the two types of tannins and emulsion systems in which they were applied. In particular, chestnut tannins proved to be more effective in EY emulsions than in SF emulsions, where quebracho tannins exhibited superior antioxidant activity. It might be pointed out that additional mechanisms could occur in the two emulsion systems. Firstly, it is essential to highlight that SF emulsions were prepared with sunflower oil stripped of tocopherols. In that system, tannins represent the unique antioxidants. Although the excellent antioxidant properties of gallic acid

are well documented (Hadidi et al., 2024; Velderrain-Rodríguez et al., 2018; Xiang et al., 2024) and that hydrolysable tannins, can undergo hydrolysis under acidic conditions or partial hydrolysis upon exposure to heat and water (Arapitsas, 2012). As a result, simpler and more polar phenolic compounds, such as gallic acid and ellagic acid, are released into the system. At neutral pH, however, the cleavage of ester bonds in hydrolysable tannins is considerably less efficient, since the hydrolysis reaction requires an excess of H^+ ions (or strongly basic conditions) to proceed effectively. The release of smaller, more polar monomeric compounds tends to shift polyphenols from the interface into the aqueous phase, where they are less effective due to their increased distance from the lipid targets (Laguerre et al., 2017). Partial hydrolysis at neutral pH could limit the dispersion of these simple polyphenols, thereby increasing their hydrophobic character and maintaining their localization at the oil–water interface. Conversely, the phenolic groups in quebracho tannins are integrated within a more complex polymeric structure. Although their availability to scavenge free radicals may be lower than that of the hydroxyl groups in hydrolysable tannins, their stable conformation in oil-in-water systems promotes their partitioning at the interface, making them more effective in reducing oxidation rates. In the EY system, the lipid phase was not deprived of carotenoids, specifically lutein and zeaxanthin (Xiao et al., 2025), which provided substantial intrinsic antioxidant protection. In fact, reduced hydroperoxide formation compared to the stripped oil, particularly under neutral pH conditions, was denoted. Lutein is the predominant fat-soluble pigment in egg yolk and is co-extracted with lipids. Chemically, lutein is an oxygenated carotenoid composed of eight isoprene units forming its structural backbone. The presence of hydroxyl groups at the C3 and C3’ positions of the terminal rings lead greater polarity to lutein compared to other carotenoids belonging to the hydrocarbon group. This amphiphilic nature, resulting from its long hydrophobic polyenic chain and polar hydroxyl groups, suggests that lutein molecules can potentially localize at oil–water interfaces. In such arrangements, the hydrophobic chain orients toward the oil phase, while the hydrophilic hydroxyl groups interact with the aqueous phase or with the polar head groups of emulsifiers (Batista

et al., 2006). Numerous studies demonstrated the antioxidant activity of lutein (Ahn & Kim, 2021; Manupa et al., 2023), as well as its synergistic effects when combined with polyphenols. For instance, Xiao et al., (2025) reported that in heated egg yolk, lutein reduced the formation of Maillard reaction intermediates. Jiang et al. (2015) observed that a combination of lipophilic (carotenoid) and hydrophilic (phenolic) extracts from vegetables, in a 1:1 ratio, exhibited the highest synergistic antioxidant activity in the DPPH assay. However, due to its highly unsaturated structure, lutein is particularly susceptible to oxidative degradation by oxygen and heat (Boon et al., 2010; Yang et al., 2023), as well as to environmental factors such as pH. Exposure to high pH value led to approximately 12% degradation, whereas at pH 2 the degradation was about 48% under the same conditions. Neutral pH is more favorable for preserving lutein content, with only about 12% loss reported (Bhat et al., 2023). Furthermore, Khalil et al. (2012) found that lutein encapsulated in emulsion-based delivery systems degraded more rapidly than lutein dispersed in bulk oil phases, highlighting the importance of developing effective strategies to inhibit carotenoid degradation in emulsions. Carotenoids act as primary antioxidants by quenching singlet oxygen and scavenging reactive species through electron or energy transfer processes. Upon oxidation, they form relatively stable radical cations that require regeneration to maintain their antioxidant function. That regeneration is facilitated by secondary antioxidants capable of donating electrons or hydrogen atoms to restore carotenoids to their reduced state (Edge et al., 1997; Fiedor & Burda, 2014; Rice-Evans et al., 1997). Under near-neutral pH, hydrolysable tannins can undergo partial hydrolysis to release low molecular weight phenolics, such as gallic acid, which own favorable redox potentials and lower pKa values. These properties enhance their efficiency in regenerating oxidized carotenoids. Therefore, in this context, chestnut tannins do not primarily act as chain-breaking antioxidants but rather function as secondary antioxidants or synergists. Their role appears to be linked to the stabilization and potential regeneration of lutein, contributing to its prolonged antioxidant activity in the emulsion system. Conversely, condensed tannins, due to their rigid polymeric structures and inherently higher pKa values, exhibit limited

proton dissociation and reduced reactivity in electron transfer reactions, resulting in less effective carotenoid regeneration. Supporting this, Weigel et al. (2018) monitored the degradation of lutein-related color in emulsions co-formulated with antioxidants, reporting that ascorbic acid was the most effective in protecting lutein from oxidation. In contrast, catechin was found to be less effective, likely due to its lower polarity—partially confirming the findings of the present study.

The oscillatory pattern observed in hydroperoxide levels suggests continuous cycles of formation and rapid degradation of hydroperoxides into secondary oxidation products. At the end of the propagation phase, primary oxidation products break down into secondary oxidation products, including aldehydes, ketones, and alcohols. In the present study, the use of sunflower oil, rich in linoleic acid, led to the formation of a high amount of hexanal, resulting from the cleavage of the C–O bond by alkoxy radicals derived from hydroperoxides (Shahidi & Hossain, 2022). Conversely, the high levels of oleic and linoleic acids in egg yolk would be expected to promote the formation of both hexanal and nonanal. In SF emulsions, hexanal was consistently detected from the initial time point, mirroring the evolution of primary oxidation products and confirming the rapid onset of lipid oxidation. Consistently with the peroxide value (PV) trends, tannins markedly reduced the formation of hexanal. In contrast, EY emulsions displayed delayed formation of volatile aldehydes, with hexanal first detected at pH 3.5 after 8 days of storage, followed by the appearance of nonanal after 10 days. Notably, at neutral pH, neither hexanal nor nonanal were detected throughout the whole storage period, which agree with the lower extent of oxidative degradation under these conditions.

Finally, the impact of tannin addition on the formation of POPs in SF emulsions and COPs in EY emulsions was also assessed. Phytosterols are a group of plant-source sterols with great physiological functions but are highly susceptible to oxidation when exposed to oxygen, heat, free radicals and metal ions. Oxidation leads to the formation of phytosterol oxidation products (POPs). Despite their importance, research on POPs remains limited, particularly regarding their biological effects in the human body. Some studies suggested that harmful effects, including cancerogenic, atherosclerotic

and mutagenic activity; other reported antidiabetic or anti-inflammatory benefits, making their health impact a topic of ongoing debate (Gachumi et al., 2021). In emulsified systems, sterols behave as surface-active compounds: their structure allows them to locate at the oil–water interface by forming hydrogen bonds between the hydroxyl group at C3 and water molecules, and through Van der Waals interactions with the hydrophobic region of the oil phase (Cercaci et al., 2007; Yang et al., 2024). Since oxidation reactions mainly take place at interface, sterols become particularly prone to degradation, leading to the formation of SOPs. The low concentrations of SOPs observed in tannin-containing emulsions could be attributed to the action of tannins along the formation pathway. Specifically, the radical-scavenging activity of tannins interferes with the initial steps of sterol oxidation, which involve reactions with free radicals in the presence of oxygen to form 7-hydroperoxysterols. These intermediates subsequently degrade into hydroxy and keto sterols (Gachumi et al., 2021). By examining the kinetics of individual oxysterol formation (Appendix table 5.6.1, 5.6.2 and 5.6.3), it was observed that hydroxy and epoxy derivatives of sitosterol and campesterol were primarily detected. After 3 days of storage, under both pH conditions, the generation of 7-ketositosterol and 7-ketocampesterol became evident. The time required to generate 7-keto derivatives is consistent with the knowledge about their oxidative pathways, where sterol hydroperoxides, under the influence of free radicals or metal ions, can decompose via multiple routes to form either hydroxylated (such as 7α-hydroxy and 7β-hydroxy sterols) or ketonic derivatives like the 7-keto sterol. The formation of 7-keto products is particularly favored under strong oxidative stress or radical propagation conditions, as they can arise directly from hydroperoxides through β-scission or via secondary oxidation of already-formed hydroxy derivatives (Lercker & Rodriguez-Estrada, 2002). Furthermore, factors such as pH and the presence of antioxidants, like tannins, may modulate the balance between these pathways, delaying the accumulation of ketonic products and favoring the transient build-up of hydroxy or epoxy intermediates (Kulig et al., 2016). When considering the individual POPs, namely the sum of α/β-hydroxy and epoxy derivatives, the first

appreciable differences between emulsions containing tannins and controls were observed from day 6 under acidic conditions (pH 3.5), except for the β-epoxide, while at neutral pH these differences emerged earlier, from day 3. However, no significant differences were observed in the levels of the POPs as related to the different tannins used. Interestingly, in EY emulsions, total COPs were detected only in control samples throughout the entire experimental time, whereas no trace amounts were observed in the tannin-containing emulsions over the same timeframe, reflecting what was observed for the primary and secondary oxidation products. Again, the strongest synergy activity between lutein and zeaxanthin with the presence of tannins, could result in an exceptional protection against the oxidation rates.

5.5 Conclusion

This study demonstrated the promising potential of chestnut and quebracho tannins as natural multifunctional agents to enhance the oxidative and physical stability of oil-in-water (O/W) emulsions. Both tannins exhibited significant antioxidant activity, markedly reducing the formation of primary and secondary oxidation products, including sterol oxidation products (SOPs). When partially replacing the synthetic surfactant Tween-20, quebracho tannin contributed to greater emulsion stability by increasing the negative surface charge, particularly at pH 3.5. Chestnut tannin, on the other hand, showed higher efficacy in egg yolk-based emulsions at pH 7.0, possibly due to interactions with endogenous compounds such as lutein.

These findings highlight the relevance of plant-derived polyphenols as clean-label ingredients capable of improving both the shelf life and, potentially, the nutritional quality of emulsified food products.

Appendix

Table 5.6.4. Phytosterol Oxidation Products (μg/kg of POPs in fat content) at pH 3.5. The results are expressed as mean ± standard deviation of 3 independent replicates (n=3).

		7OH-S	*βEP-S*	*αEP-S*	*7K-S*	*7OH-C*	*βEP-C*	*αEP-C*	*7K-C*	*7OH-St*	*7K-St*	*Total*
T0	*C*	2.70 ± 0.22	1.00 ± 0.02	1.04 ± 0.03	n.d.	3.94 ± 0.12	0.79 ± 0.05	1.38 ± 0.15	n.d.	n.d.	n.d.	11.86 ± 0.79^{ab}
	C01	2.01 ± 0.03	1.57 ± 0.13	1.15 ± 0.14	n.d.	3.81 ± 0.14	0.64 ± 0.02	1.34 ± 0.05	n.d.	n.d.	n.d.	10.51 ± 6.51^{c}
	C02	2.20 ± 0.01	1.29 ± 0.09	1.12 ± 0.06	n.d.	3.97 ± 0.04	0.65 ± 0.06	1.37 ± 0.07	n.d.	n.d.	n.d.	10.60 ± 0.39^{bc}
	Q01	2.91 ± 0.10	1.60 ± 0.17	1.30 ± 0.02	n.d.	4.01 ± 0.06	0.74 ± 0.10	1.40 ± 0.01	n.d.	n.d.	n.d.	11.95 ± 0.20^{a}
	Q02	2.14 ± 0.11	1.50 ± 0.15	1.18 ± 0.13	n.d.	3.87 ± 0.11	0.68 ± 0.05	1.42 ± 0.03	n.d.	n.d.	n.d.	10.79 ± 0.36^{abc}
	Sign.	n.s.	n.s.	n.s.		n.s.	n.s.	n.s.				*
T3	*C*	2.69 ± 0.06	2.08 ± 0.15^{a}	1.06 ± 0.21	6.69 ± 0.07	3.95 ± 0.18	0.78 ± 0.47	1.39 ± 0.17	3.80 ± 0.01	n.d.	n.d.	22.44 ± 0.34^{a}
	C01	2.15 ± 0.21	1.58 ± 0.02^{b}	1.16 ± 0.03	n.d.	3.89 ± 0.03	0.64 ± 0.01	1.34 ± 0.02	n.d.	n.d.	n.d.	10.76 ± 0.12^{b}
	C02	2.38 ± 0.39	1.49 ± 0.10^{b}	1.12 ± 0.06	n.d.	3.98 ± 0.06	0.65 ± 0.01	1.38 ± 0.02	n.d.	n.d.	n.d.	11.01 ± 0.33^{b}
	Q01	2.91 ± 0.18	1.74 ± 0.06^{b}	1.32 ± 0.06	n.d	4.03 ± 0.05	0.74 ± 0.03	1.40 ± 0.01	n.d.	n.d.	n.d.	12.14 ± 0.07^{b}
	Q02	2.12 ± 0.38	1.58 ± 0.07^{b}	1.20 ± 0.02	n.d.	3.95 ± 0.02	0.68 ± 0.03	1.42 ± 0.03	n.d.	n.d.	n.d.	10.94 ± 0.40^{b}
	Sign.	n.s.	**	n.s.	***	n.s.	n.s.	n.s.	***			***
T6	*C*	7.09 ± 1.60^{a}	3.38 ± 0.07^{a}	1.58 ± 0.01^{a}	9.63 ± 0.71	4.59 ± 0.26^{a}	1.15 ± 0.11^{a}	1.47 ± 0.03^{a}	4.30 ± 0.22	n.d.	n.d.	33.20 ± 2.63^{a}
	C01	2.47 ± 0.29^{b}	1.76 ± 0.10^{b}	1.19 ± 0.06^{b}	n.d.	3.99 ± 0.01^{b}	0.63 ± 0.02^{b}	1.34 ± 0.01^{b}	n.d.	n.d.	n.d.	11.37 ± 0.48^{b}
	C02	2.28 ± 0.41^{b}	1.49 ± 0.17^{b}	1.12 ± 0.10^{b}	n.d.	3.99 ± 0.03^{b}	0.62 ± 0.01^{b}	1.34 ± 0.03^{b}	n.d.	n.d.	n.d.	10.83 ± 0.13^{b}
	Q01	2.81 ± 0.86^{b}	1.72 ± 0.07^{b}	1.31 ± 0.02^{b}	n.d.	4.02 ± 0.07^{b}	0.68 ± 0.02^{b}	1.38 ± 0.01^{b}	n.d.	n.d.	n.d.	11.92 ± 0.85^{b}
	Q02	2.76 ± 0.12^{b}	1.78 ± 0.08^{b}	1.29 ± 0.01^{b}	n.d.	4.04 ± 0.01^{b}	0.72 ± 0.01^{b}	1.38 ± 0.01^{b}	n.d.	n.d.	n.d.	11.97 ± 0.04^{b}
	Sign.	**	***	**		*	***	*				***

T14	*C*	25.11 ± 4.84^{a}	5.35 ± 0.06^{a}	2.07 ± 0.05^{a}	10.79 ± 1.80^{a}	6.33 ± 0.62^{a}	1.64 ± 0.05^{a}	1.63 ± 0.03^{a}	4.76 ± 0.18^{a}	5.32 ± 3.68	4.44 ± 1.06	67.44 ± 1.13^{a}
	C01	2.49 ± 0.39^{b}	1.32 ± 0.13^{d}	1.03 ± 0.13^{c}	5.20 ± 0.29^{b}	4.00 ± 0.05^{b}	0.56 ± 0.05^{d}	1.27 ± 0.06^{c}	3.29 ± 0.06^{b}	n.d.	n.d.	19.15 ± 0.84^{b}
	C02	2.31 ± 0.11^{b}	1.26 ± 0.05^{d}	1.06 ± 0.05^{c}	5.07 ± 0.04^{b}	3.97 ± 0.01^{b}	0.62 ± 0.02^{cd}	1.31 ± 0.02^{bc}	3.20 ± 0.12^{b}	n.d.	n.d.	18.80 ± 0.21^{b}
	Q01	3.15 ± 0.71^{b}	1.87 ± 0.06^{b}	1.24 ± 0.05^{b}	5.20 ± 0.18^{b}	4.04 ± 0.06^{b}	0.72 ± 0.03^{b}	1.36 ± 0.05^{bc}	3.07 ± 0.01^{b}	n.d.	n.d.	20.66 ± 0.47^{b}
	Q02	1.65 ± 0.43^{b}	1.53 ± 0.03^{c}	1.16 ± 0.05^{bc}	5.24 ± 0.14^{b}	3.91 ± 0.02^{b}	0.66 ± 0.05^{bc}	1.38 ± 0.03^{b}	3.15 ± 0.11^{b}	n.d.	n.d.	18.67 ± 0.58^{b}
	Sign.	***	***	***	***	***	***	***	***	***	***	***

Abbreviations: Sign., statistical significance; n.s., not significant; the asterisks denote the level of significance: *, $p<0.05$; **, $p<0.01$; *** $p<0.001$; nd, not detected. Tukey's test was applied for multiple comparisons ($p = 0.05$), different letters in column indicate significantly different means among the samples

Table 5.6.2. Phytosterol Oxidation Products (µg/kg of POPs in fat content) at pH 7.0. The results are expressed as mean ± standard deviation of 3 independent replicates (n=3).

		7OH-S	***βEP-S***	***αEP-S***	***7K-S***	***7OH-C***	***βEP-C***	***αEP-C***	***7K-C***	***7OH-St***	***7K-St***	***Total***
T0	*C*	2.78 ± 0.14	1.91 ± 0.04	1.04 ± 0.03	n.d.	3.98 ± 0.11	0.71 ± 0.01	1.42 ± 0.04	n.d.	n.d.	n.d.	11.93 ± 0.79
	C01	2.14 ± 0.02	1.57 ± 0.08	1.51 ± 0.11	n.d.	3.78 ± 0.05	0.69 ± 0.04	1.37 ± 0.07	n.d.	n.d.	n.d.	10.66 ± 6.51
	C02	2.15 ±0.04	1.29 ±0.01	1.35 ± 0.16	n.d.	3.89 ± 0.06	0.64 ± 0.02	1.39 ± 0.02	n.d.	n.d.	n.d.	10.60 ± 0.39
	Q01	2.87 ±0.13	1.60 ± 0.03	1.61 ± 0.04	n.d.	4.21 ± 0.10	0.61 ± 0.03	1.41 ± 0.06	n.d.	n.d.	n.d.	11.98 ± 0.20
	Q02	2.21 ±0.09	1.50 ± 0.12	1.53 ± 0.01	n.d.	3.81 ± 0.04	0.69 ± 0.01	1.31 ± 0.09	n.d.	n.d.	n.d.	10.69 ± 0.36
	Sign.	n.s.	n.s.	n.s.		n.s.	n.s.	n.s.				n.s.
T3	*C*	15.00 ± 0.65^{a}	3.11 ± 0.43^{a}	1.72 ± 0.12^{a}	12.05 ± 3.52	5.41 ± 0.05^{a}	1.12 ± 0.13^{a}	1.48 ± 0.13	6.75 ± 0.18	n.d.	n.d.	46.64 ± 10.11^{a}
	C01	2.36 ± 0.03^{b}	1.59 ± 0.37^{b}	1.32 ± 0.17^{ab}	n.d.	3.98 ± 0.01^{b}	0.68 ± 0.03^{b}	1.33 ± 0.03	n.d.	n.d.	n.d.	11.25 ± 0.55^{b}
	C02	2.61 ± 0.15^{b}	1.48 ± 0.12^{b}	1.20 ± 0.09^{b}	n.d.	4.02 ± 0.02^{b}	0.63 ± 0.05^{b}	1.37 ± 0.05	n.d.	n.d.	n.d.	11.32 ± 0.10^{b}
	Q01	2.24 ± 0.67^{b}	1.60 ± 0.15^{b}	1.27 ± 0.12^{ab}	n.d.	3.97 ± 0.06^{b}	0.68 ± 0.05^{b}	1.39 ± 0.05	n.d.	n.d.	n.d.	11.15 ± 1.10^{b}
	Q02	2.68 ± 0.13^{b}	1.75 ± 0.14^{b}	1.18 ± 0.05^{b}	n.d.	3.99 ± 0.02^{b}	0.71 ± 0.01^{b}	1.37 ± 0.01	n.d.	n.d.	n.d.	11.68 ± 0.35^{b}
	Sign.	***	**	*		***	**	n.s.				**
T6	*C*	14.91 ± 3.05^{a}	4.91 ± 0.31^{a}	2.09 ± 0.06^{a}	14.34 ± 0.22	5.36 ± 0.15^{a}	1.59 ± 0.03^{a}	1.61 ± 0.07^{a}	5.25 ± 0.28	n.d.	n.d.	50.07 ± 4.05^{a}
	C01	1.59 ± 0.14^{b}	1.84 ± 0.17^{b}	1.32 ± 0.03^{b}	n.d.	3.92 ± 0.01^{b}	0.73 ± 0.01^{b}	1.42 ± 0.02^{b}	n.d.	n.d.	n.d.	10.82 ± 0.06^{b}
	C02	2.10 ± 0.84^{b}	1.82 ± 0.11^{b}	1.29 ± 0.04^{b}	n.d.	3.96 ± 0.06^{b}	0.71 ± 0.08^{b}	1.40 ± 0.02^{b}	n.d.	n.d.	n.d.	11.28 ± 0.65^{b}
	Q01	1.48 ± 0.04^{b}	2.01 ± 0.09^{b}	1.43 ± 0.05^{b}	n.d.	3.92 ± 0.01^{b}	0.74 ± 0.02^{b}	1.43 ± 0.03^{b}	n.d.	n.d.	n.d.	10.10 ± 0.05^{b}
	Q02	2.43 ± 0.15^{b}	1.76 ± 0.09^{b}	1.29 ± 0.06^{b}	n.d.	4.00 ± 0.01^{b}	0.70 ± 0.03^{b}	1.40 ± 0.01^{b}	n.d.	n.d.	n.d.	11.58 ±0 .51^{b}
	Sign.	***	***	***		***	***	**				***
T14	*C*	32.12 ± 7.78^{a}	10.53 ± 5.16^{a}	3.41 ± 1.59^{a}	18.08 ± 0.30^{a}	7.49 ± 1.04^{a}	2.99 ± 1.47^{a}	1.85 ± 0.54	6.41 ± 0.72^{a}	10.18 ± 1.99	5.28 ± 1.58	82.89 ± 10.10^{a}
	C01	2.06 ± 0.02^{b}	1.25 ± 0.05^{b}	1.36 ± 0.17^{b}	5.11 ± 0.04^{b}	3.97 ± 0.02^{b}	0.79 ± 0.05^{b}	1.25 ± 0.16	3.41 ± 0.03^{b}	n.d.	n.d.	19.21 ± 0.39^{b}
	C02	3.31 ± 1.99^{b}	2.51 ± 0.77^{b}	1.41 ± 0.21^{b}	5.13 ± 0.06^{b}	4.05 ±0.16^{b}	0.86 ± 0.19^{b}	1.44 ± 0.08	3.44 ± 0.14^{b}	n.d.	n.d.	22.15 ± 3.60^{b}
	Q01	1.72 ± 0.63^{b}	1.65 ± 0.09^{b}	1.20 ± 0.02^{b}	5.03 ± 0.01^{b}	3.90 ± 0.05^{b}	0.67 ± 0.01^{b}	1.38 ± 0.01	3.39 ± 0.05^{b}	n.d.	n.d.	18.94 ± 0.83^{b}

Q02	2.13 ± 0.08[b]	1.72 ± 0.14[b]	1.27 ± 0.01[b]	5.08 ± 0.03[b]	3.96 ± 0.02[b]	0.68 ± 0.06[b]	1.36 ± 0.01	3.42 ± 0.07[b]	n.d.	n.d.	19.62 ± 0.19[b]
Sign.	***	**	*	***	***	**	n.s.	***			***

Abbreviations: Sign., statistical significance; n.s., not significant; the asterisks denote the level of significance: *, $p<0.05$; **, $p<0.01$; *** $p<0.001$; nd, not detected. Tukey's test was applied for multiple comparisons ($p = 0.05$), different letters in column indicate significantly different means among the samples

Table 5.6.3. Cholesterol oxidation products (µg/kg, in fat content) in control samples at pH 3.5 (the presence of COPs in the other treatments was not detected). The results are expressed as mean ± standard deviation of 3 independent replicates (n=3).

		7OH-CH	*βEP-CH*	*αEP-CH*	*7K-CH*	*Total*
T0	*C*	3.12 ± 0.03[b]	0.72 ± 0.04	1.49 ± 0.07	n.d.	2.21 ± 0.21[b]
T3	*C*	4.91 ± 0.02[a]	0.66 ± 0.03	1.51 ± 0.08	5.88 ± 0.07	8.05 ± 0.14[a]
T6	*C*	4.04 ± 0.07[a]	0.67 ± 0.01	1.50 ± 0.02	5.15 ± 0.02	7.32 ± 0.10[a]
T14	*C*	5.26 ± 0.02[a]	0.67 ± 0.01	1.50 ± 0.02	5.06 ± 0.02	7.24 ± 0.08[a]
Sign.		*	n.s.	n.s.	n.s.	***

Abbreviations: Sign., statistical significance; n.s., not significant; the asterisks denote the level of significance: *, $p<0.05$; **, $p<0.01$; *** $p<0.001$; nd, not detected. Tukey's test was applied for multiple comparisons ($p = 0.05$), different letters in column indicate significantly different means among the samples

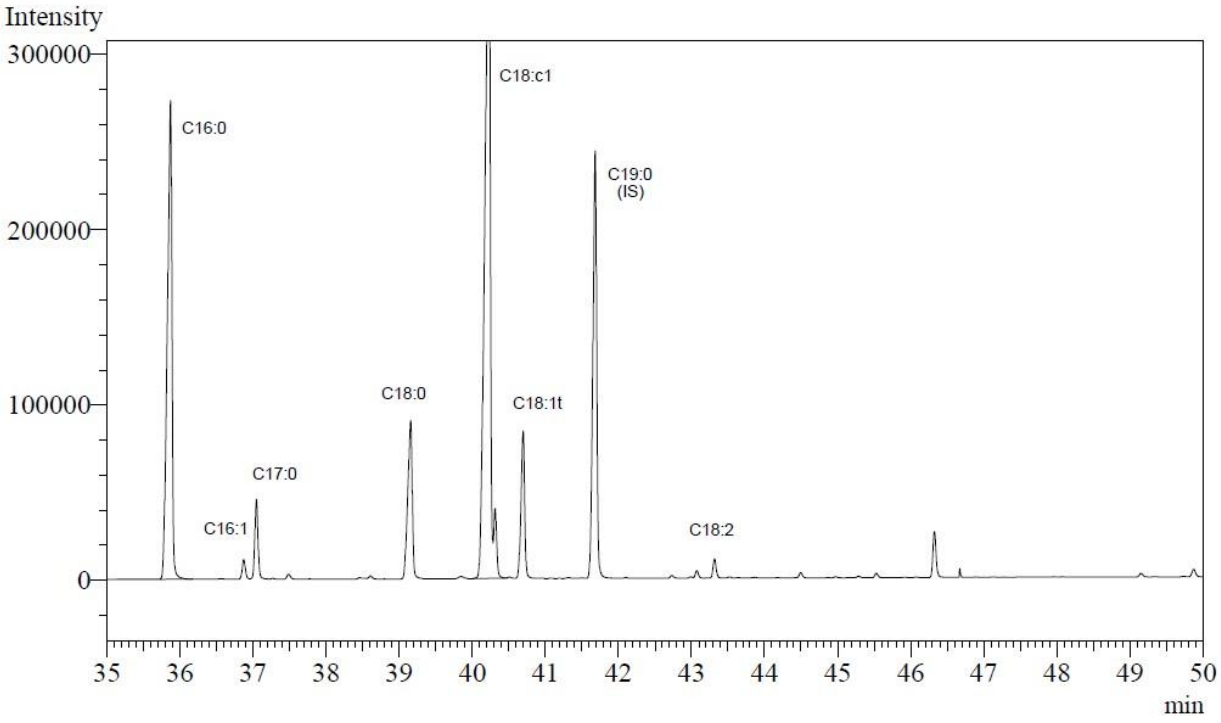

Figure 5.6.1. GC-FID chromatogram of fatty acids methyl esters (FAMEs) determined in egg yolk lipid matter. C19:0 was used as internal standard (IS)

References

Abad, A., & Shahidi, F. (2020). A robust stripping method for the removal of minor components from edible oils. Food Production, Processing and Nutrition, 2(1), 1. https://doi.org/10.1186/s43014-019-0015-2

Ahn, Y. J., & Kim, H. (2021). Lutein as a Modulator of Oxidative Stress-Mediated Inflammatory Diseases. Antioxidants, 10(9), 1448. https://doi.org/10.3390/antiox10091448

Andrade, R. G., Dalvi, L. T., Silva, J. M. C., Lopes, G. K. B., Alonso, A., & Hermes-Lima, M. (2005). The antioxidant effect of tannic acid on the in vitro copper-mediated formation of free radicals. Archives of Biochemistry and Biophysics, 437(1), 1–9. https://doi.org/10.1016/j.abb.2005.02.016

Arapitsas, P. (2012). Hydrolyzable tannin analysis in food. Food Chemistry, 135(3), 1708–1717. https://doi.org/10.1016/j.foodchem.2012.05.096

Badhani, B., & Kakkar, R. (2017). DFT study of structural and electronic properties of gallic acid and its anions in gas phase and in aqueous solution. Structural Chemistry, 28(6), 1789–1802. https://doi.org/10.1007/s11224-017-0958-3

Batista, A. P., Raymundo, A., Sousa, I., & Empis, J. (2006). Rheological characterization of coloured oil-in-water food emulsions with lutein and phycocyanin added to the oil and aqueous phases. Food Hydrocolloids, 20(1), 44–52. https://doi.org/10.1016/j.foodhyd.2005.02.009

Berton-Carabin, C. C., Ropers, M. H., & Genot, C. (2014). Lipid Oxidation in Oil-in-Water Emulsions: Involvement of the Interfacial Layer. Comprehensive Reviews in Food Science and Food Safety, 13(5), 945–977. https://doi.org/10.1111/1541-4337.12097

Bhat, I., Jose, N. M., & Mamatha, B. S. (2023). Oxidative stability of lutein on exposure to varied extrinsic factors. Journal of Food Science and Technology, 60(3), 987–995. https://doi.org/10.1007/s13197-022-05430-3

Bijlsma, J., de Bruijn, W. J. C., Hageman, J. A., Goos, P., Velikov, K. P., & Vincken, J.-P. (2020). Revealing the main factors and two-way interactions contributing to food discolouration caused by iron-catechol complexation. Scientific Reports, 10(1), 8288. https://doi.org/10.1038/s41598-020-65171-1

Bonciolini, A., Cantele, C., Salgarella, N. I., Zeppa, G., Bertolino, M., & Cardenia, V. (2023). Effect of Tannins on Cholesterol Content and Its Oxidation in Egg Pasta as Related to Different Pasta Shapes. Food and Bioprocess Technology, 16(7), 1541–1554. https://doi.org/10.1007/s11947-023-03016-1

Bonciolini, A., Vissio, A., Calaminici, R., Forte, E., & Cardenia, V. (2025). Comparative study on phytosterol oxidation products determination in high oleic sunflower oil by using cholesterol oxidation products or purified phytosterol oxidation products as reference materials. Journal of Agriculture and Food Research, 21(April), 101961. https://doi.org/10.1016/j.jafr.2025.101961

Boon, C. S., McClements, D. J., Weiss, J., & Decker, E. A. (2010). Factors influencing the chemical stability of carotenoids in foods. Critical Reviews in Food Science and Nutrition, 50(6), 515–532. https://doi.org/10.1080/10408390802565889

Cantele, C., Bonciolini, A., Rossi, A. M., Bertolino, M., & Cardenia, V. (2025). Effects of Wheat Bran-Derived Alkylresorcinols on the Physical and Oxidative Stability of Oil-in-Water Emulsions as related to pH. Food Chemistry, 464(P2), 141659. https://doi.org/10.1016/j.foodchem.2024.141659

Cercaci, L., Rodriguez-Estrada, M. T., Lercker, G., & Decker, E. A. (2007). Phytosterol oxidation in oil-in-water emulsions and bulk oil. Food Chemistry, 102(1), 161–167. https://doi.org/10.1016/j.foodchem.2006.05.010

Delfanian, M., Sahari, M. A., & Barba, F. J. (2023). Effect of lipophilized gallic acid on the oxidative stability of omega-3 fatty acids rich soy and cow milk. LWT, 190, 115475. https://doi.org/10.1016/j.lwt.2023.115475

Edge, R., McGarvey, D. J., & Truscott, T. G. (1997). The carotenoids as anti-oxidants — a review. Journal of Photochemistry and Photobiology B: Biology, 41(3), 189–200. https://doi.org/10.1016/S1011-1344(97)00092-4

Eslami, A. C., Pasanphan, W., Wagner, B. A., & Buettner, G. R. (2010). Free radicals produced by the oxidation of gallic acid: An electron paramagnetic resonance study. Chemistry Central Journal, 4(1), 15. https://doi.org/10.1186/1752-153X-4-15

Fiedor, J., & Burda, K. (2014). Potential Role of Carotenoids as Antioxidants in Human Health and Disease. Nutrients, 6(2), 466–488. https://doi.org/10.3390/nu6020466

Figueroa-Espinoza, M. C., Zafimahova, A., Alvarado, P. G. M., Dubreucq, E., & Poncet-Legrand, C. (2015). Grape seed and apple tannins: Emulsifying and antioxidant properties Dedicated to the memory of Gérard Mazerolles. Food Chemistry, 178, 38–44. https://doi.org/10.1016/j.foodchem.2015.01.056

Gachumi, G., Poudel, A., Wasan, K. M., & El-Aneed, A. (2021). Analytical Strategies to Analyze the Oxidation Products of Phytosterols, and Formulation-Based Approaches to Reduce Their Generation. Pharmaceutics, 13(2), 268. https://doi.org/10.3390/pharmaceutics13020268

Guzey, D., & McClements, D. J. (2007). Impact of Electrostatic Interactions on Formation and Stability of Emulsions Containing Oil Droplets Coated by β-Lactoglobulin−Pectin Complexes. Journal of Agricultural and Food Chemistry, 55(2), 475–485. https://doi.org/10.1021/jf062342f

Hadidi, M., Liñán-Atero, R., Tarahi, M., Christodoulou, M. C., & Aghababaei, F. (2024). The Potential Health Benefits of Gallic Acid: Therapeutic and Food Applications. Antioxidants, 13(8), 1001. https://doi.org/10.3390/antiox13081001

Hennebelle, M., Villeneuve, P., Durand, E., Lecomte, J., van Duynhoven, J., Meynier, A., Yesiltas, B., Jacobsen, C., & Berton-Carabin, C. (2024). Lipid oxidation in emulsions: New insights from the past two decades. Progress in Lipid Research, 94(October 2023). https://doi.org/10.1016/j.plipres.2024.101275

Hu, Y., Yang, G., Huang, W., Lai, S., Ren, Y., Huang, B., Zhang, L., Li, P., Lu, B. Development and validation of a gas chromatography-mass spectrometry method for determination of sterol oxidation products in edible oils, RSC Adv. 5 (2015), 41259–41268. https://doi.org/10.1039/c5ra02795k.

Inchingolo, R., Bayram, I., Uluata, S., Kiralan, S. S., Rodriguez-Estrada, M. T., McClements, D. J., & Decker, E. A. (2021). Ability of Sodium Dodecyl Sulfate (SDS) Micelles to Increase the Antioxidant Activity of α-Tocopherol. Journal of Agricultural and Food Chemistry, 69(20), 5702–5708. https://doi.org/10.1021/acs.jafc.1c01199

Jiang, H., Li*, H., Yu, C., Yang, T., Hu, J., Liu, R., & Deng*, Z. (2015). The Evaluation of Antioxidant Interactions among 4 Common Vegetables using Isobolographic Analysis. Journal of Food Science, 80(6). https://doi.org/10.1111/1750-3841.12896

Karonen, M. (2022). Insights into Polyphenol–Lipid Interactions: Chemical Methods, Molecular Aspects and Their Effects on Membrane Structures. Plants, 11(14), 1809. https://doi.org/10.3390/plants11141809

Khalil, M., Raila, J., Ali, M., Islam, K. M. S., Schenk, R., Krause, J.-P., Schweigert, F. J., & Rawel, H. (2012). Stability and bioavailability of lutein ester supplements from Tagetes flower prepared under food processing conditions. Journal of Functional Foods, 4(3), 602–610. https://doi.org/10.1016/j.jff.2012.03.006

Khatib, M., Campo, M., Bellumori, M., Cecchi, L., Vignolini, P., Innocenti, M., & Mulinacci, N. (2023). Tannins from Different Parts of the Chestnut Trunk (Castanea Sativa Mill.): a Green and Effective Extraction Method and Their Profiling by High-Performance Liquid Chromatography-Diode Array Detector-Mass Spectrometry. ACS Food Science & Technology, 3(11), 1903–1912. https://doi.org/10.1021/acsfoodscitech.3c00272

Kovalcuks, A. (2014). Purification of egg yolk oil obtained by solvent extraction from liquid egg yolk. Annual 20th International Scientific Conference Research for Rural Development.

Kulig, W., Cwiklik, L., Jurkiewicz, P., Rog, T., & Vattulainen, I. (2016). Cholesterol oxidation products and their biological importance. Chemistry and Physics of Lipids, 199, 144–160. https://doi.org/10.1016/j.chemphyslip.2016.03.001

Laguerre, M., Bily, A., Roller, M., & Birtić, S. (2017). Mass Transport Phenomena in Lipid Oxidation and Antioxidation. Annual Review of Food Science and Technology, 8, 391–411. https://doi.org/10.1146/annurev-food-030216-025812

Lercker, G., & Rodriguez-Estrada, M. T. (2002). Cholesterol Oxidation Mechanisms. In F. Guardiola, P. C. Dutta, R. Codony, & G. Savage (Eds.), Cholesterol and Phytosterol Oxidation Products: Analysis, Occurence, and Biological Effects (pp. 1–25).

Lethuaut, L., Métro, F., & Genot, C. (2002). Effect of droplet size on lipid oxidation rates of oil-in-water emulsions stabilized by protein. Journal of the American Oil Chemists' Society, 79(5). https://doi.org/10.1007/s11746-002-0500-z

Liu, Z., Luo, S., Liu, C., & Hu, X. (2024). Tannic acid delaying metabolism of resistant starch by gut microbiota during in vitro human fecal fermentation. Food Chemistry, 440, 138261. https://doi.org/10.1016/j.foodchem.2023.138261

Manupa, W., Wongthanyakram, J., Jeencham, R., & Sutheerawattananonda, M. (2023). Storage stability and antioxidant activities of lutein extracted from yellow silk cocoons (Bombyx mori) in Thailand. Heliyon, 9(6), e16805. https://doi.org/10.1016/j.heliyon.2023.e16805

McClements, D. J., Bai, L., & Chung, C. (2017). Recent Advances in the Utilization of Natural Emulsifiers to Form and Stabilize Emulsions. Annual Review of Food Science and Technology, 8(1), 205–236. https://doi.org/10.1146/annurev-food-030216-030154

McClements, D. J., & Decker, E. (2018). Interfacial Antioxidants: A Review of Natural and Synthetic Emulsifiers and Coemulsifiers That Can Inhibit Lipid Oxidation. Journal of Agricultural and Food Chemistry, 66(1), 20–25. https://doi.org/10.1021/acs.jafc.7b05066

MCCLEMENTS, D. J., & DECKER, E. A. (2000). Lipid Oxidation in Oil-in-Water Emulsions: Impact of Molecular Environment on Chemical Reactions in Heterogeneous Food Systems. Journal of Food Science, 65(8), 1270–1282. https://doi.org/10.1111/j.1365-2621.2000.tb10596.x

Molino, S., Lerma-Aguilera, A., Piskorz, M. M., López Mingorance, F., Montero, J. M., Uehara, T., Hashimoto, H., González Ballerga, E., & Olmos, J. A. (2024). Tannin-based supplementation influences gut microbiota composition and activity in IBS-D patients with a potential impact on symptoms: a pilot study. Food & Function, 15(17), 8893–8903. https://doi.org/10.1039/D4FO02236J

Molino, S., Pilar Francino, M., & Ángel Rufián Henares, J. (2023). Why is it important to understand the nature and chemistry of tannins to exploit their potential as nutraceuticals? Food Research International, 173(July). https://doi.org/10.1016/j.foodres.2023.113329

Pasch, H., Pizzi, A., & Rode, K. (2001). MALDI–TOF mass spectrometry of polyflavonoid tannins. Polymer, 42(18), 7531–7539. https://doi.org/10.1016/S0032-3861(01)00216-6

Rice-Evans, C., Miller, N., & Paganga, G. (1997). Antioxidant properties of phenolic compounds. Trends in Plant Science, 2(4), 152–159. https://doi.org/10.1016/S1360-1385(97)01018-2

Rose-Sallin, C., Huggett, A. C., Bosset, J. O., Tabacchi, R., & Fay, L. B. (1995). Quantification of Cholesterol Oxidation Products in Milk Powders Using [2H7]Cholesterol To Monitor Cholesterol Autoxidation Artifacts. Journal of Agricultural and Food Chemistry, 43(4). https://doi.org/10.1021/jf00052a017

Sanz, M., Cadahía, E., Esteruelas, E., Muñoz, Á. M., Fernández de Simón, B., Hernández, T., & Estrella, I. (2010). Phenolic Compounds in Chestnut (Castanea sativa Mill.) Heartwood. Effect of Toasting at Cooperage. Journal of Agricultural and Food Chemistry, 58(17), 9631–9640. https://doi.org/10.1021/jf102718t

Shahidi, F., & Hossain, A. (2022). Role of Lipids in Food Flavor Generation. Molecules, 27(15). https://doi.org/10.3390/molecules27155014

Shantha, N. C., & Decker, E. A. (1994). Rapid, Sensitive, Iron-Based Spectrophotometric Methods for Determination of Peroxide Values of Food Lipids. Journal of AOAC INTERNATIONAL, 77(2), 421–424. https://doi.org/10.1093/jaoac/77.2.421

Sørensen, A.-D. M., Durand, E., Laguerre, M., Bayrasy, C., Lecomte, J., Villeneuve, P., & Jacobsen, C. (2014). Antioxidant Properties and Efficacies of Synthesized Alkyl Caffeates, Ferulates, and Coumarates. Journal of Agricultural and Food Chemistry, 62(52), 12553–12562. https://doi.org/10.1021/jf500588s

Teo, A., Goh, K. K. T., Wen, J., Oey, I., Ko, S., Kwak, H.-S., & Lee, S. J. (2016). Physicochemical properties of whey protein, lactoferrin and Tween 20 stabilised nanoemulsions: Effect of temperature, pH and salt. Food Chemistry, 197, 297–306. https://doi.org/10.1016/j.foodchem.2015.10.086

Uluata, S., McClements, D. J., & Decker, E. A. (2016). Riboflavin-induced oxidation in fish oil-in-water emulsions: Impact of particle size and optical transparency. Food Chemistry, 213, 457–461. https://doi.org/10.1016/j.foodchem.2016.06.103

Vácha, R., Rick, S. W., Jungwirth, P., de Beer, A. G. F., de Aguiar, H. B., Samson, J.-S., & Roke, S. (2011). The Orientation and Charge of Water at the Hydrophobic Oil Droplet–Water Interface. Journal of the American Chemical Society, 133(26), 10204–10210. https://doi.org/10.1021/ja202081x

Velderrain-Rodríguez, G., Torres-Moreno, H., Villegas-Ochoa, M., Ayala-Zavala, J., Robles-Zepeda, R., Wall-Medrano, A., & González-Aguilar, G. (2018). Gallic Acid Content and an Antioxidant Mechanism Are Responsible for the Antiproliferative Activity of 'Ataulfo' Mango Peel on LS180 Cells. Molecules, 23(3), 695. https://doi.org/10.3390/molecules23030695

Venter, P. B., Sisa, M., van der Merwe, M. J., Bonnet, S. L., & van der Westhuizen, J. H. (2012). Analysis of commercial proanthocyanidins. Part 1: The chemical composition of quebracho (Schinopsis lorentzii and Schinopsis balansae) heartwood extract. Phytochemistry, 73, 95–105. https://doi.org/10.1016/j.phytochem.2011.10.006

Vratsanos, M. A., & Gianneschi, N. C. (2022). Direct Observation of Emulsion Morphology, Dynamics, and Demulsification. ACS Nano. https://doi.org/10.1021/acsnano.2c00199

Wang, C., Siriwardane, D. A., Jiang, W., & Mudalige, T. (2019). Quantitative analysis of cholesterol oxidation products and desmosterol in parenteral liposomal pharmaceutical formulations. International Journal of Pharmaceutics, 569, 118576. https://doi.org/10.1016/j.ijpharm.2019.118576

Waraho, T., Cardenia, V., Rodriguez-Estrada, M. T., Julian McClements, D., & Decker, E. A. (2009). Prooxidant mechanisms of free fatty acids in stripped soybean oil-in-water emulsions. Journal of Agricultural and Food Chemistry, 57(15), 7112–7117. https://doi.org/10.1021/jf901270m

Waraho, T., McClements, D. J., & Decker, E. A. (2011a). Impact of free fatty acid concentration and structure on lipid oxidation in oil-in-water emulsions. Food Chemistry, 129(3), 854–859. https://doi.org/10.1016/j.foodchem.2011.05.034

Waraho, T., McClements, D. J., & Decker, E. A. (2011b). Mechanisms of lipid oxidation in food dispersions. Trends in Food Science & Technology, 22(1), 3–13. https://doi.org/10.1016/j.tifs.2010.11.003

Weigel, F., Weiss, J., Decker, E. A., & McClements, D. J. (2018). Lutein-enriched emulsion-based delivery systems: Influence of emulsifiers and antioxidants on physical and chemical stability. Food Chemistry, 242, 395–403. https://doi.org/10.1016/j.foodchem.2017.09.060

Xiang, Z., Guan, H., Zhao, X., Xie, Q., Xie, Z., Cai, F., Dang, R., Li, M., & Wang, C. (2024). Dietary gallic acid as an antioxidant: A review of its food industry applications, health benefits, bioavailability, nano-delivery systems, and drug interactions. Food Research International, 180, 114068. https://doi.org/10.1016/j.foodres.2024.114068

Xiao, J., Ling, L., Li, X., Zhou, X., Mo, X., Wan, P., Wang, Q., & Chen, D.-W. (2025). Lutein as an antioxidant inhibits the Maillard reaction in heated egg yolk. LWT, 218, 117490. https://doi.org/10.1016/j.lwt.2025.117490

Yang, B., Zhao, T., Ji, S., Liu, Y., Xu, M., & Lu, B. (2024). Molecular dynamics simulations of the interfacial behaviors and photo-oxidation of phytosterol under different emulsion oil content. Food Chemistry, 451, 139292. https://doi.org/10.1016/j.foodchem.2024.139292

Yang, X., Xiao, J., Wan, P., Liu, J., Mo, H., & Chen, D.-W. (2023). The effect of lutein on the oxidation of egg yolk phospholipids in a liposome model. Food Chemistry: X, 20, 100945. https://doi.org/10.1016/j.fochx.2023.100945

Chapter 6

Characterization of tannin-sterol co-precipitates: insight into binding interactions and structural properties

6.1 Abstract

The present study focused on the interactions between plant-derived tannins and sterols, with a particular focus on the formation of supramolecular complexes. Two types of tannins, chestnut (*Castanea sativa* Mill.*)* and quebracho (*Quercus infectoria* G. Olivier*)* (quebracho), were evaluated for their ability to interact with cholesterol and phytosterols (β-sitosterol and stigmasterol) as related to the presence of hydrolysable (chestnut) or condensed tannins (quebracho). UV-Vis spectroscopy, surface charge (ξ-potential) analysis, Differential Scanning Calorimetry (DSC) and Scanning Electron Microscopy (SEM) were used to investigate the potential interactions and confirm the formation of an amorphous aggregate. Finally, partitioning studies in O/W emulsions showed that tannins, particularly condensed, significantly influenced the distribution of sterols between oil and aqueous phases. Overall, the present work provides new insight into the supramolecular interaction between tannins and sterols, highlighting the potential application of tannins as natural agents to modulate sterols bioavailability in food system.

6.2 Introduction

Sterols, including cholesterol and phytosterols, are lipophilic molecules present in the majority of animal- and plant-based foods. Cholesterol (CH), an important component of animal cell membranes, is an essential regulator of membrane fluidity and precursor for steroid hormone and bile acid synthesis (de Oliveira et al. 2018). In spite of recent studies (DiMarco and Fernandez 2019) challenging the relationship between elevated serum cholesterol and dietary consumption of cholesterol-containing foods in healthy individuals, oxidized cholesterol derivatives remain strongly linked with an increased cardiovascular risk (Testa et al. 2018; Gargiulo et al. 2016; Leonarduzzi et al. 2007; Husche et al. 2015; Vigne and Pot 2024) highlighting the necessity of strict control of foods' oxidative stability in addition to their overall cholesterol content. In accordance, dietary approaches trying to minimize cholesterol absorption and increase of its excretion have been of particular interest. Among these strategies, plant sterols phytosterols, i.e., β-sitosterol and stigmasterol, have been of great interest due to their blood cholesterol-lowering properties (Poli et al. 2021; Cabral and Klein 2017). However, average dietary intake of phytosterols is not sufficient to have a clinically significant cholesterol-lowering effect; effective intake levels (~2 g/day) are difficult to obtain without fortification of functional foods (Cercaci et al. 2007).

Again, the scarce solubility of phytosterols in aqueous matter, and sensitivity to oxidation compromise their bioaccessibility and stability; thus, their integration into food matrices is difficult (Zhang et al. 2022).

On the other hand, plant polyphenols, especially tannins, have appeared as potential multipurpose agents. Plant polyphenols, especially tannins, are among the bioactive food components that are extensively investigated for anti-inflammatory, antioxidant, and hypocholesterolemic properties (Molino et al. 2024; 2021; 2018; Sallam et al. 2021; Smeriglio et al. 2017).

Tannins are a class of polyphenolic compounds that are usually classified into two categories: condensed tannins and hydrolysable tannins. The latter, also referred to as proanthocyanidins, consist

of oligomers or polymers of flavan-3-ols, for example, epicatechin and catechin (Arbenz and Avérous 2015), and are usually found in fruits like grapes, apples, and in certain wood extracts such as quebracho and chestnut. Tannin have been mostly recognized for their antinutritional effects, primarily due to their high ability to complexes with macromolecules, such as protein, carbohydrates, and mineral, and thereby rendering them less bioavailable (Smeriglio et al. 2017; Adamczyk et al. 2017; Serrano et al. 2009; Schöbel et al. 2014). Apart from these interactions, tannins have also shown a great ability to bind lipid molecules. Numerous studies indicated that condensed tannins have the ability to suppress cholesterol absorption via several mechanisms that include regulation of gene expression, binding of bile acid, and micellar solubility (Ogawa et al. 2016; Ikeda et al. 1992; Li et al. 2019). However, direct molecular-level interactions in straightforward aqueous systems or within emulsion-based matrices receive little attention in the majority of the current literature (Zeng et al. 2020).

Therefore, the present study aims to investigate the direct interaction between pure sterols (cholesterol, β-sitosterol, and stigmasterol) and two tannin sources (quebracho and chestnut). Further, fractionation of oil-in-water emulsions was carried out. These findings offer novel information on tannins' molecular binding ability, which may have an impact on functional food and diet formulation targeting lipid metabolism.

6.3 Material and Methods

6.3.1 Chemicals and Materials

All solvents and reagents were of analytical grade. Cholesterol (≥99%), (+)-catechin (≥99.0%), gallic acid (≥98.0%), sulfuric acid (≥97.0%) and Tween 20, were purchase from Sigma-Aldrich (St. Louis, MO, USA). β-sitosterol (≥70.0%) were obtained from Cayman Chemical (Ann Arbor, MI, USA). Stigmasterol (≥95.0%) was supply by Chemodex (St. Gallen, Switzerland). Ethanol, methanol and

methanol + 0.1% formic acid were purchased from Honeywell (Morristown, NJ, USA). Diethyl ether, n-hexane (99.0%) and potassium hydroxy were obtained from Carlo Erba (Milan, Italy). Vanillin (99.0%) was purchased from Alfa Aesar (Haverhill, MA, USA). Potassium iodate was obtained from Merck (Burlington, MA, USA) and PBS from Zymed (South San Francisco, CA, USA).

6.3.2 UV absorption spectra

The UV absorption spectra of ethanol solution of sterols (cholesterol, β-sitosterol and stigmasterol; 2mM) without and combined with the two selected tannins at different concentrations (Chestnut, Quebracho; 0, 4, 8, 12 and 16 μg/mL) were analyzed in a wavelength range of 200-400 nm at room temperature with a Shimadzu UV-1800 UV-Vis Spectrophotometer (Shimadzu, Kyoto, Japan).

6.3.3 Determination of catechin equivalents of tannin powders

The quantification of catechins was performed through the vanillin assay described by Scalbert et al., (1989) with slight modification. Briefly, quebracho tannins water solution (0.25 mg/mL) and chestnut water solution (1 mg/mL) were added of 2 mL of vanillin-sulfuric acid mixture (1% vanillin in H_2SO_4 70%) fresh prepared and left in dark at 20 °C for 15 minutes. Then, the absorbance was measured at 500 nm with a Shimadzu UV-1800 UV-Vis Spectrophotometer (Shimadzu, Kyoto, Japan). A calibration curve was developed with catechin standard in a range 1 - 60 μg/mL ($y = 0.042x – 0.0531$, $R^2 = 0.9983$) for quantitative purpose. The results were expressed as μg of catechin equivalent (CE)/mL of aqueous tannin solution.

6.3.4 Determination of gallic acid equivalent of tannin powders

The quantification of gallic acid equivalent described by Scalbert et al., (1989), was performed through the iodate potassium assay with some modifications. One mL of tannin solution (1 mg/mL in methanol 80%, *v/v*) was added to 5 mL of aqueous solution of KIO_3 (2.5%, *w/v*), previously keep

at 30 °C for 10 minutes. The solution was left at 30 °C for 2 minutes and then the absorbance was measured at 550 nm with a Shimadzu UV-1800 UV-Vis Spectrophotometer (Shimadzu, Kyoto, Japan). For the quantification, a calibration curve of gallic acid standard (10-100 μg/mL) ($y = 0.0016x + 0.038$, $R^2 = 0.9992$) was built. The results were expressed as μg of gallic acid equivalent (GaE)/mL of aqueous tannin solution.

6.3.5 Effect of tannins on zeta potential of sterol solutions

The solutions were prepared following the method reported by Zeng et al., (2020) with some modifications. Sterol ethanol solutions (20 mg/mL) were diluted 100 times in PBS (pH 7.4). The solutions were sonicated with VCX 500 Ultrasonic Microprocessor (Sonics Material, Newtown, CT, USA) at 40 % of amplitude for 3 minutes. Reaching the dispersion, sterol solutions were combined with the tannins (chestnut and quebracho) at different concentrations (0.5, 1.0, 1.5, 2.0 mg CE/mL) in equal ratio. Then, samples were sonicated with 20% of amplitude for 1 minute. Particle dimensions and surface charge were analyzed by Zetasizer Pro (Malvern Instruments, Worcestershire, UK) through dynamic light scattering using Universal 'Dip' Cell Kit (Zen 1002, Malvern Panalytical, UK).

6.3.6 Evaluation of tannins-sterols interaction

The co-precipitate of tannins and sterols was optimized from the method describe by Zeng et al., (2020) with modifications. Twenty microliters of sterol solution (20 mg/mL) were added to 2 mL of phosphate-buffered saline (PBS) and sonicated in a water bath for 5 minutes to ensure proper dispersion. Quebracho tannin solutions at different concentrations (0.5 and 2.0 mg catechin equivalents (CE)/mL) were then added to the sterol–PBS mixtures. The samples were incubated under shaking at 40 °C for 2 hours, followed by centrifugation at 10,000 × *g* for 20 minutes at 4 °C to separate the precipitates. A proper aliquot of the supernatant was subjected to vanillin assay (paragraph 6.2.2) to quantify the decrease in catechin equivalents compared to the initial quebracho

tannin solution and to the sterol content determined via gas chromatography with flame ionization detection (GC-FID; section 6.3.6). Samples prepared with the highest tannin concentration (2.0 mg CE/mL) were also analyzed by scanning electron microscopy (SEM) and Differential Scanning Calorimetry (DSC).

6.3.7 Determination of sterol content on supernatant

One mL of supernatant (obtained in section 6.3.5) was added to 1 mL of diethyl ether, followed by vigorous shaking and centrifugation at 8000 × *g* for 5 minutes at 5 °C. The organic phase was recovered, and the extraction was repeated once. The two ether extracts were then combined, and the solvent was removed under a nitrogen flow. The sterol samples were reconstituted in 200 µL of *n*-hexane. One µL was injected (split ratio 1:30) by autosampler into a GC -FID (Shimadzu 2010, Kyoto, Japan), equipped with a CP-TAP CB capillary column (25 m × 0.25 mm × 0.10 µm; Agilent Technology, Santa Clara, CA, USA). The oven temperature ramped from 200 °C to 310 °C at 5 °C/min and increased to 360 °C at 10 °C/min, maintained for 5 minutes. The temperature of the injector and FID were set at 355 °C and 360 °C, respectively. Helium was used as carrier gas with a linear velocity of 40 cm/s. The area ratio between the sterol standard solution and the area obtained from the sample was used to evaluate sterol recovery.

6.3.8 SEM imaging

Phenom XL G2 (Thermo-Fischer Scientific, Waltham, MA, USA) scanning electron microscope was used for imaging at accelerating voltage of 5 kV. Powder of tannins, sterols and precipitate were place into the SEM sample holder and acquired at 500× and 2000× magnification at room temperature.

6.3.9 Differential Scanning Calorimetry of co-precipitate

Differential Scanning Calorimetry (DSC) analyses were carried out using a Nexta DSC200 (Hitachi, Tokyo, Japan) calorimeter to assess the thermal behavior of pure sterols (β-sitosterol, cholesterol, stigmasterol), quebracho tannins (Q), and their binary mixtures (QB, QC, QS). Approximately 5 mg of each sample was accurately weighed into standard aluminum crucibles and hermetically sealed. An empty crucible was used as reference. The thermal program consisted of three consecutive cycles, designed to evaluate both initial transitions and potential reversible or irreversible changes. A heating cycle from 20 °C to 200 °C at a constant rate of 10 °C/min, to remove any thermal history, followed by a cooling cycle decreasing the temperature until -20 °C at 10 °C/min, to impart a controlled thermal history, was performed. Finally, a re-heating from −20 °C to 200 °C, at 10 °C/min, followed by an isothermal hold of 1 minute at 200 °C, was applied to evaluate the correct and stabilized melting profile. All analyses were conducted under a nitrogen atmosphere to prevent oxidation, using a flow rate of 50 mL/min.

6.3.10 Sterols content in water phase of O/W emulsion

Oil-in-water emulsion were prepared according to Figueroa-Espinoza et al., (2015). Twenty-four hours prior to preparation, tannins (chestnut, C; Quebracho, Q) were dissolved in phosphate buffer solution (10 mmol/L, pH 7.0 or pH 3.5) at two concentrations (0.1 % and 0.2 % of the total volume of buffer, *w/v*) as a substitute for 1% of Tween 20. Subsequently, stripped sunflower oil (SF) or lipid egg yolk fraction (EY) (10% of the total weight of the emulsion; *w/v*) was added to the aqueous solution and pre-mixed using an IKA T25 digital Ultra-Turrax (IKA-Werke GmbH & Co. KG, Staufen, Germany) for 2 minutes at speed of 20,000 rpm. Then, the emulsions were obtained by sonication for 3 minutes (alternating 30 sec On and 30 sec Off) at 40 % of amplitude. The temperature was continuously monitored during the process and maintained lower than 30 °C. A control sample (C), prepared without tannins and with 1% of tween 20, was also prepared in parallel. At the end, 3

mL of emulsion were transferred in 20 mL headspace vials previously pre-cleaned with 1N HCl solution to remove metal residues. The vials were sealed with aluminum caps with PTFE/silicone septa and stored in darkness at 40°C for 14 days. At day 0, 3, 6, 9 and 14, emulsions were centrifuged at 18,200 × *g* for 50 minutes at 4 °C using Angle Rotor 11461 with a MPW 260R centrifuge (MPW Med. Instruments, Warsaw, Poland) to separate the emulsion phases. The aqueous phase was collected and saponified with 5 mL of 4N KOH methanol solution for 18 hours under continuous stirring in dark at room temperature. Then, the unsaponifiable matter was isolated with 10 mL of diethyl ether and washed twice with10 mL of bi-distilled water. The organic phases were combined, filtered with 0.2 µm PTFE filter, then the solvent removed by a rotary evaporator (Rotavapor® R-210, Büchi, Flawil, Switzerland). The sterols were dissolved in 100 µL of methanol and analyzed by HPLC-MS/MS. Two µL were injected in a Nexera X3 UHPLC system (Shimadzu, Kyoto, Japan), equipped with a Kinetex C18 column (2.6 µm, 100 Å, 100 × 2.1 mm, Phenomenex, Torrence, CA, USA) protected by a guard column, and coupled with a linear ion-trap quadrupole mass spectrometer (QTRAP 3200; AB Sciex, Concord, ON, Canada) equipped with an atmospheric pressure chemical ionization (APCI) source. In agree with Wang et al., (2019) a gradient elution with water with 0.1% formic acid (A) and methanol acidified with 0.1% of formic acid (B)was used using the following program: 0 - 0.5 min 80% B, linear gradient from 80% B to 100% B in 8 min, held for 4 min then switched back to 80% B and re-equilibrated for 4 min. The flow rate was 0.3 mL/min. The elution of analytes was carried out 40 °C. The detection and quantification were obtained in positive ionization mode. Direct infusion was performed to optimize the mass parameters of sterols standard solution.

6.3.11 Statistical Analysis

To investigate the formation of tannins-sterols aggregate, one-way analysis of variance (one way ANOVA) and Tukey's post hoc test was used to determine any statistical difference between the

samples at a confidence level of 95%. IBM SPSS statistical software (version 29; IBM, Chicago, USA) was used.

6.4 Results

6.4.1 Characterization of tannins

The characterization of tannin powder from Quebracho and Chestnut was performed through the determination of catechin equivalent and gallic acid tannin equivalent assays. As expected, quebracho tannin powder contained a significantly higher amount of catechins (137.30 µg/mL) compared to chestnut tannin powder, which registered only 7.97 µg/mL. Contrarily, regarding the hydrolysable tannins assay, the gallic acid equivalents were equal to 48.13 µg/mL and 394.76 µg/mL for quebracho and chestnut, respectively.

6.4.2 Effects of tannins on UV spectra of Sterols

The effect of tannin solutions on UV spectra of cholesterol were displayed in Figure 6.1. Considering cholesterol (Figure 6.1a and 6.1b), the characteristic maximum absorption of the 2 mM cholesterol solution was observed at 209 nm. The addition of both tannins (C and Q) led to a shift in the maximum absorption to 206 nm. Furthermore, as the concentration of C and Q increased, a linear increase in absorbance at 206 nm was observed. A similar trend was detected for β-sitosterol and stigmasterol. β-sitosterol exhibited a maximum absorbance at 206 nm. The addition of C led to a shift to 205 for C4, 204 nm for C8 and C12, while C16 shifted the absorbance to 208 nm. However, compared to cholesterol, the absorbance curves were lower than those found for single sterol. The addition of Q resulted in a shift of only 1 nm, also showing a decrease in absorbance when combined with the sterol. Regarding stigmasterol, a shift from 209 to 207 nm was observed, with an increase in absorbance at concentrations of 12 and 16 µg/mL for both C and Q. Figure 6.1 reports the resulting signal obtained

by subtraction of tannin signal (16 µg/mL) at the sum of sterol-tannin (16 µg/mL) complex signal. In the case of chestnut tannin, the theoretical sterol signal was higher than the values recorded with quebracho tannin. It was important to note that the individual tannins did not exhibit maximum absorption at the wavelengths corresponding to the sterol solution.

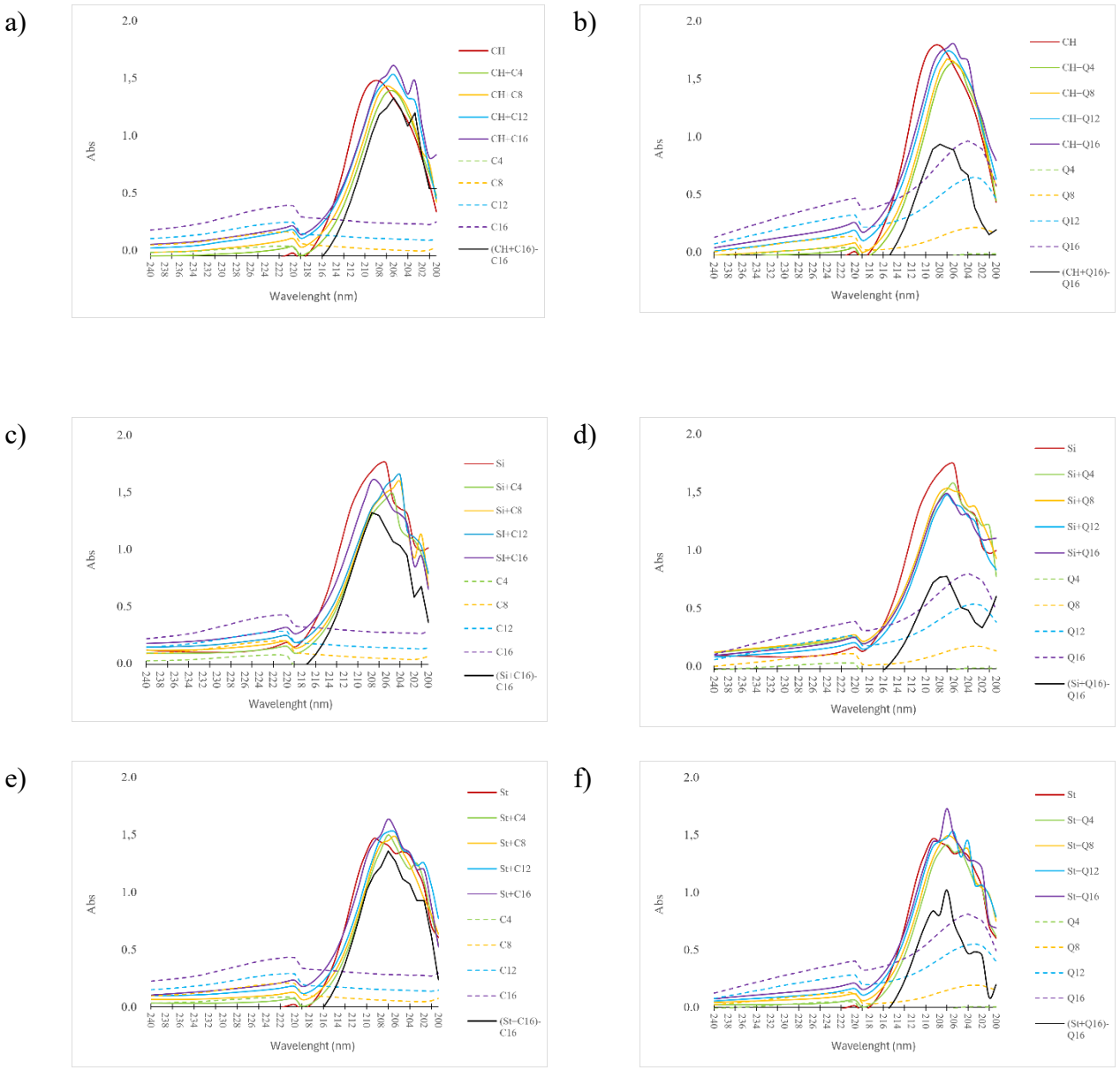

Figure 6.1. Effect of different concentration of tannin on the UV spectra of ethanol sterol solutions; a) cholesterol + chestnut; b) cholesterol + quebracho; c) β-sitosterol + chestnut; d) β-sitosterol + quebracho; e) Stigmasterol + chestnut; f) Stigmasterol + quebracho.

6.4.3 Impact of tannins on ζ-potential

In this study, zeta potential measurements were used to assess the possible interactions between sterols and quebracho tannins in aqueous dispersions. As reported in Figure 6.2, the addition of quebracho tannin to sterol solutions reduced the negative charge, with differences due to the different sterols.

Cholesterol alone showed a value of -29.46 ± 0.97 mV, indicating moderate-to-high stability of the solution. The addition of 0.5 mg CE/mL significantly increased (p<0.01) the negative surface charge. However, at higher quebracho tannin concentrations (1, 1.5, and 2 mg/mL) the zeta potential progressively decreased (p<0.001, CH+Q0.5), suggesting reduced solution stability due to potential interactions between cholesterol and tannins. A similar trend was observed for β-sitosterol (-18.47 ± 0.82 mV), where the addition of 0.5 mg CE/mL improved colloidal stability (-22.69 ± 0.83 mV). However, at higher tannin concentrations (1, 1.5, and 2 mg CE/mL) no significant changes in surface charge were detected compared to the sterol control (p>0.05), suggesting a threshold effect in the sterol–tannin interaction.

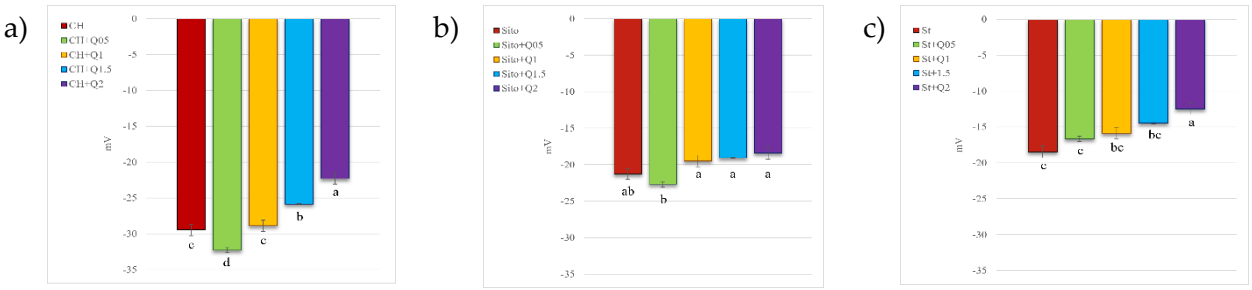

Figure 6.2. Effect of quebracho tannins on zeta potential of a) cholesterol, b) β-sitosterol and, c) stigmasterol. Results are expressed as mean ± standard deviation (n=3). Results of ANOVA with Tukey's post hoc test are reported; different letters indicate significantly different means (p<0.05) among the samples.

6.4.4 Catechin equivalent and sterols content after precipitation

Vanillin assay was employed for the quantification of catechin equivalent present in the supernatant after the formation of co-precipitate. The results are reported in table 6.1.

Table 6.1. Catechins equivalent recoveries in supernatant after the formation of co-precipitate sterol-tannin

	0.5 mg CE/mL	**2.0 mg CE/mL**	*Sign.*
Cholesterol	91.37 ± 1.33 %	87.96 ± 3.43 %	n.s.
β-sitosterol	93.90 ± 6.44 %	85.92 ± 1.67 %	n.s.
Stigmasterol	95.19 ± 1.64 %	85.95 ± 1.30 %	n.s.
Sign.	n.s.	n.s.	

Each value represents the mean ± standard deviation of three independent experiments (n=3).
Sig., statistical significance; n.s., not significant. The asterisks denote the level of significance: *, $p<0.05$; **, $p<0.01$; *** $p<0.001$.

The results suggest that the formation of the precipitate leads to a reduction in catechin content in the supernatant. Control samples (i.e., without added sterols) were set as 100%, and the values for the other samples were expressed as a percentage relative to this baseline. The observed decrease in catechin equivalents suggests the formation of tannin–sterol complexes, which remove tannins from the supernatant through co-precipitation. Furthermore, as the tannin concentration increased as a consistent reduction in residual catechin content in the supernatant was found, even if the data was not statistically significant ($p>0.05$). That suggests a possible concentration-dependent but saturable interaction between tannins and sterols under the tested conditions.

6.4.5 Differential Scanning Calorimetry – DSC

Differential Scanning Calorimetry (DSC) was employed to evaluate the interactions between quebracho tannin (Q) and the three sterols considered in this study. Individual components and their

binary mixtures with Q were analyzed. The results graphs are reported in Figure 6.7.1 (Appendix). Pure β-sitosterol (Figure 6.7.1 a) displayed a sharp endothermic peak at 136.5 °C (−18303 μW), corresponding to the melting point. In contrast, the Q+β complex showed a substantially reduced endothermic event. Overall, the curve was notably flatter and devoid of distinct thermal transitions. Pure cholesterol (Figure 6.7.1 b) displayed a pronounced endothermic event at 151.6 °C (−26032 μW). Again, complex Q+C not exhibited thermal profile. Finally, pure stigmasterol showed an endothermic peak at 172.3 °C (−30971 μW). In the QS complex, surprisingly, the endothermic peak was observable but displayed a temperature shift (160.6 °C) and markedly attenuated (−5243 μW).

6.4.6 Scanning Electron Microscopy (SEM)

To investigate the morphological changes induced by tannin–sterol interactions, pure compounds and selected co-precipitates were examined using scanning electron microscopy (SEM) at magnifications of 500× and 2000×. The resulting micrographs revealed distinct morphological differences among the individual tannins and sterols, as well as significant alterations following co-precipitation. Representative SEM images of the pure compounds are presented in Appendix figures 6.7.1. Quebracho tannin (6.7.2a, 500×; 6.7.2b, 2000×) exhibited a highly heterogeneous morphology, characterized by irregular globular aggregates with concave surfaces and occasional filamentous structures, likely corresponding to residual of lignin. In contrast, chestnut tannin (6.7.2c, 500×; 6.7.2d, 2000×) appeared more homogeneous, forming finer and more uniform particles. While similar globular features were occasionally observed, they were less abundant and smaller in size. Additionally, small spherical aggregates clustered together were visible, suggesting a more compact and uniform structure. The sterol standards also showed unique and well-defined morphologies. Cholesterol (6.7.2e, 500×; 6.7.2f, 2000×) formed compact, overlapping flake-like structures. Stigmasterol (6.7.2g, 500×; 6.7.2h, 2000×) displayed elongated, hexagonal crystals with lengths of

approximately 20 µm, resembling a well-organized crystalline conformation. β-sitosterol appeared as long, rod-like filaments, also measuring around 20 µm in length. Upon co-precipitation, significant morphological changes were observed across all tannin–sterol complexes. Appendix figures 6.7.3c, show the co-precipitates formed with cholesterol (6.7.3a), stigmasterol (6.7.3b), and β-sitosterol (6.7.3c), respectively. In all cases, the distinctive morphologies of the individual components disappeared. Instead, dense, amorphous deposits were formed, characterized by irregular, flake-like structures lacking the crystalline features seen in the pure compounds. These observations support the formation of new supramolecular assemblies, likely stabilized by non-covalent interactions, as suggested by spectroscopic and colloidal analyses.

6.4.7 Sterols content in water phase of O/W emulsions

The cholesterol and β-sitosterol content are depicted in Figure 4. Cholesterol content was ranged from 0.11 ± 0.01 to 0.47 ± 0.22 µg/mL of emulsion. The 0.2Q at pH 3.5 showed the highest cholesterol content, followed by 01Q at the same pH on day 0. After 3 days, cholesterol retention in water phase significantly dropped for all samples except for 01C pH 3.5 and 0.2C pH 7. At the final stage of the shelf life, no significant differences (p>0.05) were observed between all samples.

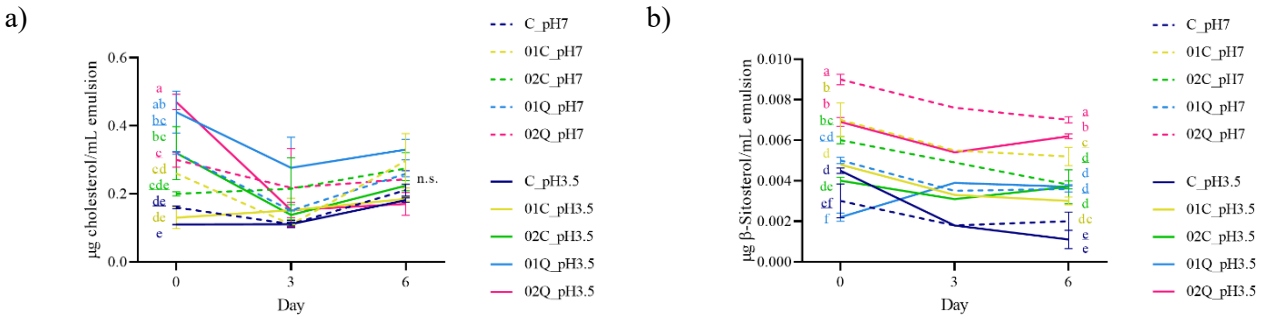

Figure 6.3. Cholesterol (a) and β-sitosterol (b) content in water phase of O/W emulsions. Results are expressed as mean ± standard deviation (n=3). Results of ANOVA with Tukey's post hoc test are reported; different letters indicate significantly different means (p<0.05) among the samples.

β-sitosterol content was lower than cholesterol, ranging from 0.0022 ± 0.0002 to 0.0090 ± 0.0001 μg/mL of emulsion. Again, 0.2Q was the samples with higher amounts of β-sitosterol but, in this case, at pH 7.0, followed by 0.1C pH 7.0 and 0.2Q pH 3.5. A decrease in β-sitosterol content was also observed but at day 6 the samples maintained significant differences (p<0.05) between them, confirming 0.2Q at both pH conditions the samples able to drive in water phase sterols compounds. Control samples were lower (p<0.01) respect to the samples-tannin emulsions.

6.5 Discussion

The present study explored the physicochemical interactions between two types of tannin extracts with both plant and animal sterols, aiming to investigate their potentially complexation behavior. The UV absorption spectra was used as a preliminary tool to evaluate the possible interaction. Based on the different absorption spectra, the formation of an aggregate was hypothesized. In the presence of tannins, particularly quebracho, upon mixing with cholesterol, β-sitosterol, and stigmasterol, a hypsochromic (blue) shift of the maximum absorption peak was produced, and in some cases, concentration-dependent absorbance intensity changes were found. These spectral shifts, often accompanied by an observed loss of absorbance in some cases, suggest changes in sterol microenvironment polarity and tighter packing in the aggregate. Such changes in spectra are consistent with non-covalent complexes with different degrees of hydrophobic interaction, hydrogen bond formation, and π–π stacking (Song et al., 2015; Zeng et al., 2020). Zeng et al. (2020), similarly reported blue shifts upon combining condensed tannins from apple with cholesterol, confirming the utility of UV spectroscopy for detecting tannin–sterol interactions. To the best of our knowledge, no studies have been conducted on the interaction of tannins with phytosterols. A key observation was the difference in theoretical absorbances: according to the research conducted by Song and collegues (2015), if no interactions occurred between two molecular components, their combined absorption spectrum should have remained similar to that of the primary molecule. The observed decrease in

absorbance when combining Q with sterols may be attributed to signal quenching due to the formation of tightly bound aggregates. The lower theoretical absorbance in the presence of quebracho tannin (composed predominantly by condensed tannin, such as catechin and fisetinidol units (Molino et al. 2018)) suggested a stronger interaction with sterols, leading to a greater deviation from the sterol-alone spectrum respect to those noted with chestnut (mainly composed by hydrolysable tannins, such as castalagin and vescalagin), indicating a signal more similar to that of the sterol alone, implying a weaker interaction. Based on the vanillin assay performed on the tannin powders, quebracho showed a concentration of 207.96 μg CE/mL, whereas chestnut exhibited only 7.97 μg CE/mL content, confirming the higher value in Q of catechin units. These differences in interaction ability may stem from structural factors: condensed tannins own a rigid and aromatic-rich structure that can interact with sterols via stacking or H-bonding, while hydrolysable tannins are more polar and flexible, which may limit their ability to form stable complexes in a lipid-like environment. Supporting this, Zheng et al. (2020) confirmed via computational simulations that four types of catechins form stable complexes with cholesterol, with high adsorption energies and the presence of hydrogen bonds. Their results indicate that the molecular interaction is mainly driven by hydrogen bonds and π-interactions (charge transfer of aromatic rings of tannins) without requiring covalent bonds. Given that quebracho tannins are predominantly composed of catechin units, their stronger interaction with sterols observed in this study aligns with the proposed mechanism. Catechin-based interaction with sterols has been shown to decrease cholesterol micelle formation, supporting the idea that quebracho tannins are more effective in sterol binding than hydrolysable tannins from chestnut. Several research have been demonstrated that tannins could interact directly with cholesterol (and analogous), forming complex or no-covalent precipitates. For instance, Ogawa et al. (2016) and Ikeda et al. (1992) reported that the addition of epigallocatechin gallate to bile micellar solution and cholesterol lead to the formation of a precipitate formed by cholesterol and catechin, reducing the amount of cholesterol in solution. Other studies support the theory of strong binding forces exerted by catechin toward lipid molecules,

particularly focusing on the lipid membrane. The interaction between catechins and lipids primarily involves the galloyl moiety, which plays a significant role in their binding to phospholipid membranes (Matsuzaki et al., 2017). Molecular dynamics simulations further reveal that the presence of hydroxyl groups in catechins enhances hydrogen bonding with lipid headgroups, particularly in the absorbed state (Sirk et al., 2008).

Further insight into the colloidal behavior of the systems was obtained from ζ-potential analysis. The addition of quebracho tannin significantly altered the surface charge of sterol suspensions in a dose-dependent manner. ζ-potential is defined as the electrical potential at the slipping plane of the electric double layer surrounding a particle in a colloidal dispersion. It is a critical parameter for understanding the stability and behavior of colloidal systems, being influenced by the surface charge of particles, the ionic strength, and the pH of the solution. A high zeta potential, whether positive or negative, indicates strong electrostatic repulsion between particles, which prevents aggregation and enhances colloidal stability (Feng, Kilker, and Lee 2020). At low concentrations, quebracho tannin likely adsorbs onto both cholesterol and β-sitosterol particle surfaces, exposing its functional groups (e.g., phenolic and carboxyl groups), which contribute to a more negative charge. In contrast, increasing tannin concentrations likely lead to a higher degree of interaction or aggregation, progressively masking the negative surface charge and thus reducing the zeta potential. Conversely, stigmasterol exhibited a distinct behavior. The control sample showed the highest negative charge, and the progressive addition of tannins led to a gradual decrease in zeta potential ($p<0.01$), indicating reduced colloidal stability as tannin concentration increased. These differences may be attributed to slight variations in molecular structure: stigmasterol owns a double bond in the aliphatic side chain (C22-C23), which is absent in cholesterol and β-sitosterol. This unsaturation may influence hydrophobic interactions with tannins, possibly altering their affinity or aggregation behavior (Haç-Wydro et al., 2010). Additionally, the presence of a double bond in the side chain may affect molecular packing and aggregation tendencies, making stigmasterol more prone to forming dense

aggregates in the presence of tannins. This structural specificity likely explains the progressive masking of surface charge observed with increasing tannin concentration. To further confirm the aggregation hypothesis, particle size measurements were attempted. However, the results were inconsistent and poorly reproducible due to the high instability of the system (data not shown). The observed fluctuations suggest that tannin-induced aggregation occurs dynamically, leading to irregular particle size distributions and further supporting the hypothesis of sterol–tannin interactions affecting colloidal stability.

Differential Scanning Calorimetry (DSC) analysis was conducted to investigate the thermal transitions of pure sterols (cholesterol, C; β-Sitosterol, B., stigmasterol, S) and their respective complexes with quebracho tannins. The DSC thermograms revealed distinct thermal behaviors between the pure sterols and their complexes, suggesting significant interactions affecting their crystallinity and thermal stability. Quebracho tannin alone exhibited a largely featureless DSC profile, consistent with its amorphous nature. In general, condensed tannins are low-density amorphous non-crystalline solid oligomers/polymers (García et al., 2016). As a plant-derived polyphenolic extract, quebracho is composed of structurally diverse oligomeric and polymeric units that do not crystallize under standard conditions. On the other hand, the pure sterols – cholesterol, β-sitosterol, stigmasterol – displayed well-defined peaks, exhibiting characteristic endothermic peaks corresponding to their melting transitions, indicative of their crystalline nature, confirmed by the SEM analysis describe subsequently. The Differential Scanning Calorimetry (DSC) analysis revealed significant alterations in the thermal behavior of sterol–quebracho tannin complexes compared to their pure sterol counterparts. Upon complexation with quebracho tannins, these thermal events were notably diminished or absent, suggesting a disruption of the sterols' crystalline structure. That observation implies the formation of amorphous complexes, where sterol molecules are likely dispersed within the tannin matrix, hindering their ability to undergo typical phase transitions. The degree of thermal transition suppression varied among the sterols studied, indicating differential interactions with the

tannin. Specifically, in the case of β-sitosterol, the thermal profile of the Q+BETA complex lacked the characteristic melting peak observed in the pure compound. Nevertheless, while pure quebracho tannin (Q) displayed a broad and smooth baseline consistent with its amorphous nature, the Q+BETA curve presented notable deviations in both signal intensity and curve shape. These differences suggest that β-sitosterol, although not exhibiting its typical phase transition, was still present in the system in a thermally modified state. Similar result was obtained with cholesterol. A clearly endothermic peak was obtained, while in the QC complex, the endothermic melting transition is completely absent, indicating that cholesterol is no longer present in a crystalline form. This suggests that the sterol is either molecularly dispersed within the tannin matrix or structurally disordered to an extent that suppresses its phase transition. Sreij et al. (2019) reported that the interaction between cholesterol and aescin led to an increase in the intensity of thermal signals. Similarly, binary interactions between cholesterol and phospholipids - mediated by van der Waals forces between the sterol backbone and lipid membranes - were shown to result in a broader endothermic signal and a downward shift in the transition temperature. Moreover, Esperança et al. (2022) reported that the addition of γ-oryzanol to cholesterol hindered its normal crystallization, promoting the formation of mesophases that melted at lower temperatures. Finally, the thermal behavior of pure stigmasterol was again characterized by a distinct endothermic melting transition. However, upon the complexion with quebracho tannins, the transition was still observable in the QS sample but appeared significantly attenuated and shifted. Unlike β-sitosterol and cholesterol, whose thermal signals were fully suppressed, stigmasterol retained its fundamental thermal behavior, suggesting limited structural perturbation. The preservation of both transitions in the QS complex indicates that stigmasterol maintains a significant degree of crystallinity even after interaction with the tannin. This suggests that the interaction is relatively weak, insufficient to fully disrupt its organized structure. Again, one possible explanation is related to the double bond at the C22-C23 position, as described above.

Scanning Electron Microscopy (SEM) provided additional evidence supporting the morphological transformations induced by tannin–sterol interactions. Pure sterols displayed distinct and recognizable morphologies: crystalline flakes for cholesterol, rod-like structures for β-sitosterol, and well-defined polyhedral crystals for stigmasterol. In contrast, the co-precipitates exhibited a markedly different and amorphous appearance. The transition from well-organized crystalline forms to irregular, dense aggregates suggest a significant molecular rearrangement promoted by interaction with quebracho tannins. The co-precipitates appeared as compact, granular masses lacking visible structural order, implying a disruption of the original molecular packing and a substantial loss of crystallinity. This amorphization is likely driven by non-covalent forces - such as hydrogen bonding and hydrophobic interactions - that facilitate the rearrangement of sterol molecules into less ordered configurations (Kong et al., 2022). Furthermore, the increased compactness observed in all complexes compared to their pure counterparts supports the hypothesis of supramolecular organization between tannins and sterols. The SEM findings align closely with the DSC results. The loss or attenuation of characteristic thermal transitions observed in the DSC thermograms strongly corroborates the morphological evidence of crystallinity disruption. Together, the thermal and morphological analyses provide a consistent picture of molecular-level interaction and structural modification upon complexation, with variations in the degree of disorder depending on the specific sterol involved. The disappearance of the melting peak in the cases of cholesterol and β-sitosterol may suggest stronger interactions between the two components, leading to the formation of a completely amorphous structure devoid of crystallinity. In contrast, for stigmasterol, the persistence of the melting peak could indicate weaker interaction with quebracho tannin or a better-organized system, thus retaining a certain degree of crystallinity.

Finally, to determine whether the presence of cholesterol and β-sitosterol in the aqueous phase was associated with the surfactant-like activity of tannins, control emulsions - formulated without tannins - were also analyzed. Although sterol concentrations were lower in control samples and both

cholesterol and β-sitosterol were still detectable in the aqueous phase. That suggests that solubilization, albeit limited (∼10 - 60 nM in pure water) (Vinarova et al., 2015), can be facilitated by emulsifiers. Indeed, Inchingolo et al. (2021) and Mitra & Dungan (2001) demonstrated that an excess of emulsifier can drive lipophilic molecules from the dispersed oil phase into the continuous aqueous phase. Tween 20, a non-ionic surfactant used in the present study, has a low critical micelle concentration (CMC), which favors micelle formation and the incorporation of sterols even at relatively low concentrations. Additionally, Mitra & Dungan (2001) demonstrated the transfer potential of cholesterol from oil to water in emulsions stabilized by saponins, highlighting the role of surfactant concentration, temperature, and pH. Their findings identified an optimal pH around 4.0 for cholesterol transfer, with pH 3.2 being the least effective, and neutral pH exhibiting intermediate behavior. This pattern may explain the small, non-significant differences (p>0.05) observed in sterol content in control emulsions across pH conditions. However, further research is needed to explore how pH influences micelle structure and surface activity, particularly for non-ionic surfactants like Tween 20. Interestingly, sterol structure appears to be a critical factor in aqueous phase transfer; β-sitosterol, compared to cholesterol, exhibited an opposite trend, with increased aqueous solubilization under neutral conditions.

The addition of tannins, particularly quebracho tannin, significantly enhanced the initial solubilization of both cholesterol and β-sitosterol compared to controls. This observation is consistent with previous UV-Vis spectrophotometric studies, where condensed tannins, such as quebracho, demonstrated a stronger ability to interact with sterols than hydrolysable tannins, such as chestnut. These findings suggest that tannins may act as dispersing or complexing agents, facilitating sterol transfer into the aqueous phase through interactions at the oil–water interface or within the micellar environment. Supporting that, in a previous study (Bonciolini et al., 2023) oak wood tannin extract and tara tannin extract, both belong to the hydrolysable category, showed the ability to drive cholesterol from fresh egg pasta to cooking water. Similarly, in the present O/W emulsions, a

comparable effect was observed for hydrolysable tannins, particularly under neutral pH, where both cholesterol and β-sitosterol levels increased in the aqueous phase. Zeng et al. (2019) reported that tannic acid and gallic acid exerted stronger inhibitory effects on the cholesterol solubility in mixed micelles and liquid egg yolk in a dose-dependent relationship. Again, Ngamukote et al. (2011) reported that 0.2 mg/mL, gallic acid, catechin, and epicatechin reduced the formation of cholesterol micelles in a range from 11.88 to 27.26 %.

The time-course analysis revealed distinct behaviors between cholesterol and β-sitosterol. Cholesterol content in the aqueous phase declined significantly by T3 and smoothed across all samples at T6, suggesting potential reorganization at the interface, re-incorporation into oil droplets, or oxidative degradation. In contrast, β-sitosterol maintained significant differences between samples even at T6, with 0.2% quebracho consistently achieving the highest aqueous phase retention. This could be due, in part, to differences in the sample matrices: egg yolk emulsions contain additional components compared to sunflower oil ones, which could modulate interfacial dynamics during storage. In contrast, emulsions prepared with stripped sunflower oil offered a simpler, more controlled lipid environment, potentially allowing a clearer observation of sterol-tannin interactions during oxidative shelf life. Importantly, the observed differences between sterols in emulsions align with the solid-state characterization results. DSC and SEM analyses demonstrated that β-sitosterol undergoes stronger disruption of crystalline organization upon complexation with quebracho tannins, leading to an amorphous phase, while cholesterol retains partial structure. These findings suggest that the greater aqueous phase retention of β-sitosterol in emulsions could be linked to its higher propensity to form disordered, solubilized complexes with tannins, thereby improving its dispersion in the aqueous environment. Conversely, cholesterol's more rigid partially crystalline organization may limit its long-term retention in the aqueous phase under oxidative stress conditions. Overall, these results underscore the complexity of sterol–polyphenol interactions in emulsified systems and highlight how

both the chemical nature of the sterol and the structural features of the tannin influence not only initial solubilization but also sterol redistribution and stability during shelf life.

6.6 Conclusion

This study investigated the interaction between tannins and sterols, highlighting the capacity of condensed tannins, particularly those from quebracho, to form supramolecular complexes with both cholesterol and phytosterols. Spectroscopic analyses first demonstrated systematic shifts in absorbance intensity and wavelength upon tannin addition, indicating alterations in the microenvironment due to non-covalent interactions. Zeta potential measurements further confirmed this hypothesis, showing that quebracho tannins modulate the electrostatic properties of the system in a concentration-dependent manner. Differential Scanning Calorimetry (DSC) provided additional evidence of molecular interactions, revealing shifts and modifications in thermal transition profiles in the co-precipitates compared to the isolated sterols and tannins. These findings were corroborated by morphological analysis using Scanning Electron Microscopy (SEM), which confirmed the formation of amorphous, densely packed aggregates following tannin–sterol co-precipitation. Moreover, partitioning studies conducted in emulsified systems revealed that tannins significantly influenced sterol distribution between the lipid and aqueous phases, supporting the hypothesis of complex formation under dynamic conditions. However, further investigations are necessary to better understand the differential behavior observed between sterols, particularly stigmasterol. Additional studies are also required to elucidate the actual impact of tannin–sterol interactions during human digestion and metabolism.

Appendix

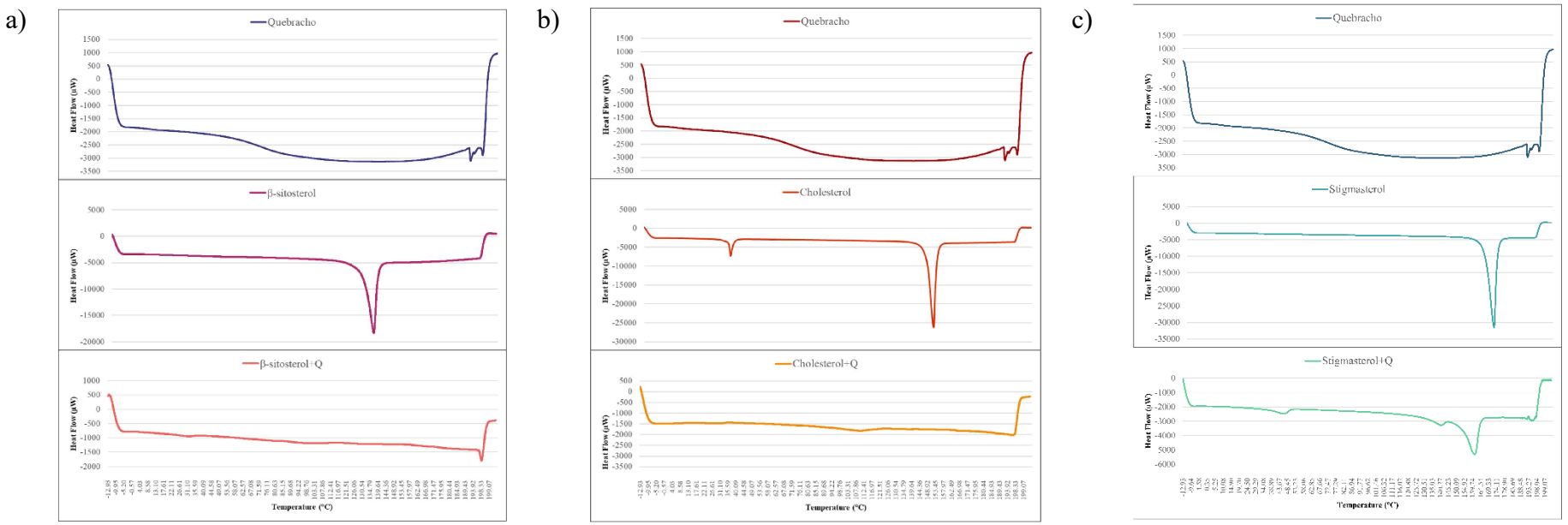

Figure 6.7.1. Differential Scanning Calorimetry (DSC) thermograms of the co-precipitates. (a) β-sitosterol series; (b) cholesterol series; (c) stigmasterol series. In each series, the first graph represents quebracho tannin alone; the second graph represents the pure sterol; the third graph represents the quebracho–sterol co-precipitate.

a)

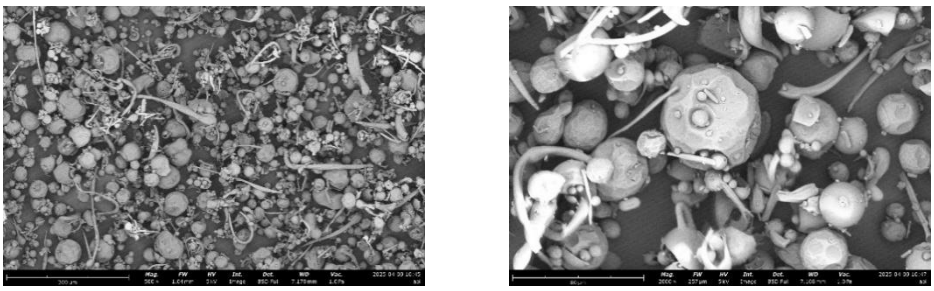

b)

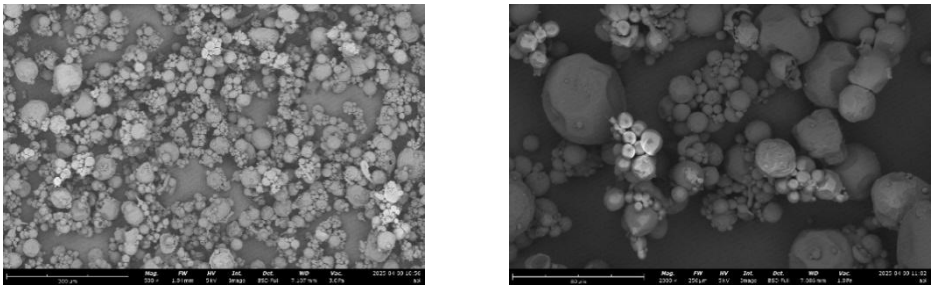

c)

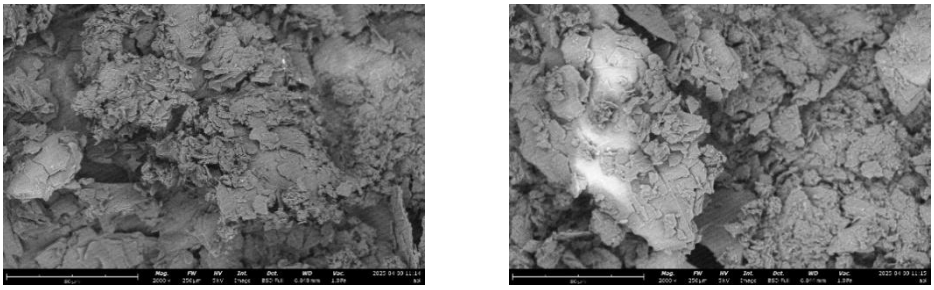

d)

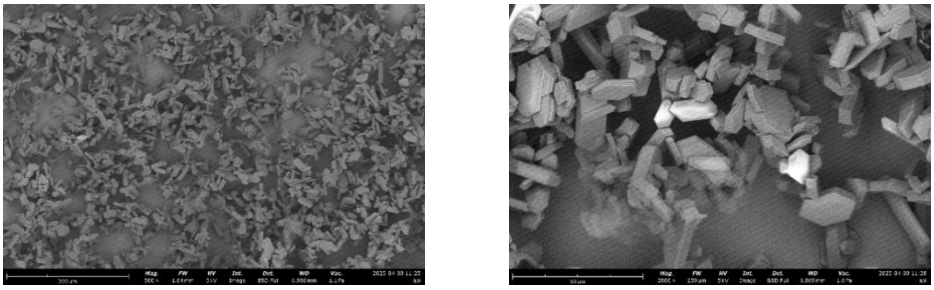

e)

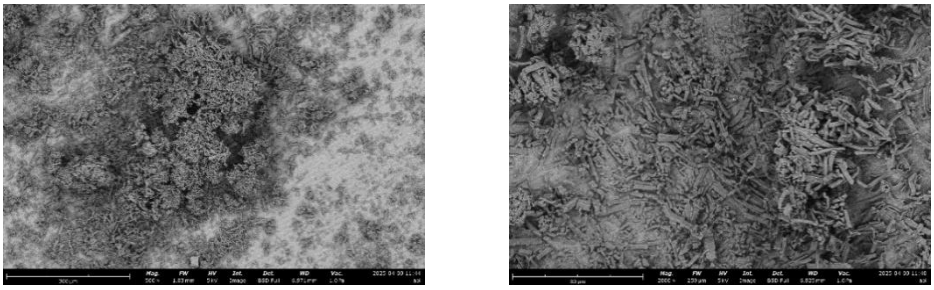

Figure 6.7.2. SEM micrographs of a) quebracho tannin; b) chestnut tannin; c) cholesterol; d) stigmasterol; e) β-sitosterol. Images in the first column were acquired at 500× magnification, and those in the second column at 2000× magnification.

a) 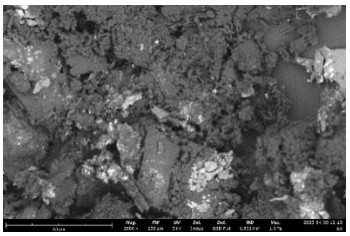 b) 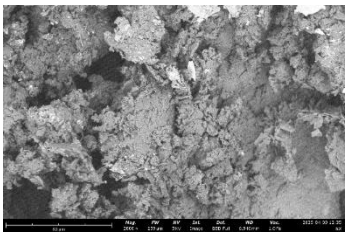 c) 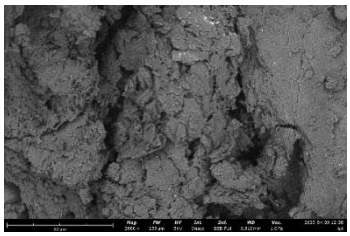

Figure 6.7.3. SEM micrograph (Magn. 2000×) of quebracho tannins co-precipitate with a) cholesterol; b) β-sitosterol; c) stigmasterol.

References

Adamczyk, B., Simon, J., Kitunen, V., Adamczyk, S., & Smolander, A. (2017). Tannins and their complex interaction with different organic nitrogen compounds and enzymes: old paradigms versus recent advances. ChemistryOpen, 6(5), 610–614. https://doi.org/10.1002/open.201700113

Arbenz, A., & Avérous, L. (2015). Chemical modification of tannins to elaborate aromatic biobased macromolecular architectures. Green Chemistry, 17(5), 2626–2646. https://doi.org/10.1039/c5gc00282f

Bonciolini, A., Cantele, C., Salgarella, N. I., Zeppa, G., Bertolino, M., & Cardenia, V. (2023). Effect of tannins on cholesterol content and its oxidation in egg pasta as related to different pasta shapes. Food and Bioprocess Technology, 16(7), 1541–1554. https://doi.org/10.1007/s11947-023-03016-1

Cabral, C. E., & Klein, M. R. S. T. (2017). Phytosterols in the treatment of hypercholesterolemia and prevention of cardiovascular diseases. arquivos brasileiros de cardiologia. https://doi.org/10.5935/abc.20170158

Cercaci, L., Rodriguez-Estrada, M. T., Lercker, G., & Decker, E. A. (2007). Phytosterol oxidation in oil-in-water emulsions and bulk oil. Food Chemistry, 102(1), 161–167. https://doi.org/10.1016/j.foodchem.2006.05.010

de Oliveira, V. S., Ferreira, F. S., Cople, M. C. R., Labre, T. da S., Augusta, I. M., Gamallo, O. D., & Saldanha, T. (2018). Use of natural antioxidants in the inhibition of cholesterol oxidation: a review. In Comprehensive Reviews in Food Science and Food Safety (Vol. 17, Issue 6, pp. 1465–1483). Blackwell Publishing Inc. https://doi.org/10.1111/1541-4337.12386

DiMarco, D. M., & Fernandez, M. L. (2019). Differences in response to egg-derived dietary cholesterol result in distinct lipoprotein profiles while plasma concentrations of carotenoids and choline are not affected in a young healthy population. Journal of Agriculture and Food Research, 1, 100014. https://doi.org/10.1016/j.jafr.2019.100014

Esperança, E. S., Bonatto, M. S., Silva, K. C. G., Shimamoto, G. G., Tubino, M., Costa, M. C., Rodrigues, C. E. C., Meirelles, A. J. A., Sato, A. C. K., & Maximo, G. J. (2022). Phytosterols and γ-oryzanol as cholesterol solid phase modifiers during digestion. Foods, 11(22), 3629. https://doi.org/10.3390/foods11223629

Feng, Y., Kilker, S. R., & Lee, Y. (2020). Surface charge (zeta-potential) of nanoencapsulated food ingredients. In Characterization of nanoencapsulated food ingredients (pp. 213–241). Elsevier. https://doi.org/10.1016/B978-0-12-815667-4.00007-9

Figueroa-Espinoza, M. C., Zafimahova, A., Alvarado, P. G. M., Dubreucq, E., & Poncet-Legrand, C. (2015). Grape seed and apple tannins: Emulsifying and antioxidant properties Dedicated to the memory of Gérard Mazerolles. Food Chemistry, 178, 38–44. https://doi.org/10.1016/j.foodchem.2015.01.056

García, D. E., Glasser, W. G., Pizzi, A., Paczkowski, S. P., & Laborie, M.-P. (2016). Modification of condensed tannins: from polyphenol chemistry to materials engineering. New Journal of Chemistry, 40(1), 36–49. https://doi.org/10.1039/C5NJ02131F

Gargiulo, S., Gamba, P., Testa, G., Leonarduzzi, G., & Poli, G. (2016). The role of oxysterols in vascular ageing. Journal of Physiology, 594(8), 2095–2113. https://doi.org/10.1113/JP271168

Haç-Wydro, K., Flasiński, M., Broniatowski, M., Dynarowicz-ŁĄtka, P., & Majewski, J. (2010). Comparative studies on the influence of β-sitosterol and stigmasterol on model sphingomyelin membranes: A grazing-incidence X-ray diffraction study. Journal of Physical Chemistry B, 114(20), 6866–6871. https://doi.org/10.1021/jp101196e

Husche, C., Sch, H. F., Weing, O., Lütjohann, D., & Laufs, U. (2015). Vascular effects of oxysterols and oxyphytosterols in apoE À / À mice. 240, 73–79. https://doi.org/10.1016/j.atherosclerosis.2015.02.032

Ikeda, I., Imasato, Y., Sasaki, E., Nakayama, M., Nagao, H., Takeo, T., Yayabe, F., & Sugano, M. (1992). Tea catechins decrease micellar solubility and intestinal absorption of cholesterol in rats. Biochimica et Biophysica Acta (BBA) - Lipids and Lipid Metabolism, 1127(2), 141–146. https://doi.org/10.1016/0005-2760(92)90269-2

Inchingolo, R., Bayram, I., Uluata, S., Kiralan, S. S., Rodriguez-Estrada, M. T., McClements, D. J., & Decker, E. A. (2021). Ability of sodium dodecyl sulfate (sds) micelles to increase the antioxidant activity of α-tocopherol. Journal of Agricultural and Food Chemistry, 69(20), 5702–5708. https://doi.org/10.1021/acs.jafc.1c01199

Kong, F., Kang, S., Zhang, J., Jiang, L., Liu, Y., Yang, M., Cao, X., Zheng, Y., Shao, J., & Yue, X. (2022). The non-covalent interactions between whey protein and various food functional ingredients. Food Chemistry, 394, 133455. https://doi.org/10.1016/j.foodchem.2022.133455

Leonarduzzi, G., Poli, G., Sottero, B., & Biasi, F. (2007). Department of Clinical and Biological Sciences of University of Turin, San Luigi Hospital, 10043 Orbassano, Turin, Italy. 791–799.

Li, X., Jiang, H., Pu, Y., Cao, J., & Jiang, W. (2019). Inhibitory effect of condensed tannins from banana pulp on cholesterol esterase and mechanisms of interaction. Journal of Agricultural and Food Chemistry, 67(51), 14066–14073. https://doi.org/10.1021/acs.jafc.9b05212

Matsuzaki, T., Ito, H., Chevyreva, V., Makky, A., Kaufmann, S., Okano, K., Kobayashi, N., Suganuma, M., Nakabayashi, S., Yoshikawa, H. Y., & Tanaka, M. (2017). Adsorption of galloyl catechin aggregates significantly modulates membrane mechanics in the absence of biochemical cues. Physical Chemistry Chemical Physics, 19(30), 19937–19947. https://doi.org/10.1039/C7CP02771K

Mitra, S., & Dungan, S. R. (2001). Cholesterol solubilization in aqueous micellar solutions of quillaja saponin, bile salts, or nonionic surfactants. Journal of Agricultural and Food Chemistry, 49(1), 384–394. https://doi.org/10.1021/jf000568r

Molino, S., Fernández-Miyakawa, M., Giovando, S., & Rufián-Henares, J. Á. (2018). Study of antioxidant capacity and metabolization of quebracho and chestnut tannins through in vitro gastrointestinal digestion-fermentation. Journal of Functional Foods, 49(July), 188–195. https://doi.org/10.1016/j.jff.2018.07.056

Molino, S., Lerma-Aguilera, A., Jiménez-Hernández, N., Gosalbes, M. J., Rufián-Henares, J. Á., & Francino, M. P. (2021). Enrichment of food with tannin extracts promotes healthy changes in the human gut microbiota. Frontiers in Microbiology, 12(March). https://doi.org/10.3389/fmicb.2021.625782

Molino, S., Lerma-Aguilera, A., Piskorz, M. M., López Mingorance, F., Montero, J. M., Uehara, T., Hashimoto, H., González Ballerga, E., & Olmos, J. A. (2024). Tannin-based supplementation influences gut microbiota composition and activity in IBS-D patients with a potential impact on symptoms: a pilot study. Food & Function, 15(17), 8893–8903. https://doi.org/10.1039/D4FO02236J

Ngamukote, S., Mäkynen, K., Thilawech, T., & Adisakwattana, S. (2011). Cholesterol-lowering activity of the major polyphenols in grape seed. Molecules, 16(6), 5054–5061. https://doi.org/10.3390/molecules16065054

Ogawa, K., Hirose, S., Nagaoka, S., & Yanase, E. (2016). Interaction between tea polyphenols and bile acid inhibits micellar cholesterol solubility. Journal of Agricultural and Food Chemistry, 64(1), 204–209. https://doi.org/10.1021/acs.jafc.5b05088

Poli, A., Marangoni, F., Corsini, A., Manzato, E., Marrocco, W., Martini, D., Medea, G., & Visioli, F. (2021). Phytosterols, cholesterol control, and cardiovascular disease. Nutrients, 13(8), 2810. https://doi.org/10.3390/nu13082810

Sallam, I. E., Abdelwareth, A., Attia, H., Aziz, R. K., Homsi, M. N., von Bergen, M., & Farag, M. A. (2021). Effect of gut microbiota biotransformation on dietary tannins and human health implications. Microorganisms, 9(5), 965. https://doi.org/10.3390/microorganisms9050965

Scalbert, A., Monties, B., & Janin, G. (1989). Tannins in wood: comparison of different estimation methods. Journal of Agricultural and Food Chemistry, 37, 1324–1329.

Schöbel, N., Radtke, D., Kyereme, J., Wollmann, N., Cichy, A., Obst, K., Kallweit, K., Kletke, O., Minovi, A., Dazert, S., Wetzel, C. H., Vogt-Eisele, A., Gisselmann, G., Ley, J. P., Bartoshuk, L. M., Spehr, J., Hofmann, T., & Hatt, H. (2014). Astringency is a trigeminal sensation that involves the activation of G protein-coupled signaling by phenolic compounds. Chemical Senses, 39(6), 471–487. https://doi.org/10.1093/chemse/bju014

Serrano, J., Puupponen-Pimiä, R., Dauer, A., Aura, A.-M., & Saura-Calixto, F. (2009). Tannins: Current knowledge of food sources, intake, bioavailability and biological effects. Molecular Nutrition & Food Research, 53(S2), S310–S329. https://doi.org/10.1002/mnfr.200900039

Sirk, T. W., Brown, E. F., Sum, A. K., & Friedman, M. (2008). Molecular dynamics study on the biophysical interactions of seven green tea catechins with lipid bilayers of cell membranes. Journal of Agricultural and Food Chemistry, 56(17), 7750–7758. https://doi.org/10.1021/jf8013298

Smeriglio, A., Barreca, D., Bellocco, E., & Trombetta, D. (2017). Proanthocyanidins and hydrolysable tannins: occurrence, dietary intake and pharmacological effects. British Journal of Pharmacology, 174(11), 1244–1262. https://doi.org/10.1111/bph.13630

Song, H., Chen, C., Zhao, S., Ge, F., Liu, D., Shi, D., & Zhang, T. (2015). Interaction of gallic acid with trypsin analyzed by spectroscopy. Journal of Food and Drug Analysis, 23(2), 234–242. https://doi.org/10.1016/j.jfda.2014.09.001

Sreij, R., Dargel, C., Schweins, R., Prévost, S., Dattani, R., & Hellweg, T. (2019). Aescin-cholesterol complexes in dmpc model membranes: a dsc and temperature-dependent scattering study. Scientific Reports, 9(1), 5542. https://doi.org/10.1038/s41598-019-41865-z

Testa, G., Rossin, D., Poli, G., Biasi, F., & Leonarduzzi, G. (2018). Implication of oxysterols in chronic inflammatory human diseases. Biochimie, 153, 220–231. https://doi.org/10.1016/j.biochi.2018.06.006

Vigne, S., & Pot, C. (2024). Implication of oxysterols and phytosterols in aging and human diseases. In Advances in experimental medicine and biology (Vol. 1440). https://doi.org/10.1007/978-3-031-43883-7_12

Vinarova, L., Vinarov, Z., Atanasov, V., Pantcheva, I., Tcholakova, S., Denkov, N., & Stoyanov, S. (2015). Lowering of cholesterol bioaccessibility and serum concentrations by saponins: in vitro and in vivo studies. Food & Function, 6(2), 501–512. https://doi.org/10.1039/C4FO00785A

Wang, C., Siriwardane, D. A., Jiang, W., & Mudalige, T. (2019). Quantitative analysis of cholesterol oxidation products and desmosterol in parenteral liposomal pharmaceutical formulations. International Journal of Pharmaceutics, 569, 118576. https://doi.org/10.1016/j.ijpharm.2019.118576

Zeng, X., Du, Z., Ding, X., & Jiang, W. (2020a). Characterization of the direct interaction between apple condensed tannins and cholesterol in vitro. Food Chemistry, 309(July 2019), 125762. https://doi.org/10.1016/j.foodchem.2019.125762

Zeng, X., Du, Z., Ding, X., & Jiang, W. (2020b). Characterization of the direct interaction between apple condensed tannins and cholesterol in vitro. Food Chemistry, 309, 125762. https://doi.org/10.1016/j.foodchem.2019.125762

Zeng, X., Du, Z., Ding, X., & Jiang, W. (2020c). Characterization of the direct interaction between apple condensed tannins and cholesterol in vitro. Food Chemistry, 309. https://doi.org/10.1016/j.foodchem.2019.125762

Zeng, X., Sheng, Z., Li, X., Fan, X., & Jiang, W. (2019). In vitro studies on the interactions of blood lipid level-related biological molecules with gallic acid and tannic acid. Journal of the Science of Food and Agriculture, 99(15), 6882–6892. https://doi.org/10.1002/jsfa.9974

Zhang, R., Han, Y., McClements, D. J., Xu, D., & Chen, S. (2022). Production, characterization, delivery, and cholesterol-lowering mechanism of phytosterols: a review. Journal of Agricultural and Food Chemistry, 70(8), 2483–2494. https://doi.org/10.1021/acs.jafc.1c07390

Zheng, K., Guo, K., Xu, J., Liu, W., Chen, J., Xu, C., & Chen, L. (2020). Study on the interaction between catechin and cholesterol by the density functional theory. Open Chemistry, 18(1), 357–368. https://doi.org/10.1515/chem-2020-0038

Chapter 7

Conclusions and Future Perspectives

7.1 Conclusive remarks

This PhD project was carried out in a historical context increasingly marked by the public's attention to health-related nutrition and the demand for functionalized foods with added value for human well-being. However, the intrinsic instability of many food products during processing and storage leads to the formation of harmful compounds, ranging from well-known entities such as free radicals and *trans* fats to more recently studied molecules like sterol oxidation products. The most effective strategy to mitigate oxidative degradation is the incorporation of antioxidants. However, the amphiphilic mismatch between the typically hydrophobic lipids and hydrophilic antioxidants represents a critical challenge, often limiting the efficacy of such interventions. In this regard, tannins may represent an innovative bridge between lipid and phenolic systems, offering a promising avenue to preserve lipid stability.

The aim of this research study was to evaluate the antioxidant effect and colligative properties of two classes of tannins—specifically chestnut (rich in hydrolysable tannins) and quebracho (rich in condensed tannins)—through a dual approach. Tannins are widely known for their antioxidant activity, as well as for their so-called antinutritional properties, owing to their ability to bind macromolecules such as proteins, vitamins, metals, and, although less studied, lipids, potentially reducing their bioavailability.

Initially, since the determination of phytosterol oxidation products (POPs) is challenging, due to limited availability of reference material except for 7-ketositosterol, a comparative study to set up a proper and robust analytical approach was developed. That study isolated pure POPs using a semi-preparative HPLC method and compared their effectiveness in quantifying POPs with that of cholesterol oxidation products (COPs), which are the most commonly used reference. Two

chromatographic techniques were compared; liquid chromatography coupled to high-resolution mass spectrometry (LC-Orbitrap-HRMS) and gas chromatography combined with mass spectrometry (GC-MS). The study for the first time demonstrated that the choice of the right reference material plays a crucial role in order to reach robust and reproducible results and the use of pure COPs as chemical standards for POPs quantification needs to be reconsidered.

Then, the antioxidant capacity of tannins was assessed in oil-in-water (O/W) emulsion systems using two different lipid phases: stripped sunflower oil and lipid matter isolated from egg yolk. The emulsions were also studied under two pH conditions (3.5 and 7.0). Both oxidative stability and physical stabilization—via interfacial activity—were monitored throughout 14 days of shelf-life at 40 °C. The main findings can be summarized as follows:

i. Both tannins delayed lipid oxidation. However, their activity varied according to the lipid matrix and pH. Quebracho proved particularly effective in O/W emulsions with sunflower oil. Conversely, in egg yolk emulsions, the co-presence of lutein and hydrolysable tannins suggested a potential synergistic mechanism, in which tannins may have acted as secondary antioxidants, regenerating the natural antioxidant component (lutein).

ii. Quebracho tannins significantly increased the negative surface charge across all systems tested, contributing to improved emulsion stability.

iii. Both tannins substantially reduced the formation of sterol oxidation products (SOPs), including cholesterol and phytosterol derivatives. Again, the cholesterol oxidation was most effectively counteracted by the combined action of lutein and tannins.

The second part of the research explored, for the first time, the ability of tannins to complex with sterols. The results were promising, particularly with quebracho tannin, composed predominantly of catechin units. The interaction with cholesterol, β-sitosterol, and stigmasterol revealed a strong binding capacity, opening new perspectives for tannin applications in food systems. The transfer of

sterols into the aqueous phase in emulsified systems may offer the opportunity to reduce potentially harmful components like cholesterol in specific food formulations, or alternatively, to enhance and stabilize phytosterols—recognized for their cholesterol-lowering effects—in aqueous matrices.

7.2 Future Perspectives

Further investigations will be required to elucidate potential synergistic effects between tannins and other antioxidant molecules—particularly those belonging to the carotenoid family. Additional research is currently underway to deepen the understanding of tannin–sterol interactions, with a specific focus on the behavior of hydrolysable tannins. Ongoing studies include nuclear magnetic resonance (NMR) analysis aimed at characterizing the nature of the bonds formed during complexation.

A crucial point for future investigation will be to clarify the functional implications of tannin–sterols complexation—namely, whether tannins act as sequestrating agents that hinder sterol absorption during digestion, or conversely, as carriers capable of enhancing sterol bioavailability. Understanding this duality will be essential for determining the potential applications of tannins in functional food design and lipid-related health interventions.

LIST OF PUBLICATIONS

Bonciolini, A., Vissio, A., Calaminici, R., Forte, E., Cardenia, V. Comparative study on phytosterol oxidation products determination in high oleic sunflower oil by using cholesterol oxidation products or purified phytosterol oxidation products as reference materials. *Journal of Agriculture and Food Research* (2025), 21, 101961.

Cantele, C., **Bonciolini, A.**, Rossi, A.M., Bertolino, M., Cardenia, V. Effects of Wheat Bran-Derived Alkylresorcinols on the Physical and Oxidative Stability of Oil-in-Water Emulsions as related to pH. *Food Chemistry* (2025), 464, 141659.

Salgarella, N.I., **Bonciolini, A.**, Glicerina, V., Greco Miani, M., Tatar, H.D., Cardenia, V. Durum wheat oil oleogels: A study on rheological, thermal, and microstructural properties. *Food Structure* (2024), 42, 100397.

Shiva, G., Cardenia, V., **Bonciolini, A.**, Santos, R.D., Al-Rasadi, K., Sahebkar, A. Lipidomic profiling in patients with familial hypercholesterolemia: Abnormalities in glycerolipids and oxysterols. *Clinical Biochemistry* (2024), 131-132, 110812.

Cantele, C., Potenziani, G., **Bonciolini, A.**, Bertolino, M., Cardenia, V. Effect of Alkylresorcinols Isolated from Wheat Bran on the Oxidative Stability of Minced-Meat Models as Related to Storage. *Antioxidants* (2024), 12, (8), 930.

Ossola, M., Ferrocino, I., Franciosa, I., Aimasso, U., Cravero, L., **Bonciolini, A.**, Cardenia, V., Merlo, F.D., Anrò, M., Chiarotto, A., Bosa, C., Cocolin, L. Does Microbiome Matter in Chronic Intestinal Failure Due to Type 1 Short Bowel Syndrome in Adults? *Nutrients* (2024) 16, (14), 2282.

Traina, C., Ferrocino, I., **Bonciolini, A.**, Cardenia, V., Lin, X., Rantsiou, K., Cocolin, L. Monitoring the yeasts ecology and volatiles profile throughout the spontaneous fermentation of Taggiasca cv. table olives through culture-dependent and independent methods. *International Journal of Food Microbiology* (2024), 417, 110688.

Bonciolini, A., Cantele, C., Piochi, M., Di Lecce, G., Risso, D., Cardenia, V. New insights on phytocannabinoids role in antioxidant activity of hemp inflorescences extract in high-oleic sunflower oil. *LWT* (2023), 194, 115807.

Bonciolini, A., Cantele, C., Salgarella, N.I., Zeppa, G., Bertolino, M., Cardenia, V. Effect of Tannins on Cholesterol Content and Its Oxidation in Egg Pasta as Related to Different Pasta Shapes. *Food and Bioprocess Technology* (2023), 16, (7), 1541-155